Centralised Battery Flexibility Assessment for Imbalance Management in Spain considering Li-Ion Degradation Mechanism

Master's Thesis

Leon Maximilian Haupt

Escola Tècnica Superior d'Enginyeria Industrial de Barcelona

Universitat Politècnica de Catalunya

Barcelona, September 18, 2018

Programme: InnoEnergy Master SELECT

Environomical Pathways for Sustainable Energy Systems

Conducted at: Royal Institute of Technology, Stockholm

Universitat Politècnica de Catalunya, Barcelona

Degree: Master in Energy Engineering

Supervisors: Francisco Díaz-González

Pol Olivella-Rosell

Convocation: October 2018

In cooperation with: CITCEA & Estabanell Energia

In association with: Europe-funded H2020 project INVADE

Co-funded by the Horizon 2020 programme of the European Union

Abstract

The rise of Distributed Energy Resources (DER) cause more uncertainty for the Balance Responsible Party (BRP) with regards to precise forecasting of supply and demand. In case of an imbalance, ancillary services have to be activated resulting in monetary deviation penalties for the respective BRP. The implementation of reliable communication technology enables the use of aggregated flexibility, utilising smart industrial and residential applications, heating systems, electric vehicles, distributed generation and energy storage.

This work analyses the use case of centralised Lithium-Ion battery providing flexibility for BRPs. The analysis was conducted using Spanish electricity market data and real imbalance data from the year 2017.

The model developed in this work integrates battery cycle aging using a piecewise linear cost function. This approach provides a close approximation of the battery degradation mechanism of electrochemical batteries and can be incorporated easily into existing market dispatch programs with short time window. Having battery degradation implemented in the decision making reveals a more considerate operation of the battery, which prolongs the battery's lifetime and improves the project's profitability. Moreover, the analysis revealed that the Lithium-Ion Titanate (LTO) chemistry performs the best from an operational and project-based perspective. Eventually, the business case of usin ng centralised battery flexibility for deviation management using the example of Spain was assessed and concluded to be insufficient to reach break-even for the investment.

Contents

List of Figures

List of Tables

List of Abbreviations

AC	Alternating Current
AGR	Aggregator
BDEW	German Association of Energy and Water
BESS	Battery Energy Storage System
BMS	Battery Management System
BOS	Balance of System
BRP	Balance Responsible Party
CAPEX	Capital Expenditures
COS	Cost of Storage
DC	Direct Current
DER	Distributed Energy Resources
DMP	Daily Market Price
DoD	Depth of Discharge
DSO	Distribution System Operator
EBITDA	Earnings Before Savings Interest and Tax Depreciation and Amortisation
EES	Electric Energy Storage
ENTSO-E	European Network of Transmission System Operators for Electricity
EoL	End of Life
EPC	Engineering, Procurement and Construction
EPESA	Estabanell y Pahisa Energia, S.A
ESU	Energy Storage Unit

EV	Electric Vehicle
FCR	Frequency Containment Reserves
FO	Flexibility Operator
FRR	Frequency Restoration Reserves
ICT	Information and Communications Technology
IRENA	International Renewable Energy Agency
IRR	Internal Rate of Return
KPI	Key Performance Indicator
LCOS	Levelized Cost of Storage
LEC	Local Energy Community
LFM	Local Flexibility Market
LFP	Lithium Iron Phosphate
LiB	Lithium Batteries
LMO	Lithium Manganese Oxide
LTO	Li-Ion Titanate
LV	Low Voltage
MIBEL	Mercado Ibérico de la Electricidad
MILP	Mixed-Integer-Linear-Problem
MPC	Model Predictive Control
MV	Medium Voltage
NCA	Lithium Nickel Cobalt Aluminium Oxide
NMC	Nickel Manganese Cobalt Oxide
NPV	Net Present Value
OCV	Open Circuit Voltage
OPEX	Operational Expenditures
P/E Ratio	Power to Energy Ratio

PBC	Programa Diario Base
PCU	Power Conversion Unit
PHES	Pumped Hydro Energy Storage
PHF	Programa Horario Final
PHO	Programa Horario Operative
PLC	Power Line Communications
PV	Photovoltaic
PVD	Viable daily Definitive program
PVP	Programa Diario Viable Provisional
REE	Red Eléctrica de España
RR	Replacement Reserves
SEI	Solid Electrolyte Interphase
SESP	Smart Energy Service Provider
SoC	State of Charge
SoH	State of Health
TE	Transactive Energy
TLC	Traffic Light Concept
TSO	Transmission System Operator
UCTE	Union for the Coordination of Transmission of Electricity
UPC	Universitat Politècnica de Catalunya
UPS	Uninterruptible Power Supply
USEF	Universal Smart Energy Framework
VS	Value Stream
WAC	Weighted Average of Cost

List of sets, parameters and variables

Economic Assessment

Project Parameters

Symbol	Value assumed	Unit	Description
$T_{project}$	10	years	Horizon for the project indexed in years by t
d_{op}	365	days/year	Number of days of operation in the year
i	5	%	Expected interest rate of the project
i_{tax}	25	%	Corporate tax rate in Spain [1]
$i_{inflation}$	2.3	%	Inflation rate according to Spanish Consumer Price Index (CPI) [2]
T_{deprec}	5	years	Years of depreciation

Battery Specifications

Symbol	Unit	Description
P	kW	Power capacity of the system
$E_{installed}$	kWh	Installed energy storage capacity of the system
c_e	€/kWh	Specific cost per storage capacity unit
c_p	€/kW	Specific cost per power capacity unit
c_{other}	€/kWh	Other investment cost with the installation of the BESS
c_f	€/(kW·year)	Fix cost for operating and maintenance function of power capacity
c_r	€	Replacement cost of the BESS
D_{cycles}	number of cycles	Number of cycles guaranteed by the battery manufacturer
D_{DoD}	%	Depth of discharge, with which the guaranteed number of cycles D_{cycles} can be achieved
D_{EoL}	%	End of life capacity after the battery exceeded D_{cycles}, guaranteed by the manufacturer. Given in relation to the installed energy storage capacity $E_{installed}$
T_{bat}	years	Expected calendar lifetime of the battery, guaranteed by the manufacturer
μ	%	Roundtrip energy efficiency (AC/AC)
DoD	p.u.	Maximum usable capacity limited by upper and lower boundaries
E_{usable}	kWh	$E_{usable} = E_{installed} \cdot DoD \cdot \mu$, the actual usable energy storage capacity

Other Project-related Parameters

Symbol	Unit	Description
T_{optim}	h	Optimisation time horizon given in hours
$E_{discharged}^{TOTAL}$	kWh	Total energy discharged by the BESS in T_{optim}
$E_{charged}^{TOTAL}$	kWh	Total energy charged by the BESS in T_{optim}
L_{degr}	%	Total life loss of the BESS calculated by the algorithm within time T_{optim}
$T_{expected}$	years	Calculated life expectancy based on life loss L_{degr} and guaranteed battery life T_{Bat}
c_{opport}	€/kWh	Calculated average opportunity cost by the use caused by discharging the battery
c_{elec}	€/kWh	Calculated average price of electricity caused by charging the battery within T_{optim}
i_{opport}	%	Expected increase or decrease of c_{opport} per year
i_{elec}	%	Expected increase or decrease of c_{elec} per year

Optimisation

Sets

Symbol	Code	Description
T	`model.t`	Number of time intervals in the optimisation horizon, indexed by t
J	`model.s`	Number of segments in the cycle aging cost function, indexed by j
B	`model.b`	Number of batteries in the optimisation indexed by b

General Parameters

Symbol	Code	Description
d_t^{BRP}	`model.imbalance`	Imbalance data of the BRP at time t [MWh], negative if upwards imbalance (more generation, less consumption) and positive if downwards imbalance (less generation, more consumption)
p_t^{IB}	`model.p_imbalance`	Imbalance price at time t [€/MWh]
p_t^{ID}	`model.p_intraday`	Intraday price of session 1 for delivery at time t [€/MWh]
v^{ID}	`Intraday_on_off`	Intraday trading can be switched on and off depending on the scenario. $v^{ID} = 0$, no Intraday trading is performed
M	`M`	Duration of market dispatch time interval [h]

Battery Parameters

Symbol	Code	Description
$E_b^{installed}$	`model.bat_o_rated`	Installed capacity of battery unit b [MWh]
Q_b^{in}	`model.bat_q_ch`	Maximum charging power allowed for battery unit b [MW]
Q_b^{out}	`model.bat_q_dis`	Maximum discharging power allowed for battery unit b [MW]
η_b^{ch}	`model.bat_eta_ch`	Efficiency parameter for charging storage unit b [%]
η_b^{dis}	`model.bat_eta_dis`	Efficiency parameter for discharging storage unit b [%]
S_b^{min}	`model.bat_SOC_min`	Minimum state of charge allowed of battery b [p.u.]
S_b^{max}	`model.bat_SOC_max`	Maximum state of charge allowed of battery b [p.u.]
$O_b^{initial}$	`model.bat_o_in`	Initial state of charge of battery b [MWh]
O_b^{final}	`model.bat_o_fin`	Final state of charge of battery b [MWh]
S_b^{ch}	`model.s_ch`	Threshold in battery unit b charging process [p.u.]
S_b^{dis}	`model.s_dis`	Threshold in battery unit b discharging process [p.u.]
A_b^{high}	`model.bat_avg_SOC_high`	Upper limit for the average SoC of battery unit b [p.u.]
A_b^{low}	`model.bat_avg_SOC_low`	Lower limit for the average SoC of battery unit b [p.u.]
$c_{r,b}$	`init_R`	Battery replacement cost of battery b in [€/MWh]

Symbol	Code	Description
$k_{1,b}$	`init_a`	Cycle depth stress function parameter k_1 of battery unit b
$k_{2,b}$	`init_c`	Cycle depth stress function parameter k_2 of battery unit b
D_b^{EoL}	`init_D_eol`	End of life capacity after the battery unit b exceeded D_{cycles} [p.u.]
T_{bat}	`init_life_exp`	Expected calendar lifetime of battery unit b [years]
$c_{b,j}$	`model.segm_c_j_dis`	Marginal aging cost of cycle depth segment j of battery unit b [€/MWh]
$o_{b,j}^{initial}$	`model.segm_o_in`	Initial state of charge of cycle depth segment j in period $t = 0$ of battery unit b [MWh]
$o_{b,j}^{max}$	`model.segm_o_max`	Maximum state allowed charge of cycle depth segment j of battery b in period T [MWh]

Battery Health Parameters

Symbol	Initial Value	Code	Description
L_b^{cyc}	0	`status_total_cycles`	Total cycle degradation of battery unit b [%]
L_b^{cal}	0	`status_total_calendar`	Total calendar degradation of battery unit b [%]
T_b^{status}	0	`status_time_of_usage`	Total time of usage of battery unit b [h]
A_b^{status}	0.5	`status_avg_SOC`	Average state of charge of all past optimisation periods [p.u.]
SoH_b	1	`status_total_SOH`	State of health of battery unit b [p.u.]

Decision Variables

Symbol	Code	Description
$\sigma^{ch}_{t,b,j}$	`model.sigma_ch`	Amount of electricity charged to cycle depth segment j of battery unit b at time t [MW]
$\sigma^{dis}_{t,b,j}$	`model.sigma_dis`	Amount of electricity discharged from cycle depth segment j of battery unit b at time t [MW]
$\sigma^{SoC}_{t,b,j}$	`model.sigma_soc`	Energy stored in segment j in battery unit b at time t [MWh]
σ^{ID}_{t}	`model.intraday`	Amount of electricity traded for delivery at time t on the intraday market [MWh]
$C_{t,b}$	`model.total_charging`	Total charging of battery at time t of battery unit b [MWh]
$D_{t,b}$	`model.total_discharging`	Total discharging of battery at time t of battery unit b [MWh]
$v_{t,b,j}$	`model.activity`	Operating mode of the BES: if at time t the BESS is charging then $v_{t,b,j} = 1$; if it is discharging then $v_{t,b,j} = 0$

Chapter 1

Introduction

Increasing implementation of renewable energy production into the distribution grid compromises power quality in terms of voltage limit violations, line overloads or instabilities [3]. Moreover, it causes more uncertainty for the Balance Responsible Party (BRP) with regards to precise forecasting of supply and demand. In case of an imbalance, ancillary services have to be activated resulting in monetary deviation penalties for the respective BRP [4]. One key element to improve security of prediction is the implementation of Information and Communications Technology (ICT) on both sides, the production and the consumption, enabling a secure bidirectional information flow, thus a smart grid [5], [6]. This opens the market for new services based on aggregated flexibility, utilising smart industrial and residential applications, heating systems, electric vehicles, distributed generation and alike, which are counteracting to modify the electricity production and consumption with regards to unexpected resiliency [7].

The aggregator (AGR) is the entity responsible of accumulating flexibility in active demand and supply. The AGR seeks the lowest costs to meet the energy demand of his portfolio taking the costs for capacity usage into account. Four flexibility customers can be defined: Distribution System Operators (DSO), Balance Responsible Parties (BRP), Transmission System Operators (TSO), and Prosumers. DSO and TSO are interested to purchase flexibility to manage grid congestions and reduce upgrading grid costs. BRP and retailers can use flexible resources to manage their portfolio and reduce deviation penalties and operation costs. Finally, prosumers can use their flexibility capabilities to reduce the electricity bill [7], [8].

An obligation of the BRP is to continuously achieve balance between the electricity supplied and withdrawn. A given imbalance has to be balanced by a given control energy mechanism activated by the TSO, which results in financial penalties for the respective BRP [9]. Fast development and implementation of internet of energy enables the aggregation and utilisation of distributed flexibility [10].

In this work, the business opportunities for a BRP being active as its own flexibility aggregator managing centralised batteries in order to reduce deviation penalties are assessed and by means of real data simulated and verified.

In this context, this research aims to analyse the economics of large-scale stationary Battery Energy Storage Systems (BESS). The complex degradation mechanisms deriving from the electrochemical processes are difficult to implement in dispatch algorithms. Thus, the operational regime of batteries are commonly constraint. This prevents operators from taking advantage of a BESS's operational flexibility and significantly lessens its profitability. To take full advantage of the ability of a BESS, its lifetime can no longer be considered as being fixed. Instead, the significant part of the battery degradation cost that is driven by cycling should be treated as an operating expense and implemented in the decision-making [11]. The work comprises a profound literature research on this topic resulting in a methodology to compare prevailing Lithium-chemistries from a operational and project-based point of view.

The result of this thesis will give financial indication of using such flexibility as an alternative to conventional control measures.

1.1 Partnerships

The work was conducted in cooperation with the technology transfer centre CITCEA-UPC[1] and the Catalan utility Estabanell[2], which are both participating in the Europe-funded Horizon 2020 project INVADE[3] [7]. The project is considering current development in regulatory market designs and state-of the art technology. Consequently, the design choices and assumptions made throughout this work will be aligned with the INVADE project, in order to obtain significant conclusions.

1.1.1 Horizon 2020 Project INVADE

The European INVADE project is a cloud-based flexibility management system integrated with electric vehicles (EVs) and battery storages at mobile, distributed and centralised levels. The goal of INVADE is to change the way energy is used, stored and generated by utilising renewable energy more effectively, optimising the supply of electricity and making services more end-user centric. The project integrates different components such as flexibility management systems, energy storage technologies, electric vehicles and novel business models.

INVADE's integration of ICT cloud-based battery and flexibility management systems with renewable resources represents the missing link in this market and is therefore highly sought for by European energy industries and the authorities. Prosumers, who both consume and produce electricity, will be empowered by utilising the strength of novel ICT solutions to optimise their own flexibility in energy consumption, production and storage, including the storage capacity of their electric vehicles. The project aims to

[1] CITCEA - Mecatrònica i Enertrònica: http://www.citcea.upc.edu/
[2] Estabanell Energia | Eficiència en distribució elèctrica: https://www.estabanell.cat/
[3] INVADE - The new Horizon 2020 EU project: http://h2020invade.eu/

empower the use of more environmentally-friendly energy, and to optimise the European energy system by reducing energy losses, improving the energy balance and increasing the security of supply [7], [12].

1.1.2 CITCEA

CITCEA-UPC is a technology transfer centre of the Technical University of Catalonia (UPC), specialised in responding to the needs of enterprises to build functional prototypes that can be industrialised and commercialised.

Within the INVADE Project, UPC is responsible to define the overall architecture, the detailed control algorithm of the flexibility management system, and operate the test-lab for the INVADE platform, as well as giving support for other tasks. UPC leads the work package Dissemination and Communication, and the Overall INVADE architecture [12].

1.1.3 Estabanell Energia

Estabanell y Pahisa Energia, S.A. (EPESA) has a network of over 1,100 km from Camprodon to Granollers, servicing more than 56,000 power customers, with two substations where it connects to the transmission network at 220 kV, distributing electricity through more than 800 secondary substations. EPESA combines the roles of DSO and retailer, in the electricity domain, deploying a customer focused relationship marketing, and as telecom operator, providing dark fibre and PLC based telecommunications. Being a part of INVADE, EPESA is providing reinforcement of all activities related to Demand Response, definition of the technical requirements and relationship with the prosumers and the municipality. Moreover, their main responsibility is task 10.7: The pilot implementation in Spain [12].

1.2 Thesis Outline

The present thesis aims at improving the planning and operation of Lithium-Ion based energy storage systems in electricity market operations considering Lithium-Ion degradation mechanism using the example of imbalance markets in Spain.

In greater detail, it provides solutions to the following research questions:

1. How to accurately model the battery degradation when dispatching batteries in electricity markets.
2. Which Lithium-Ion chemistry performs better from a operational and project-based perspective when applied to a specific use case.
3. What is the financial performance of providing battery flexibility for imbalance management in Spain.

Thus, the research of this thesis is diverse and structured by chapter:

- In *Chapter 2*, the customers of the battery system within the novel framework of the Local Flexibility Market are defined.
- In *Chapter 3*, state-of-the-art Lithium-battery technologies and the respective economics are investigated resulting in a project-based assessment of battery energy storage.
- In *Chapter 4*, a linear battery model for market dispatch is developed. It implements cycle and calendar degradation mechanism of Lithium-batteries.
- In *Chapter 5*, remuneration mechanism for imbalance services in the Spanish electricity market are assessed.
- In *Chapter 6*, the modelling problem of a battery energy storage used for imbalance management is formulated and thereafter by means of a sensitivity analysis validated.
- In *Chapter 7*, an operational hourly analysis of the algorithm applied to the imbalance market is conducted.
- In *Chapter 8*, the value of the use case of battery energy storage interacting in imbalance markets considering intraday trading and degradation mechanism is quantified. The first case investigates the profitability of Estabanell's battery. The second study case compares the performances of different Lithium-Ion technologies.
- In *Chapter 9*, a project summary including a budget estimation and environmental impact assessment is provided.

Chapter 2

Local Flexibility Market Concept

The Local Flexibility Market (LFM) is the key concept creating the framework for the business opportunity assessed in this thesis. The subject is investigated by many researchers, companies and policymakers world-wide. Therefore, it is important to define consistently the characteristics of the LFM and its integrated concepts. This chapter is divided as follows: Initially, the need for a new market design in a holistic view is addressed, in the following, key terminologies are defined in order to ensure comparability with other works. Thereafter, several flexibility services and their customer are introduced. Eventually, the chapter concludes with the justification of centralised Battery Energy Storage System (BESS) for flexibility use. The LFM frameworks used in this work are summarised in Appendix A.

2.1 The Need for a New Market Design

The market-driven increase of distributed energy resources (DER) and the resulting high intermittency, is a main driver for the development of new control mechanisms in order to decrease resiliency imposed on the grid. Moreover, the urge of moving to a sustainable future is linking the fossil-fuel-intensive transportation industry with the electricity sector providing a new layer of complexity in terms of electrical power and energy management.

The electricity supply is a sensitive parameter for economy, society and environment, thus regulated and controlled by policies. New market designs have to comply with these aspects, by providing security of supply, affordability and environmental protection [13]. This trade-off accounts for one of the main objectives of the energy transition, which challenges policymakers, industries and citizen as a whole in order to ensure equitable distribution of energy supply, decouple carbon emissions from economic growth, rationalise domestic consumption as well as industrial demand, and foster sustainability of power companies [14].

Common sense in policy making has led to major movements in the energy transition achieving the target triangle by focusing on the five concepts: Democratisation, decarbonisation, deregulation, decentralisation, and digitalisation.

- **Democratisation:** This concept relates to measures which enable access to green electricity contracts and affordable distributed energy resources, such as PV modules, and therefore give citizens the possibility to actively choose the quality of supply. Moreover, the technologies enabling transparent insights in consumer profiles raises the consumer awareness. This way, individuals are put in the driver's seat and empowered to choose responsibly, rather than being exposed to large enterprise and government decisions, which are imposing a certain quality of supply.
- **Decarbonisation:** As a main pillar of the energy target, the decrease of the carbon intensity of the energy supply is the key towards the long-term goal of keeping the increase in global average temperature to well below 2 °C above pre-industrial levels as ratified in the Paris climate conference (COP21) in December 2015 [15]. This is achieved on the one hand by gradually fading out fossil-fuel based thermal power plants, such as coal, oil and natural gas while nurturing alternative, renewable production.
- **Deregulation:** The energy industry along with its governing policies evolved over long period of time. These policies are ensuring security of supply while keeping the engine for a growing economy running on a reasonable cost-competitive level. As a result, an inefficient energy industry with high entrance barriers for new companies emerged. Policy makers are walking the thin line between opening the market to new competitors in order to enable innovation and development while maintaining the security of supply. This is achieved by unbundling the value chain of electricity and partly opening the market to third-parties in the sector of production and retail, while keeping the monopoly of the transmission and distribution grid. Competition embraces cost efficient solutions and an organic growth of new technologies. Moreover, it attracts private equity and gives more profit margin for new solutions.
- **Decentralisation:** Induced by the democratisation and the empowerment of the citizen, the decentralisation is a consequent step to distribute the influence of energy enterprises and move away from a demand-oriented production with a unidirectional distribution, towards a supply-oriented demand with a bidirectional flow of electricity and information. The ability to store energy is the key to decentralisation of electric power. Excess energy generated, whether from rooftop solar panels on a home or by a wind farm, requires large amount of energy storage systems implemented in the grid. Therefore, an increasing number of business models are tackling storage solutions for prosumers which could also provide advanced services to the grid.
- **Digitalisation:** High intermittency, bidirectional electricity flows, penetration of energy storage and EVs in the grid are only made possible by the implementation of ICT and the concomitant ability to process large amount of data. Digitalisation is the preceding enabler of many new business models in the energy sector, such as real-time markets, accurate weather and demand forecasting or smart energy management systems for small appliances. It is expected that the full potential in the distributed system is not yet harvested. A lack of standardised frameworks and slow-moving regulations are holding back companies making investments due to possible lock in effects, e.g.

in Germany where the smart meter rollout will only start from 2018 replacing analogue metering devices with digital meters [6]. However, these energy management products empower customers to minimise demand and make informed decisions to reduce their electricity bills.

The European Commission's 2030 policy framework for climate and energy aims at decarbonising the energy system. This implies growing need for system flexibility in order to accommodate growth of electrification and the increasingly variable renewable energy share, while also keeping in mind the potential problems of ageing infrastructure [9], [16]. The associated logic is illustrated in Figure 2.1. Consequently, the LFM and the new role, the flexibility aggregator, are filling the gap between small energy producer, consumer and smart prosumer, and energy wholesale markets which are typically accessed by retailers and large utilities. The framework of the LFM, which will be elaborated in the following, is aiming to satisfy all the five criteria introduced above.

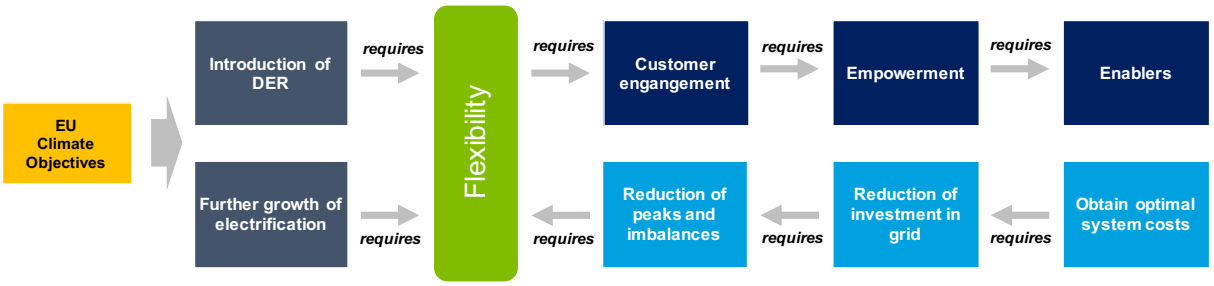

FIGURE 2.1: The necessity of flexibility in a developing grid which complies with the EU climate objectives [9].

The Smart Grid Task Force [9] concluded importantly: "While it should be noted that flexibility will not replace traditional investment, increased integration of distributed energy resources (DER) and the growing peak demand for electricity will drive the need for increased flexibility, customer engagement and empowerment in order to maintain an affordable energy system."

2.2 What is Flexibility?

"[...] flexibility is the modification of generation injection and/or consumption patterns in reaction to an external signal (price signal or activation) in order to provide a service within the energy system. The parameters used to characterise flexibility in electricity include: the amount of power modulation, the duration, the rate of change, the response time, the location etc" [9].

Flexibility can be generated on both sides of the energy value chain, thus its characterisation divides in upward regulation, which is defined as increasing generation or decreasing demand, and downward regulation, which means decreasing generation or increasing demand [7], [17].

Flexibility can be provided by different flexibility sources that can be grouped into energy storage, load, generation, and electric vehicles. It needs to be noted that different classification might be used in literature, this work however will follow the methodology of the Horizon 2020 INVADE project [7].

Sources are most commonly distinguished by their controllability. The sources get categorised into uncontrollable (no flexibility), curtailable, shift-able, buffered and freely controllable sources (full flexibility), as shown in Figure 2.2. Curtailable loads, for example, are those that do not need to recover the curtailed energy once they are reconnected. In contrast, shift-able loads are those which can be moved in time. However, the amount of energy consumed does not change, it only gets shifted in the time-domain. As initially stated, flexibility is also provided on generation-side with curtailable generation plants such as solar PV. Other load types can have several flexibility properties and its categorisation depends on the way they are operated, like EVs, which can be categorised as both curtailable, shift-able and buffered [7].

Aside from the regulation capabilities (upward vs downward regulation) and controllability, flexibility can be classified based upon its scale, whether it provides low, medium and high flexibility, and domain of interaction with the grid; behind-the-meter, low-voltage or medium-voltage grid.

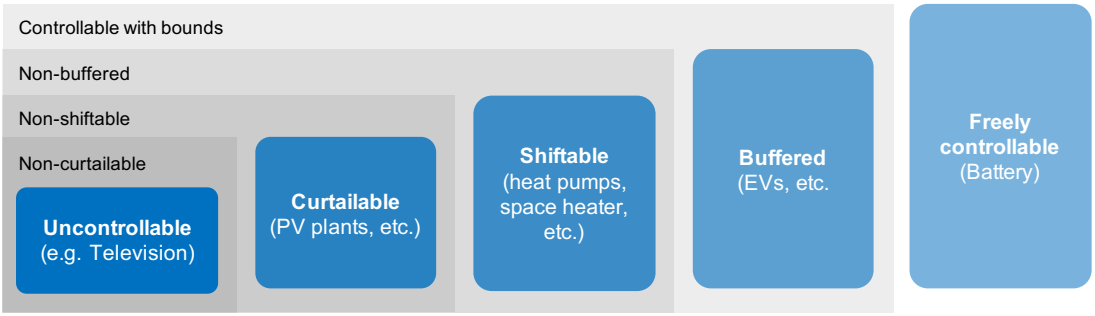

FIGURE 2.2: Categorisation of flexibility sources [7].

Table 2.1 gives an overview of flexibility sources which have been identified within the INVADE project, and their respective potential. This work will mainly focus on centralised BESS as the flexibility provider, which typically provide medium ($> 50\,\text{kWh}$ and $< 1\,\text{MWh}$) to high flexibility capacity ($> 1\,\text{MWh}$).

2.3 LFM Overview

With the different flexibility sources identified, a platform to offer and trade this flexibility has to be created. Conventional electricity markets are not suitable to perform this action, due to lack of bidding products and high entry barriers. The LFM aims to satisfy this need by providing a local flexibility trading platform for exchanging and scheduling flexibility. In the course of the establishment of the LFM, two new market roles are emerging; the Flexibility Aggregator which acts as the local market facilitator and the Local Energy Community (LEC), which is a citizen-led association aiming for the empowerment

TABLE 2.1: Flexibility sources and their potential identified by INVADE. The green mark-up represents the focus of this work [7].

Classification		Regulation capabilities		Domain			Scale		
Class	Type	Downward regulation	Upward regulation	Customer premises	LV grid	MV grid	Low flexibility	Medium flexibility	High flexibility
Storage control	Battery at households	X	X	X			X		
	Centralized battery (LV grid)	X	X		X			X	X
	Centralized battery (MV grid)	X	X			X		X	X
Load control	Disconnectable load		X	X			X		
	Shiftable load (constant profile)	X	X	X			X		
	Adjustable or shiftable load (constant energy)	X	X	X			X		
Generation control	Disconnectable DER	X		X	X		X		
	Adjustable DER	X	X	X	X		X		
	Disconnectable DER plant	X			X	X		X	X
	Adjustable DER plant	X	X		X	X		X	X
EV control	EV charging station (multiple charging points)		X		X			X	X
	EV charger at household		X	X			X		
	EV public charge point		X		X		X		
	EV charging station with V2G (multiple charging points)	X	X		X			X	X
	EV charger at household with V2G	X	X	X			X		
	EV public charge point with V2G	X	X		X		X		

of end-users and prosumers to manage energy at community level in an efficient way. As can be seen in Figure 2.3, the Aggregator establishes a new value chain which spreads out along the unidirectional electricity flow. The flexibility, which is mainly provided by the LEC, can be traded through the LFM to potential customers, such as the BRP, DSO or among prosumers themselves [7], [17], [18].

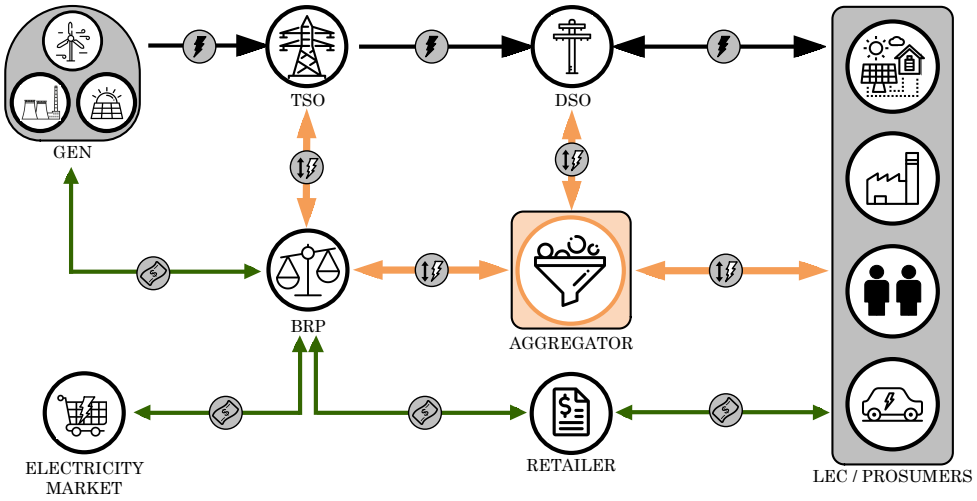

FIGURE 2.3: Local flexibility market overview. Aggregator and Local Energy Community [18].

2.3.1 Aggregator

Many flexibility sources are considered very small, therefore the empowerment of many end-users to offer their flexibility and the aggregation of these are the key to reach a critical threshold of flexibility. Since no conventional role is eligible for this task, the aggregator as an emerging role is the answer. It acts as a legal partner for flexibility contracts, interacts with LECs and ensures liquidity in the LFM.

The role of the Aggregator is not yet defined by regulators, thus the question of how the LFM integrates in the current market is still open. On the one hand a Transactive Energy System (TE) promises to provide the flexibility without the need of an additional centralised role. This concept is more user-focused and follows the idea of peer-to-peer trading. TE embodies almost complete decentralisation and attracts much attention lately, due to the Blockchain technology, which ensures integrity of data without the need of a centralised trustworthy body. On the other hand, a centralised approach simplifies the trading by creating a body which is responsible for the contracting and supervision of flexibility [17]. However, both proposals, local markets and transactive energy systems, are following the EU recommendation to put consumers at the heart of the energy markets by ensuring that they are empowered and better protected [19]. The centralised approach, even though providing less decision power to the customer, are favoured in this work, due to a higher predictability of flexibility and the lack regulatory frameworks supporting TE. In Figure 2.4 the centralised approached is shown. For completeness the TSO has been named as a potential customer of flexibility, though being out of scope of the INVADE project.

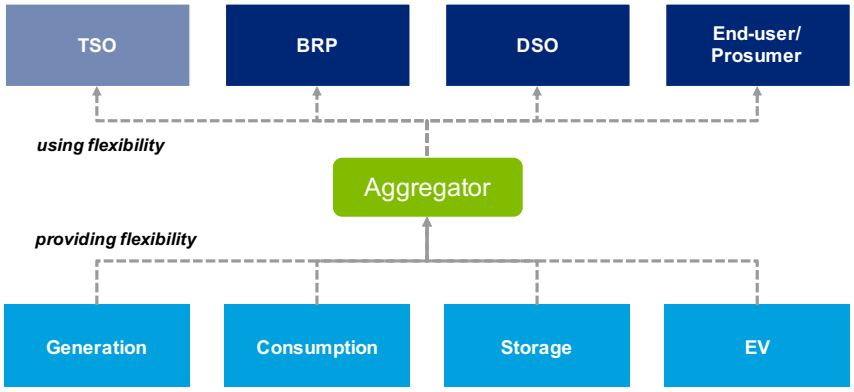

FIGURE 2.4: Flexibility flow using a centralised Aggregator to bridge the gap between sources and customers [7].

The role of the Aggregator, also commonly referred as the Flexibility Operator (FO) [7] or Smart Energy Service Provider (SESP) [17], can also be to interact within the wholesale market. Therefore, it is necessary for the Aggregator to be a BRP from a regulatory point of view. Moreover, the activities of a local aggregator are also restricted with respect to the geographical position of the providers of flexibility. As can be seen Figure 2.5, different customers have to be part of the same portfolio for the BRP to utilise their flexibility for its balancing area [7], [17], [20].

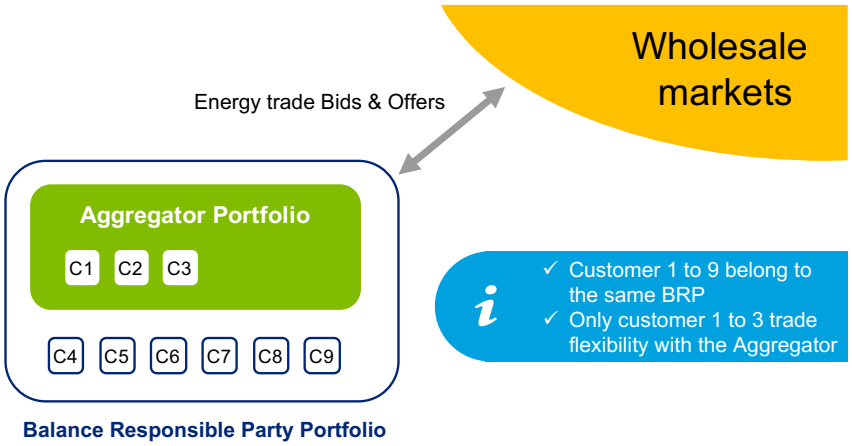

FIGURE 2.5: Aggregator interaction with BRP portfolio and wholesale market [7].

2.3.2 Local Energy Community

While literature widely agrees with the scope of the aggregator, the concept of the LEC is still to be defined consistently. LECs can be organised in different ways, therefore some characteristics and examples are given in the following.

The LEC can be considered a complement to the LFM in order to enhance interaction and contribution of end-users. Their organisation, due to the fact that these are citizen-led, varies from very informal to quite formal [21]. All in common the visionary incentive of sustainable local community. The advantage of proximity allows LECs to be more relatable for the citizen in terms of their potential impact [22]. E.g. an LEC can be a housing association investing in a local roof-top PV plant. Another example is the virtual microgrid, for example the Brooklyn Microgrid [23], which successfully creates financial incentives and business models that encourage community investment in local renewable energy. This local empowerment already has been identified by the European regulatory bodies and incorporated in a proposal for a directive on common rules for the internal electricity market [19]. Eventually, there is a synergy for LEC to be managed by LFMs and to monetise the flexibility sold within the community.

2.4 Flexibility Services and their Customer

The flexibility services have been tailored for three different customers of focus (refer to Figure 2.4); the Prosumer, DSO and BRP. Starting from the existing flexibility sources, which are introduced in Section 2.2, use cases for flexibility services can be conducted. This takes into consideration different flexibility sources which have different characteristics (refer to Table 2.1) and are better suited for specific services.

2.4.1 Prosumer Services

Prosumers' contribution to the LFM is the key element to success and needs to be encouraged and financially incentivised at all times. Its terminology derives from a market participant which is capable of producing and consuming electricity. Ideally, the flexibility provided by different means of sources, such as load, generation or storage, will be dealt by the aggregator in the LFM. The emerging challenge is to utilise the prosumer's flexibility without compromising their level of comfort, which could weaken the prosumer's willingness to participate in the LEC. Four services have been identified within the INVADE project. By nature of prosumer's connection to the grid, only flexibility sources behind-the-meter can contribute to the prosumer services [7], [8].

- **Time-of-Use optimisation** is based on load shifting from high-price intervals to low-price intervals. This requires tariff schemes which favour off-peak consumption.
- **Demand Charge Reduction / kWmax control** is based on reducing the maximum load (peak-shaving), and results in a smaller contracted capacity and thus a cost reduction for the prosumer.
- **Self-balancing** signifies the best usage of production, self-consumption and selling electricity to the grid based on divergence of prices.

- **Controlled islanding** during grid outages to maintain electricity supply behind the meter. Prosumers in this context can be larger buildings, such as hospitals which already have Uninterruptible Power Supply (UPS) devices in place.

2.4.2 Distribution System Operator Services

DSOs are facing an increase of resiliency in the distribution grid and are therefore forced to introduce countermeasures. Historically, the only way would be the fortification of the grid, but with the rise of reliable ICT and Smart Grids such investment can be optimised or completely avoided. The DSO importance within the LFM is twofold, primarily as beneficiary of flexibility, which provides congestion relief and secondarily ensuring the security of the grid with regards to system balancing, portfolio optimisation or transmission constraints management. Its involvement in the different stages of flexibility activation process is therefore necessary. Furthermore, the provision of a security mechanism which gives the DSO the sovereignty to act in the grid to avert security concerns is important. As the Aggregator does not know the grid status, a Traffic Light Concept (TLC) is introduced, which is explained more closely in Annex A. The INVADE project is focused on the following services that the ICT platform can provide to the DSO, and they are:

- **Congestion management** refers to avoiding the thermal overload of system components by reducing peak loads where failure due to overloading may occur.
- **Voltage / Reactive power control** is enacted to use load flexibility as an option to avoid exceeding the voltage limits, which are typically caused by PV systems.
- **Controlled islanding** is to prevent supply interruption in a given grid section when a fault occurs.

2.4.3 Balance Responsible Party Services

While the DSO is mainly facing physical constraints, the BRP's focus is the economic balance of its respective balance area. Imbalances in the grid occur due to forecasting errors of demand or supply. Conventionally, such imbalances, if forecasted properly, are mitigated by trading energy on the intraday market. With the rise of smart grids, it appears to be cheaper to handle these up- and downward imbalances utilising existing flexibility sources. Similarly, to the DSO, the BRP is also interested in knowing upcoming changes in balances caused by flexibility activation and should be involved in the settlement process accordingly. This potential scenario can be avoided by linking the BRP to the Aggregator, much like a supplier. Thus, all the actions of the aggregator lead to a respective change in the portfolio of the BRP without requiring any direct intervention on the markets [7], [8], [18]. Flexibility services to BRPs could be:

- **Day–ahead portfolio optimisation** aims to shift loads from a high-price time-interval to a low-price time interval before the day-ahead market closure. It enables the BRP to reduce its overall electricity purchase costs. This service is used by BRP to prepare day-ahead market bids.
- **Intraday portfolio optimisation** closely resembles day-ahead optimisation, but the time frame is constrained after closing of the day-ahead market. This enables intraday trading; load flexibility can be used to create value on this market, equivalent to the day-ahead market. This service is used by BRP to prepare intraday market bids.
- **Self-balancing portfolio optimisation** is the reduction of imbalance by the BRP within its portfolio to avoid imbalance charges. The BRP does not actively bid on the imbalance market using its load flexibility but uses it within its own portfolio.

2.5 Centralised BESS Flexibility Use Case

The use cases of BESS depend on the location of implementation and the service customer. Literature distinguishes between centralised, such as transmission and distribution grid connected systems and decentralised, so called behind-the-meter connected systems. The more downstream the energy storage system is located, the more services it can provide and consequently the more profitable the system is. On the other hand, bigger centralised systems profit of economy of scale-effects. This is why small residential solutions might not be the most cost effective option and need more than one revenue stream in order to amortise [24].

Within the INVADE project, battery storage systems on different levels have been identified as flexibility, providing value to DSO, BRP and Prosumer. The focus of this work is the application of a centralised solution. For that reason, other flexibilities services are not described hereafter.

As can be seen in Table 2.2, the main profit from a centralised system get DSO and BRP. The high energy capacity combined with the fast versatility to regulate up and down, makes the centralised battery storage highly attractive to almost all use cases. The use case, especially for the BRP has already been already extensively discussed. Malhotra et al. [25] and Battke et al. [26] provide a comprehensive overview of publications defining stationary electricity storage applications, concluding with the most prevailing use cases for batteries. The result is in concordance with Fitzgerald et al. [24], which states, that a cost efficient usage of batteries is only possible when stacking several services on each other. In this context two services are assessed; the intraday portfolio and the self-balancing portfolio optimisation. The day-ahead portfolio optimisation has been ruled out due to a lack of standardised bidding products. Additionally the intraday and balance market are considered more lucrative [26]. This complies as well with the plans of the ambition of the INVADE proposal to implement this business case in a pilot project in Spain, which consists among others of a centralised storage system (refer to Table 2.2). The flexibility services for the DSO are not integrated in this work, though being part of the Spanish pilot project. Again,

the services for the BRP are considered more remunerative, due to prevailing priority in the context of the Traffic Light Concept (refer to Annex A.2).

TABLE 2.2: Added value of centralised storage to different flexibility services, their relevance for the INVADE pilot in Spain and in the context of this work [7], [27].

Flexibility customer	Flexibility service	Use case relevance for centralised storage	INVADE Spanish pilot	Focus of this work
DSO	Congestion management	High	Yes	No
	Voltage/ Reactive power control	High	Yes	No
	Controlled Islanding	High	Yes	No
BRP	Day-ahead portfolio optimisation	Low	to be discussed	No
	Intraday portfolio optimisation	High	Yes	Yes
	Self-balancing portfolio optimisation	High	Yes	Yes
Prosumer	Time-of-Use optimisation	None	No	No
	kWmax control	None	No	No
	Self-balancing	None	No	No
	Controlled-islanding	None	No	No

2.6 Communication between Aggregator, BRP and BESS

Another important assumption in this work relies on the way information is communicated among the LFM participants. The aforementioned LFM structure embraces a centralised communication through the Aggregator which ensures a marketwise control of the available flexibility (refer to Figure 2.6). In

this context, it is reminded that the DSO only possess priority if the grid state is in amber state (refer to Appendix A.2). Within this work the DSO is neglected, and the amber state will not occur.

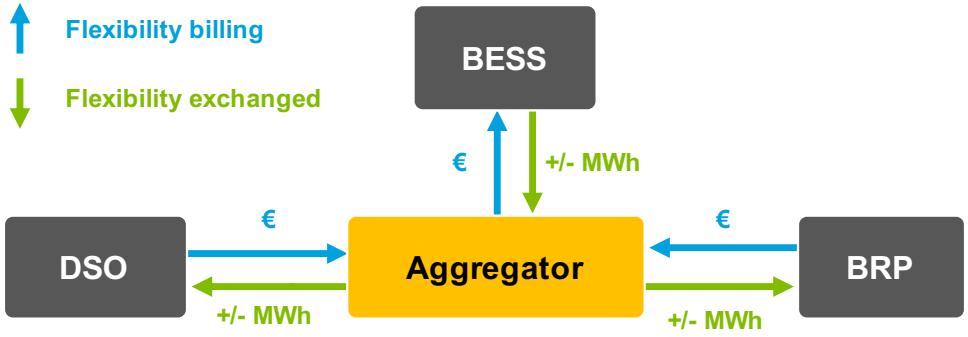

FIGURE 2.6: Interaction between aggregator, DSO, BRP and the BESS.

A flexibility framework includes flexibility dispatch processes for each participant role, which can be divided in plan, validate, operate and settle.

In this project the information sovereignty is ensured by BRP and Aggregator being one integrated entity. This way the BRP is not exposed to the risk that the Aggregator will optimise against the BRP's portfolio. However, this is a general problem the LFM faces. Every time the Aggregator reschedules loads without the consent of the BRP, the BRP needs to correct its forecast. This problem intensifies with a larger penetration of flexibility interacting in the LFM. The INVADE project proposes a baseline, which represents agreed consumption and generation transparently communicated to all market participants, when doing the settlement [7]. This baseline is calculated by the Aggregator and is accepted by DSO and BRP. In future this task should be done by a purposely created entity. This is, due to current regulatory framework, not possible.

Another communication process, which has been simplified in this project, is the exchange of information about the physical condition of the battery. A respective process could be as follows:

1. BRP calculates an approximate flexibility need based on forecasted imbalances and the market prices of imbalances, day-ahead and intraday, and provides first assumption of the battery cost.
2. This information is handed through to the prosumer and its battery. Based on the prosumer's personal need and the calculated degradation the proposed price will be either confirmed or updated and sent back to the BRP.
3. The BRP can accept the new calculated price and continue to schedule the loads. In case the new price does not comply with the BRP's interest, the process starts again from 1. This process iteratively will achieve a settlement.

Again, perfect information is assumed, which means that the BRP knows the current state of the battery and all necessary parameters to calculate the cost. In this context, the importance of degradation is

shown. In case the BESS is used for another service, the cycle-based degradation is one of the main cost drivers, and if neglected the BESS owner needs to replace the degraded battery at an early stage at their own expense.

Chapter 3

Battery Energy Storage Systems for Stationary Application

The ability to of storing energy temporarily in order to mitigate imbalances caused by daily and seasonal fluctuations in demand has been around since 1930, when the first reversible pumped hydroelectric energy storage (PHES) was installed in the USA [28]. Ever since then, the importance of energy storage as part of the power network has increased and reached an installed power capacity of more than 170 GW world-wide by 2017 [29]. Despite the fact, that PHES represents with more than 95 percent the biggest stake in the energy storage market, electrochemical battery storage systems are on the rise. Although it is unlikely, that batteries will outstrip the dominance of PHES in near future, their high modularity, low cost and wide range of application play a crucial role. This urge for more energy storage origins of the fast proceeding implementation of volatile renewable energy sources, which provoke more resiliency and therefore imbalances in the power system [30]. The resulting deviations are causing an increasing financial incentive for battery storage to be used [25].

Stationary electrical energy technologies are ranging widely in size and application. Therefore, it is advisable to follow common criteria to classify storage systems according to the nature of the energy conversion process, such as electro-mechanical, electro-magnetic and electro-chemical, and the timescale of response of the storage systems [31]. Figure 3.1 graphically depicts the storage classification presented above [25].

The field of electrochemical electrical energy storage covers a wide range of technologies with different performances and fields of application. However, in focus of this work are Lithium-Ion (Li-Ion) based secondary batteries for stationary use cases. With their significant drop in price per usable cycle, they have been become the most popular energy storage technology in mobile and stationary applications [24]. Lead-acid batteries have been used for many years in these applications and are technically well suited, although they have been rapidly replaced by Li-Ion batteries in many markets due to their superior performance. Another upcoming and promising technology is the Redox-flow battery, which is good for community storage solutions and large village electrification. Since the focus of this work will be on electro-chemical Li-Ion battery storage systems, further classification for reasons of comparison is

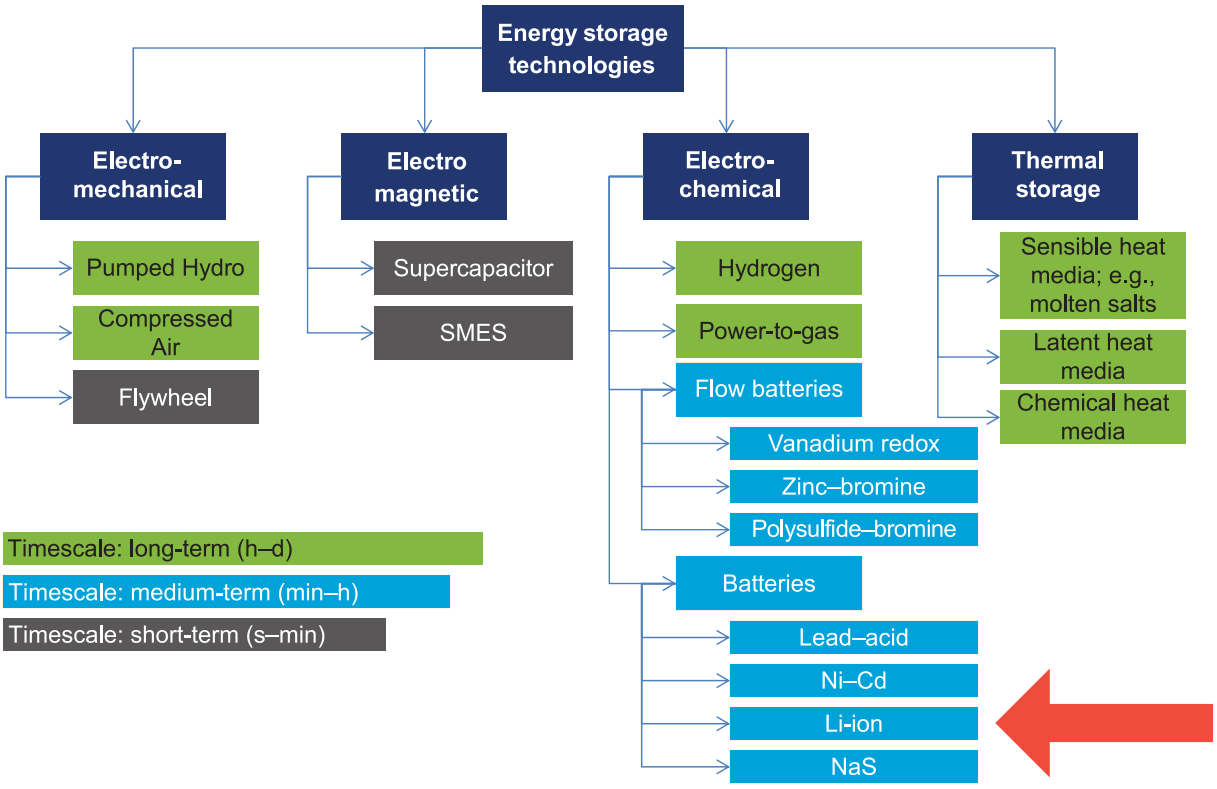

FIGURE 3.1: Energy storage technologies [31].

needed due to differences of performance and degradation mechanism within the sub-types of Li-Ion systems [32]. In the following chapters, an overview on different Li-Ion technologies and their respective application use cases and costs are presented.

3.1 BESS Application

The use cases of energy storage have been profoundly researched already. These differ mainly in terminology and their boundary definition. References [24], [31]–[33], are aiming to classify the services. An overlap resulting in 16 defined services divided in up to four categories is presented in Figure 3.2. The services depend on the level of implementation, whether the BESS is centralised and connected on transmission or distribution level or decentralised and integrated behind the meter. Thus, the business case and the primary service has a high impact on the choice of energy storage technology, as the duty cycles and required cycle life are heavily affected. Hence, the choice of technology must be considered case by case. As already mentioned in Section 2.5, the use case of this work will focus on a centralised approach on a distribution level [34].

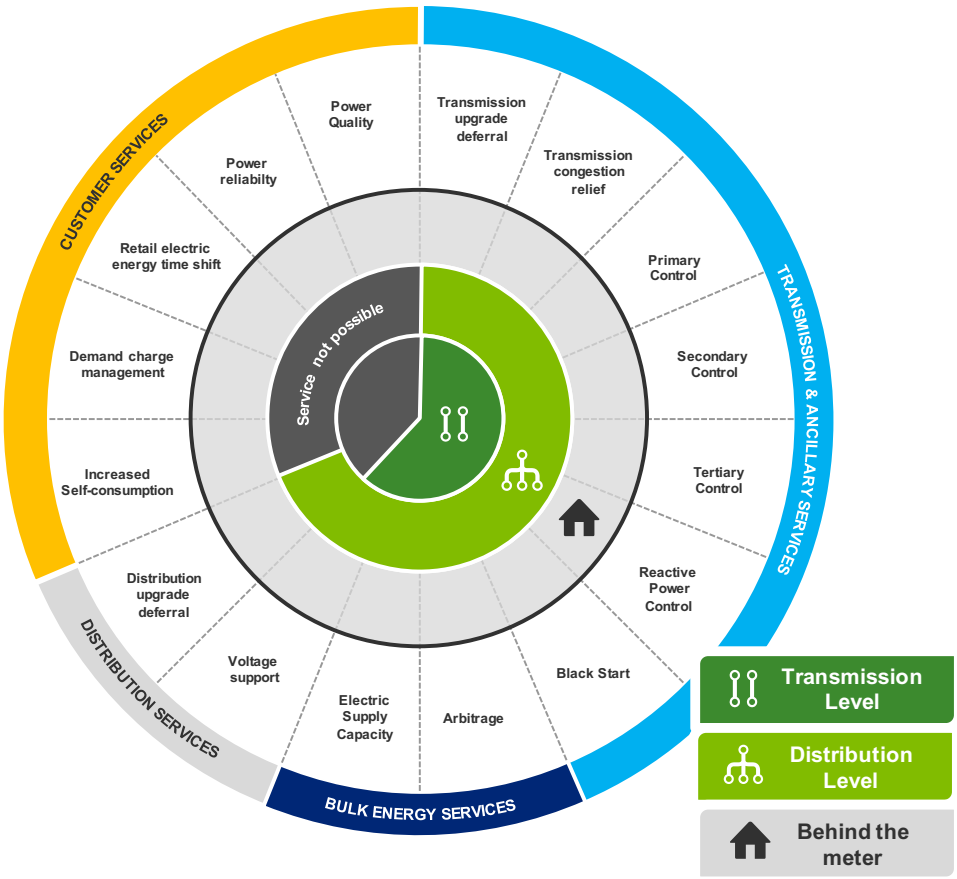

FIGURE 3.2: Services provided by energy storage [24], [31]–[33].

3.2 Lithium-based Batteries

"A battery energy storage system (BESS) converts electrical energy into potential chemical energy while charging and releases electrical energy from chemical energy while discharging. In general terms, it is based on reduction and oxidation reactions (commonly called redox reactions)" [31].

Li-Ion Batteries (LiB) implement this behaviour, by providing active material in the cathode (positive electrode), which is usually a Lithium metal oxide, such as lithium cobalate ($LiCoO_2$) and a negative electrode, which is made of carbon. The Li-Ion act as internal charge carrier flowing in reverse to the external flow of electrons in the applied circuit. Typically, the electrolyte is an organic solution containing lithium-based dissolved salts, which offers good Li-Ion transport properties. Eventually, a separator is an insulator embedded in between the electrodes, protects from an electrical short circuit, and allows ions to flow from one electrode to the other [34]. The oxidation and reduction processes taking place at the respective electrodes are as follows [31]:

$$\mathrm{Li(C)} \rightleftharpoons \mathrm{Li^+ + e^-} \tag{3.1}$$

$$\mathrm{Li^+ + e^- + CoO_2} \rightleftharpoons \mathrm{LiCoO_2} \tag{3.2}$$

$$\mathrm{Li(C) + CoO_2} \rightleftharpoons \mathrm{LiCoO_2} \tag{3.3}$$

A schematic of an Li-Ion battery is shown in Figure 3.3.

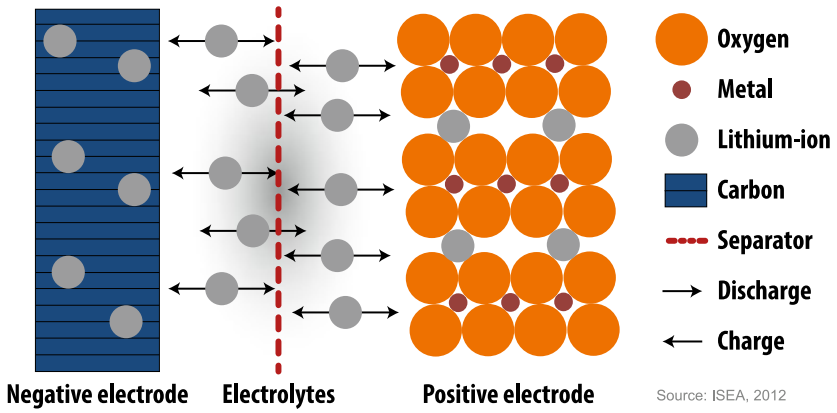

FIGURE 3.3: Operating principle of a lithium-based cell [32].

3.2.1 Different Electrode Compositions and their Characteristics

Active anode and cathode material composition and characteristics dictate the capacity and open-circuit voltage (OCV) of a battery, and thus, they also determine the baseline for the energy density and inherent safety features. Historically different sub-types of Li-Ion batteries have been developed. The following sub-types can be mentioned as commercialised. It should be noted that current research is investigating many more technologies, such as Lithium Sulphur, Solid-state Li-Ion or Lithium Air, though these are not yet considered as technologically ready [32].

- **Nickel Manganese Cobalt Oxide (NMC)** is one of the most successful Li-Ion systems. It uses a cathode combination of nickel-manganese-cobalt (NMC). These systems can be tailored to serve as energy or power cells. NMC is the battery of choice for power tools, e-bikes and other electric powertrains. The cathode combination is typically one-third nickel, one-third manganese and one-third cobalt, also known as 1-1-1. Battery manufacturers move away from cobalt systems toward nickel cathodes because of the high cost of cobalt. Nickel-based systems have higher energy density, lower cost, and longer cycle life than the cobalt-based cells but they have a slightly lower voltage. There is a move towards NMC-blended Li-Ion as the system can be built economically and achieves a good performance. The three active materials of nickel, manganese and cobalt can easily be blended to suit a wide range of applications for automotive and energy storage systems

(EES) that need frequent cycling [35]. Tesla, as an important player in the EVs and BESS sector uses NMC exclusively for stationary, residential and industrial applications.

- **Lithium Manganese Oxide (LMO)** cells have high power capabilities and have the advantage of relying on manganese, which is about five times less expensive than cobalt. LMO cells, however, have a lower energy performance and only moderate life cycle properties. These disadvantages may have an impact on the attractiveness for stationary applications, and the BES systems in this segment often apply a blend of NMC and LMO cells [32].
- **Lithium Nickel Cobalt Aluminium Oxide (NCA)** cells have high energy and power densities, as well as good life span, which make NCA a candidate for EV powertrains. The relatively high power and energy density comes with a higher price, therefore NCA has not been used in residential applications. Electrochemical and thermal stability properties, have led to the rise of NCA battery chemistries and their increased use in the mobility market, e.g. notably in Tesla EVs [32].
- **Lithium Iron Phosphate (LFP)** offers good electrochemical performance with low resistance. This is made possible with nano-scale phosphate cathode material. The key benefits are a high current rating and a long cycle life, besides good thermal stability, enhanced safety and tolerance if used intensively. LFP has a higher self-discharge than other Li-Ion batteries, which can cause balancing issues with ageing. This can be mitigated by using sophisticated single-cell management systems which increases the cost [35].
- **Li-Ion Titanate (LTO)** batteries have not been extensively commercialised due to their comparatively high cost, but some are being used today for self-consumption. LTO replaces the graphite in the anode of a typical lithium-ion battery and the material forms into a spinel structure. The cathode can be lithium manganese oxide or NMC. LTO can be fast charged and delivers a high discharge current of 10 C, or 10 times the rated capacity. LTO excels in safety, low-temperature performance and life span. Efforts are being made to improve the specific energy and to lower the cost [35].

In the Table 3.1 the most important parameters of the aforementioned chemistries are summarised. In Appendix B the respective advantages and disadvantages of each chemistry are summarised.

3.2.2 Energy Capacity

Depending on the desired performance characteristics, the battery cell can be optimised for either energy or power application. In any case the energy capacity is one of the key parameters and it usually defined in kWh. Especially in grid application, the real usable capacity differs from the installed capacity, due to state of charge (SoC) constraints and real-life conditions, such as temperature and high charging and discharge ranges (C-Rate) which lead to deviation from nominal parameters. The SoC is commonly constrained in order to avoid critical operation states, e.g. deep discharge, and thus increase the lifetime.

TABLE 3.1: Different Li-Ion battery chemistries and their characteristics.

Technology	NMC	LMO	NCA	LFP	LTO
Cathode	$LiNi_xMn_yCo_{1-x-y}O_2$	$LiMn_2O_4$ (spinel)	$LiNiCoAlO_2$	$LiFePO_4$	variable
Anode	C (graphite)	C (graphite)	C (graphite)	C (graphite)	$Li_4Ti_5O_{12}$
Specific Energy (Wh/kg) [36]	140-180	105-120	80-220	80-130	70
Energy Density (Wh/L)[36]	325	250-265	210-600	220-250	130
Specific Power (W/kg) [36]	500	1000	1500-1900	1400-2400	750
Power Density (W/L) [36]	3000	2000	4000-5000	4500	1400
Cycle life (equivalent full cycles at 100 % DoD) [32]	2000	2000	1000	2500	10000
Efficiency (%) [32]	95	95	95	92	96
Energy installation cost (EUR/kWh) [32]	420	420	352	578	1050
Monthly Self Discharge	< 5 % [37]	< 5 % [37]	< 5 % [37]	< 3 % [37]	2 - 10 % [36]
Maximum rate of discharge [37]	5 C cont. / 30 C peak	10 C cont. / 40 C peak	1C cont.	35 C cont. / 125 C peak	not available

With increasing temperatures and decreasing C-rates the energy capacity is increasing and vice versa [34].

In order to keep the battery in a safe and stable state of operation, the SoC constraint of the battery in the context of this work has been defined to a minimum of 15 % and a maximum of 95 % of SoC. This will ensure validity of the deterministic model [38].

3.2.3 Power Rating and C-Rate

In describing batteries, discharge current (and power) is often expressed as a C-rate in order to normalise against battery capacity, which is often very different between batteries. A C-rate is a measure of the rate at which a battery is discharged relative to its maximum capacity. A 1C rate means that the discharge current will discharge the entire battery in 1 hour. For a battery with a capacity of 100 kWh, this equates to a discharge current of 100 kW. A 5 C rate for this battery would be 500 kW, and a C/2 rate would be 50 kW. Similarly, an E-rate describes the discharge power. An E-rate of 1 is the equivalent discharge power to discharge the entire battery in 1 hour.

It needs to be noted, that a BESS is on the one hand limited to its C-Rate which is determined by the cell chemistry, but on the other hand by the Balance-of-System (BOS) components such as the inverter. In this context the terms C-rate and power/energy (P/E) ratio are used interchangeably. Especially in large grid-scale projects, the limiting factor is not the C-Rate of the individual cells but rather the rated power of the inverter converting the DC-flux into AC. Thus, the power rating is an important design criterion and highly depends on the application of the respective BESS. For example, BESS for frequency regulation typically provides a Power-to-Energy-Ratio (P/E-Ratio) of more than 2, while BESS for arbitrage typically have 0.5. The use case of this work experiments with P/E-ratios between 1 and 2 [34], [38].

Moreover, the maximum charging and discharging is not considered to be constant in high and low SoC respectively. Therefore, the charging and discharging is reduced in the model accordingly in order to reflect this behaviour in the deterministic model.

3.2.4 Efficiency

When determining the energy efficiency of a storage system, one must take into account also the losses that occur in the power electronic converters and grid interface. The efficiency of the power electronic converters depends on the operating point. However, a constant efficiency will be used. The use of constant efficiency is expected to cause only a small modelling error in most cases [34].

3.2.5 Self-Discharge

Self-discharge is not taken into account in the model, because Li-Ion batteries have very low rates of only a few percent in a month (see Table 3.1) [34].

3.3 Battery Economics

Due to the huge diversity of characteristics of Li-Ion Batteries in regards to their dimension and application, the business models developed around BESS are numerous [24]. Nonetheless, the associated cost blocks, though sometimes named differently in literature, are the same. In the following, the for this project relevant costs are introduced.

3.3.1 Current Trends

Due to the significant increase of demand in LiB in the last decade, the investment in Li-Ion production facilities is booming and expected to grow quick enough, to be able to satisfy the demand by the energy and transportation industries. LiB is expected to be a key technology, not only in the stationary application, but also in the car industry, which is picking up pace by implementing high performance LiB in EVs.

In this context it is expected that with rising demand, the cost of production of Li-Ion will undergo a learning curve caused by economics of scale and improvement in production. Nykvist et al. [39] describes this phenomenon and puts expected price developments of industry and research in comparison, concluding that a consistent price below USD 300 per kWh will boost the application of LiB. Moreover, it is predicted that, if costs reach as low as USD 150 per kWh it will initiate a fundamental paradigm shift in the transportation sector. These results from 2015 have been recently confirmed in their trend by the International Renewable Energy Agency (IRENA) [32]. IRENA is predicting a significant decrease of installation cost. It is also expecting a prolonged calendar and cycle life of LiB systems (refer to Appendix B.1).

This increase will inevitably result in a compelling market share of LiB in all kinds of energy storage applications. In the context of this work, this exemplifies the urgency for an appropriate financial assessment of all involved costs, explicitly including the degradation cost.

3.3.2 Cost Breakdown of BESS

Project related costs are commonly divided in Capital Expenditures (CAPEX) and Operational Expenditures (OPEX). In the context of BESS, the investment is split up as follows (refer to Figure 3.4):

- **Battery packs** consisting of the individual battery cells. The battery packs usually already implement a Battery Management System (BMS) which controls the appropriate charge and discharge control of the respective chemistry. All combined they make up the Energy Storage Unit (ESU).
- **Inverter** as the main component of the Power Conversion Unit (PCU), which is responsible for the AC/DC conversion and thus connects the ESU with the application.
- **Periphery** accounts for housing or containerisation, air conditioning and other supportive devices which do not directly belong to ESU or PCU. Commonly, these expenses are referred to the Balance of System (BOS).
- **Soft cost & EPC** correspond to the installation, such as cost emerging from engineering, procurement and construction (EPC), administration and legal work.

The proportions of the respective blocks depend on the size and use case of the system. E.g. the installation and inverter cost of a home storage is proportionally smaller than for a centralised grid-scale solution [40].

The OPEX break into the following matter of expenses (refer to Figure 3.4):

- **Electricity cost** is the inevitable cost of the energy consumed by the BESS.
- **Replacement / degradation cost** represent an important cost - though commonly simplified or neglected [41] - due to capacity reduction inherent with each charging cycle of the BESS. When reaching the technological end-of-life, the asset needs to be replaced, thus replacement costs occur. The replacement cost is not necessarily a cashflow, however it needs to be considered for the calculation of the Levelized Cost of Storage (LCOS).
- **Operation and Management** is usually negligible in small-scale solution. However, in large-scale application this accounts for the temperature control, and maintenance cycles in which the battery cannot be used other wise.
- **Self-discharge and efficiency losses** are occasionally considered and directly relate to the electricity cost and the technological performance of the BESS.

Similar to other energy resources the operation cost correlates positively with the usage of the BESS. While electricity costs can be expressed in linear relationship, the replacement costs of the BESS follow a highly non-linear relationship, as the degradation is highly complex to model due to the intricate battery electrochemistry. Nevertheless, this relationship is further explored in the next chapter.

For the sake of consistency, Figure 3.4 also shows the revenues, generated by the BESS, which can consist of one or multiple opportunity costs of different use cases. Current BESS applications are only remunerative as a result of stacking several revenue streams together and thus exceed the total cost caused by CAPEX and OPEX. In this regard the concepts of Levelized Cost of Storage (LCOS) and Cost of Service (COS) are commonly used [24], [32].

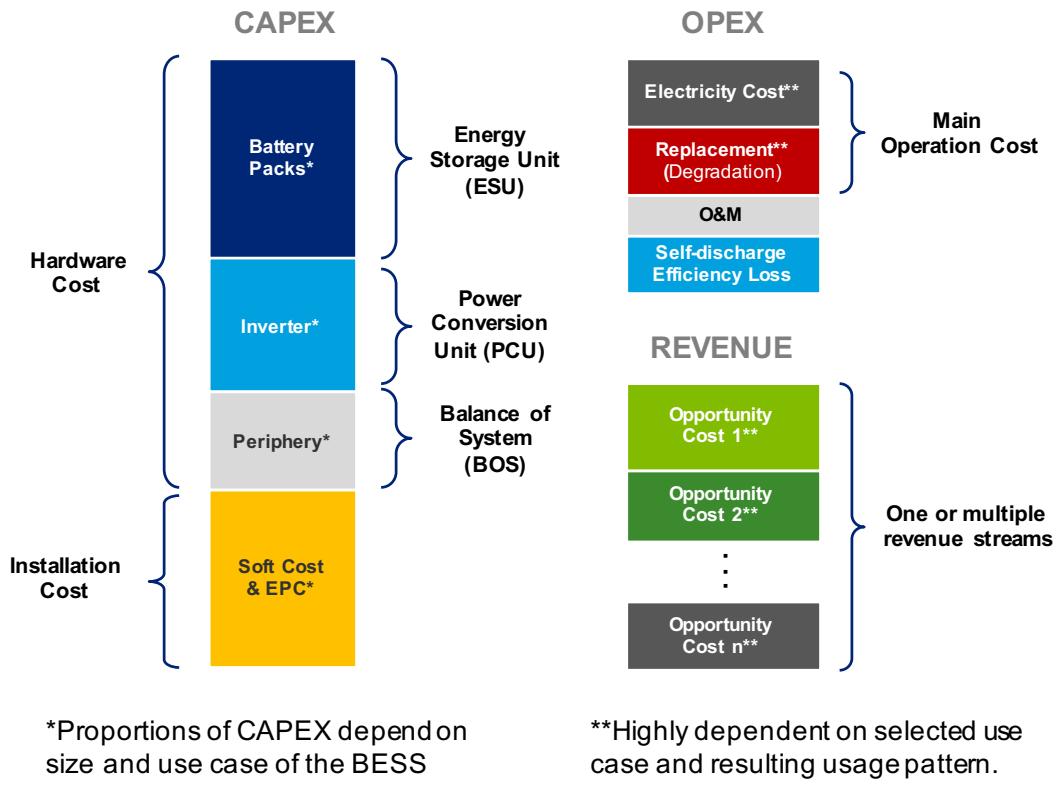

FIGURE 3.4: Cost breakdown of a BESS.

3.3.3 Economic Assessment Methodology

The use case described within this project focusses on the optimisation of usage for a time horizon of a couple of days. Even though operational profits might be recorded, it is not necessarily assured that the use case is profitable from a project point of view. Therefore, it is indispensable, to introduce metrics to validate the profitability of the use case as a whole. Moreover, the techno-economic feasibility of the project is exposed to technology related aspects, such as capital costs, energy efficiency, life expectance, but also to factors related to final application such as electricity price, opportunity costs and usage.

Especially in the context of batteries, the LCOS is commonly used. It defines operational parameters associated with systems designed for each of the most prevalent use cases of storage [42]. It is given in money per energy delivered (commonly €/kWh) and represents minimum remuneration needed to exceed the break-even point and become profitable. This measure is inevitable for the holistic economic assessment and therefore it will be used within this work besides conventional project Key Performance Indicators (KPIs) such as Net Present Value (NPV) and Internal Rate of Return (IRR).

The economic, project-related, together with the technology-related parameters to calculate these measures are introduced in the preface of this work. The power capacity installed capacity and performance

characteristics, such as cyclability and roundtrip efficiency are design choices and are of course depended on the use case. It is expected, that the performance parameters are provided by the manufacturer.

As aforementioned, the operating cost are sensitive to the use case and rely on the output of the model. The challenge of moulding the dynamic short-term assessment of up to two days into a holistic project assessment with a time horizon of 10 years, certain assumptions are made and by the means of a sensitivity analysis further assessed.

To extrapolate the output values of the algorithm to a yearly basis the factor α is calculated:

$$\alpha = \frac{d_{op} \cdot [\text{hours/day}]}{T_{optim}} \tag{3.4}$$

The total investment I_t^{CAPEX} [€/year] costs are calculated as follows:

$$I_t^{CAPEX} = P \cdot c_p + E_{installed} \cdot (c_e + c_{other}) \tag{3.5}$$

Usually the investment is allotted only in year $t = 0$. However, since the life expectancy of the BESS $T_{expected}$ can be smaller than the project horizon $T_{project}$, reinvestments after $T_{expected}$ years are expected to keep the system performance constant until the end of the project horizon. Dependent on the size of the BESS the replacement cost can be related to the BESS as a whole or only to the ESU, which is considered to be affected the most by degradation.

The total operational costs per year C_t^{OPEX} [€/year] divide in fixed operation and management, variable electricity, degradation cost, and salvage costs related to the disposal of the BESS. In this context the replacement cost is only considered if the LCOS is calculated, since the replacement cost does not account for a physical cashflow:

$$C_t^{OPEX} = C_t^{O\&M} + C_t^{ELEC} + C_t^{R} + C_T^{SALVAGE} \tag{3.6}$$

With its elements defined as follows:

$$C_t^{O\&M} = c_f \cdot E_{installed} \cdot (1 + i_{inflation})^t \tag{3.7}$$

$$C_t^{ELEC} = c_{elec} \cdot E_{charged}^{TOTAL} \cdot \alpha \cdot (1 + i_{elec})^t \tag{3.8}$$

$$C_t^{R} = c_r \cdot \alpha \cdot L_{degr} \tag{3.9}$$

In contrast to the other cost, the salvage cost $C_T^{SALVAGE}$ is only accounted in the last year of the project. In case the BESS still has a remaining value, it is considered as income. However, if the remaining market value is too little to sell the system, it's neglected. For simplicity, the remaining book value has been assumed.

It has been assumed, that the charging is the main cause of electricity cost, while the discharging cost is responsible for providing the service. The values for $E_{charged}^{TOTAL}$ and $E_{discharged}^{TOTAL}$ are obtained by the optimisation algorithm, and they are already considering the actual usable energy storage capacity E_{usable}.

In the context of this project only one revenue stream is considered, therefore the revenue per year $R_t^{Project}$ [€/year] can be written as:

$$R_t^{Project} = E_{discharged}^{TOTAL} \cdot \alpha \cdot c_{opport} \cdot (1 + i_{opport})^t \tag{3.10}$$

Consequently, the Earnings Before Savings Interest and Tax Depreciation and Amortisation (EBITDA$_t$) for every year can be calculated.

$$\text{EBITDA}_t = R_t^{Project} - I_t^{CAPEX} - C_t^{OPEX} \tag{3.11}$$

Linear depreciation is assumed. The depreciation time is assumed to be no longer than 5 years or the expected lifetime of the battery. In case the expected lifetime is less than the depreciation time $T_{expected} < T_{deprec}$, the depreciation time equals the expected life time $T_{deprec} = T_{expected}$.

$$I_t^{depreciation} = \frac{I_t^{CAPEX}}{T_{deprec}} \text{ for } \sum_{t=0}^{t} I_t^{CAPEX} > I_t^{depreciation} \tag{3.12}$$

This is valid, as long the total investment has not been depreciated. The EBITDA$_t$, the earnings including depreciation deductions, result as follows:

$$\text{EBITA}_t = \text{EBITDA}_t - I_t^{depreciation} \tag{3.13}$$

The EBITDA$_t$ is only used to calculate the applicable tax saving imposed by the depreciation.

$$\text{TAX}_t = \text{EBITA}_t \cdot i_{tax} \tag{3.14}$$

Therefore, in case the TAX$_t$ is negative, it is not being added to the cash flow, assuming that the company, which is conducting the project won't be able to deduct all the taxes. The final cash flow CF_t of each year t is obtained by subtracting the calculated total taxes from the EBITDA$_t$.

$$CF_t = \text{EBITDA}_t - \text{TAX}_t \tag{3.15}$$

The net present value, inflation-adjusted and after tax, is calculated as follows:

$$\text{NPV} = \sum_{t=0}^{T_{project}} \frac{CF_t}{(1+t)^t} \tag{3.16}$$

The internal rate of return of the project is obtained, when setting the NPV equal, and solving for i. It is given in [%].

$$0 = \sum_{t=0}^{T_{project}} \frac{CF_t}{(1+\text{IRR})^t} \tag{3.17}$$

The LCOS gives more clarification about the actual operational cost and what value has to be obtained in minimum to make the project commercially valuable. It is important to mention that the LCOS does not represent the income through the analysed. The LCOS is the constant, thus levelized price per kWh at which the net present value of the BESS project is zero.

$$\text{LCOS} = \frac{I_t^{CAPEX} + \left(C_t^{OPEX} \cdot \sum_{t=1}^{T_{bat}} \frac{1}{(1+r)^n}\right) - \left(\frac{C_T^{SALVAGE}}{(1+r)^{N+1}}\right)}{D_{cycles}/T_{bat} \cdot E_{usable} \cdot \sum_{t=1}^{T_{project}} \frac{(1-DEG \cdot t)}{(1+r)^n}} + \frac{c_{elec}}{\mu} \tag{3.18}$$

The nominator of equation 3.18 represents the NPV with; the investment cost in $t = 0$, the discounted operating expenses and the deducted salvage value. The last term considers the energy lost due to inefficiencies. The denominator calculates the discounted total usable energy over the project horizon considering the maximum possible cycles per year guaranteed by the manufacturer $D_{cycles}/T_{expected}$, the total usable capacity E_{usable} and the yearly discount factor together with the yearly expected degradation factor DEG in percent. The degradation is obtained as follows:

$$DEG[\%] = \frac{D_{cycles}}{T_{expected} \cdot D_{cycles}} \cdot (100\,\% - D_{EoL}) \tag{3.19}$$

An alternative way to calculate the LCOS would be simply the discounted cashflows divided by the total discounted discharged energy. Although a bit counterintuitive, it is important to "discount" also the usable energy (electricity discharged), as can be seen in the derivation of the LCOS formula 3.20:

$$\text{LCOS} = \frac{\sum_{t=0}^{T_{project}} \frac{CF_t}{(1+t)^t}}{\sum_{t=0}^{T_{project}} \frac{E_{discharged}^{TOTAL} \cdot \alpha}{(1+t)^t}} \tag{3.20}$$

Note, that in contrast to NPV and IRR, the LCOS does not provide any significance whether a project is cost competitive and profitable. It solely generates estimates of the installed cost over the indicated

TABLE 3.2: Project parameter depended on the use case, centralised vs decentralised. Values from [32].

Symbol	Unit	Decentralised BESS $<$ 30 kWh	Centralised BESS $<$ 1 MWh
P/E	kW/kWh	0.5	1
c_p	€/kW	200	400
c_{other}	€/kWh	not available	300
c_f	€/kW/yr	not available	10
c_r	€	I_{total}^{CAPEX}	$E_{ESU} = E_{installed} \cdot c_e$

project life required to achieve certain levelized returns for various technologies, designed for a series of identified use cases.

3.3.4 Battery Parameter

As for the battery energy storage system, the cost break-down differs and depends on the size and the chemistry used. In the INVADE project, two kind of use cases for stationary storage are identified, centralised and decentralised. For simplicity two kinds of cost structured have been assumed; smaller than 30 kWh with a P/E-ratio of around 0.5 for the household application and smaller than 1 MWh with a P/E-ratio of 1, for the application on a grid level. Lithium-based energy storage projects bigger than 1 MWh are out of scope in the INVADE project, since these are usually conducted on transmission level and the TSO is not a identified customer in the INVADE project [7]. Table 3.2 shows the project parameters for the centralised and decentralised approach.

Various Lithium-chemistries are performing differently, due to dissimilarities in expected lifetime and cycle life. A comparison of current values is presented in Table 3.3.

TABLE 3.3: Algorithm input in dependency on the BESS chemistry used in the project. Values from [32].

Symbol	Unit	LFP	LTO	NCA	NMC/LMO
c_e	€/kWh	578	1050	352	420
D_{cycles}	number of cycles	3600	15000	500	3000
D_{DoD}	%	100	100	100	100
D_{EoL}	%	80	80	80	80
T_{Bat}	years	12	15	12	12
μ	%	92	96	95	92
DoD	%	90	95	90	90
E_{usable}	%	82.8	91.2	85.5	82.8

Chapter 4

Li-Ion Battery Degradation

Eventually, important degradation mechanisms caused by the process of charging and discharging are highlighted. Despite the importance of battery storage, the literature lacks consensus on how to model the cost of operation appropriately and efficiently. A simplification of a model has been described aiming for the compromise of modelling the degradation cost of the battery correctly, while keeping the computational resources needed quite low. This ensures an application of the algorithm for market clearing processes while maintaining accuracy. The novelty of this innovative approach will contribute to the holistic assessment of the business case in this work [43].

This chapter is structured as follows. Firstly, the importance of the battery degradation model and all involved parameters are presented. Next, a reliable operational regime is presented, which aims to simplify the modelling and reduces potentially harmful operation conditions and thus increases the validity of the algorithm. Section 4.2 and 4.3 introduce stress factors related to calendar and cyclic ageing, respectively. These parameter result in the description of the State of Health in Section 4.4. Section 4.5 is introducing the Rainflow algorithm for cycle counting in battery fatigue, followed by a literature review on degradation models in general. Eventually, a linearisation approach to obtain a marginal degradation cost function to be used in optimisation algorithm is explained.

4.1 Importance of Degradation Modelling

Electrochemical batteries are complex devices which operation and degradation are dominated by high degree of non-linearity and interdependency of parameters. The limited cycle life of batteries origins mainly from the fading of active materials caused by the charging and discharging cycles. This cycle aging is caused by the growth of cracks in the active materials, a process similar to fatigue in materials subjected to cyclic mechanical loading. Birkl et al. [44] breaks down operation-related parameters and connects these to degradation mechanism and eventually clusters them into loss of lithium inventory, active anode material and active cathode material (refer to Figure 4.1).

Current battery degradation models can be classified into theoretical models and empirical models. Current theoretical degradation studies [45], [46] usually focus only on the most dominant mechanisms, such as the formation and growth of the solid electrolyte interphase (SEI). Though receiving good results under limited conditions, these models are unsuitable to be used for operation planning of BESS [47]. On the other hand empirical models are bridging the gap between being considerable precise and easier to implement on an operational level, in which the operating regime is narrow and favours simplified modelling strategies [48]–[50].

In the context of this work, an empirical approach has been chosen. In line with literature, the project group INVADE has identified the following battery degradation mechanism as relevant in order to achieve a high accuracy of the battery algorithm.

- **Non-Operational/calendar ageing factors:** ambient temperature, battery state of life, calendar time [50]–[52].
- **Operational/cycle ageing factors:** Cycle depth, over charge, over discharge, current rate, and average SoC [45], [50], [52].

Two means of coping with degradation factors have been considered; on the one hand the appropriate modelling using state of the art empiric description and on the other hand the limitation of operation to a better controllable environment to ensure a reliable operating area. The respective measures are explained in the following.

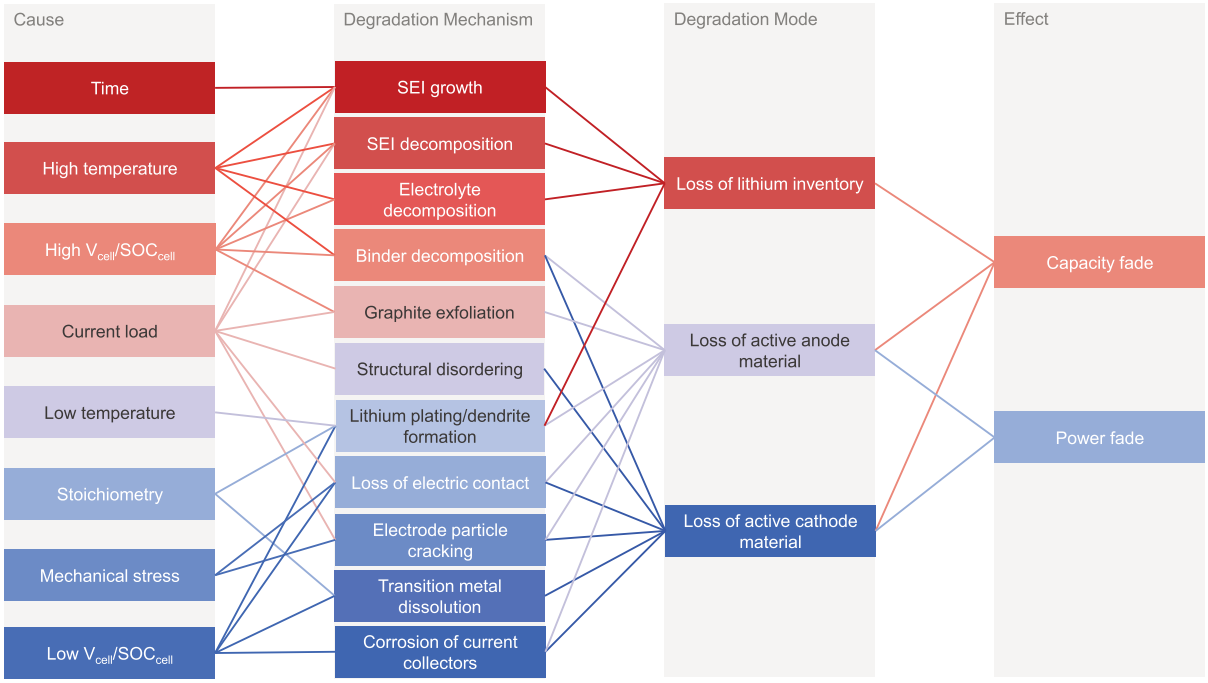

FIGURE 4.1: Cause and effect of degradation mechanisms and associated degradation modes [44].

4.2 Calendar Aging

Calendar aging refers to degradation, which will occur regardless of the operation strategy chosen. It depends on the cell temperature and the average SoC of the battery and the elapsed time in comparison to the estimated lifetime, which is guaranteed by the manufacturer.

4.2.1 Battery Cell Temperature

Usually the calendar aging is not the limiting factor in the lifetime of a battery, however the temperature influence can be considered the most important non-operational degradation factor, as can be seen in Figure 4.2.

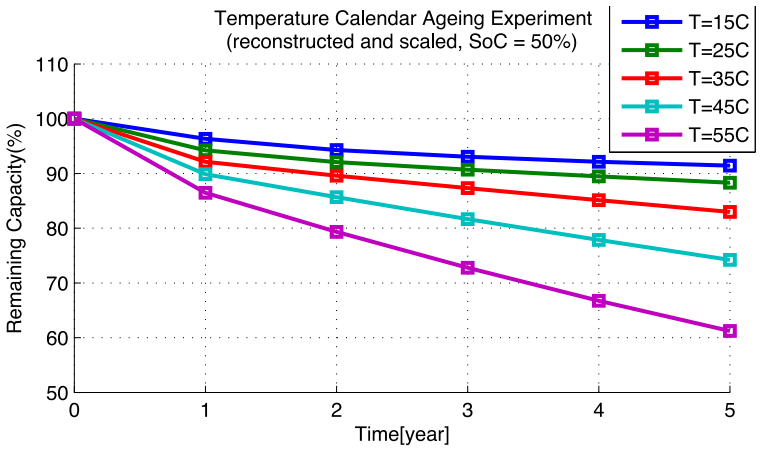

FIGURE 4.2: Calendar aging as a function of varying temperature [52].

Hereby, two extrema can be distinguished; charging in low temperature leads to decomposition of the anode, while at high temperature the solid electrolyte interface (SEI) will breakdown if cell operating temperatures exceed 90 °C [34].

An empirical stress model, following the Arrhenius equation for temperature is described by Xu [52]. In this work however, the temperature induced stress is not considered, due to missing temperature data from the batteries used in the INVADE pilot projects. In the case of the centralised battery, it will be assumed that certain measures to maintain the battery optimal operating temperature are implemented.

4.2.2 State of Charge

Studies by M. Ecker et al. [53] on calendar ageing parameters have shown that the average state of charge plays a considerable role, as well. As can be seen in Figure 4.3, the capacity fade is more pronounced for cells cycled at different cycle depths around an average SoC of 50 %. Cells that performed 100 % cycles

showed the fastest degradation. Millner et al. [49] proposes a stress model, which penalizes operation with big difference to a chosen reference SoC condition.

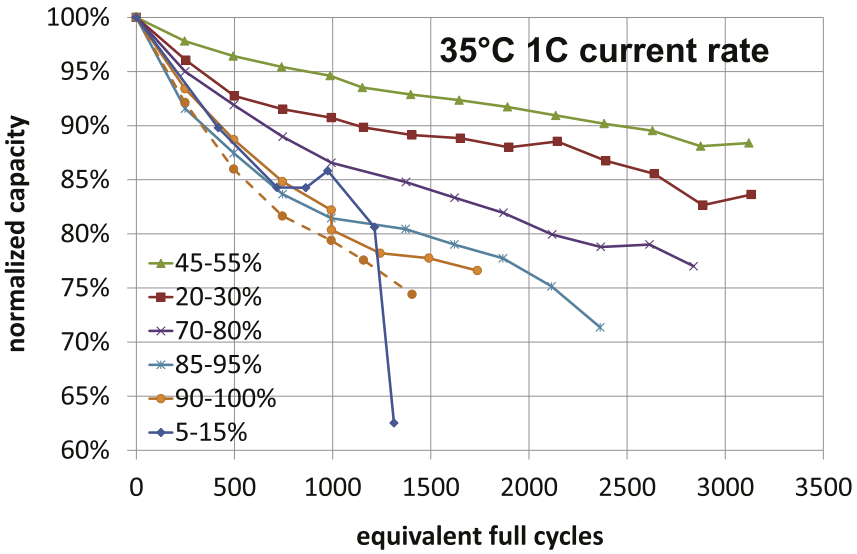

FIGURE 4.3: Calendar ageing as a function of the average SOC [53].

Within this work this degradation stress factor has been taken into consideration in two different ways; firstly, by imposing an average SoC band between 40 to 60 percent over the time horizon of the project and secondly, by limiting the upper SoC to 95 %.

4.2.3 Time Degradation

The useable energy capacity is impacted by the performance degradation due to time induced ageing [34]. The time-scale of ageing is much longer than the prediction horizon of the optimisation algorithm. Over time the usable capacity is reduced and if not taken into consideration the error of the algorithm would be tremendous. Therefore, the usable capacity needs to be measured from time to time to norm the algorithm. Aside from the maintenance cycles an empirical value is assumed by integrating the expected calendar life of the battery's manufacturer. The energy efficiency may be impacted by the performance degradation due to ageing. However, this effect is not considered in the model. The data of elapsed calendar time and the resulting calendar induced degradation will be updated in an external status file, which is keeping track of the State of Health (SoH) of the different batteries.

4.3 Cycle Aging

Cycle aging is the life lost each time the battery cycles between charging and discharging. It is commonly described as the function of the Depth of Discharge (DoD) and the applied C-rate. Additionally, extreme

events such as over charge and discharge can affect the cycle ageing significantly. The importance in the context of the degradation model decreases accordingly [45], [52].

For simplicity, cycle-based degradation treats each cycle as a single stress event independent of others, thus the accumulated degradation is the sum of the capacity reduction caused by each cycle [47], [50].

4.3.1 Depth of Discharge Stress Function

The depth of discharge is the main contributor to cycle-based ageing in a battery degradation. Thus, it will be assessed more closely in this work.

Within this work, the DoD δ is defined as the relative percentage change of electricity during a finite charging or discharging process:

$$\delta = \left| \frac{\sigma^{SoC}(t_{end}) - \sigma^{SoC}(t_{start})}{E_{installed}} \right| \cdot 100\,\% \tag{4.1}$$

with σ^{SoC} representing the absolute SoC and the available energy left in the battery. The relative value is also referenced, which is calculated as follows:

$$SoC(t) = \frac{\sigma^{SoC}(t)}{E_{installed}} \cdot 100\,\% \tag{4.2}$$

The modelling follows the concept as used in material science, known as fatigue. It's an empirical approach to predict the resiliency of a material or component as a function of the applied stress and the number of events applied [47]. Due to similarities between classical mechanical fatigue processes and the behaviour in lithium-based electrochemical batteries, the fatigue methodology can be applied. It is widely accepted that the cycle DoD has a nonlinear impact on degradation [50], [54]–[57]. For the same amount of energy processed by a battery, a higher cycle DoD leads to more degradation. Manufacturers therefore provide this information on the product data sheet, e.g. Victron Energy guarantees 3000 equivalent cycles at a DoD of 80 % for its LFP-based LiB [58]. The emerging problem is the appropriate fitting of the few experimental data in order to represent and predict the electrochemical processes. Xu et al. [50] compares nonlinear DoD stress models from literature, which can be grouped into two classes, exponential and quadratic models (refer to Figure 4.4). The accuracy of the proposed fitting methods highly depend on the present chemistries, thus does not perform well in some cases, e.g. for LMO.

In the context of this work, a simplified, quadratic approximation with two fitting parameters for all chemistries has been assumed. Thus, the cycle depth stress function $\Phi(\delta)$ can be written as follows:

$$\Phi(\delta) = k_1 \cdot \delta^{k_2} \tag{4.3}$$

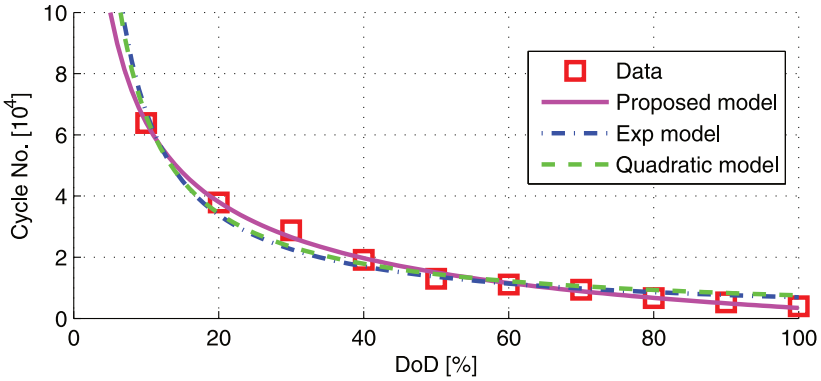

FIGURE 4.4: Expected cycle life as a function of the DoD using experimental data and different fitting methodologies [50].

TABLE 4.1: Fitting parameters for different Lithium battery cells.

Parameter	**LFP**	**LTO**	**NCA**	**NMC/LMO**	**NMC - Laresgoiti**
D_{cycles}	3600	15000	1000	3000	n/a
D_{DoD}	100 %	100 %	100 %	100 %	n/a
k_1	0.02778 %	0.0067 %	0.1 %	0.033 %	0.0524 %
k_2	2	2	2	2	2.03

Laresgoiti et al. [47] researched the degradation processes in NMC and achieved good results with $k_1 = 5.24 \times 10^{-4}$ and $k_2 = 2.03$. For different chemistries different approximation methods for fitting are used, which complicates the comparison. Since this work's scope does not comprise the experimental validation of degradation, a satisfactory simplification is proposed. This method is assuming $k_2 = 2$, based on the results by Laresgoiti et al. and calculates the fitting parameters k_1 as follows:

$$k_1 = \frac{D_{cycles}}{D_{DoD}} \tag{4.4}$$

With D_{cycles} as the number of cycles, guaranteed by the battery manufacturer, and D_{DoD} as the correlating depth of discharge the number of cycles D_{cycles} can be achieved.

The obtained values for the respective chemistries are shown in Table 4.1. The values for the different cycle life have been taken from Table 3.3.

Figure 4.5 shows the predicted cycle life loss if the battery undergoes a change of its SoC given in percentage of its own capacity. While the cycle life loss represents the incremental loss per cycle, the

expected cycle count illustrates the total expected lifetime of the battery. It is calculated as the reciprocal value of the cycle life loss.

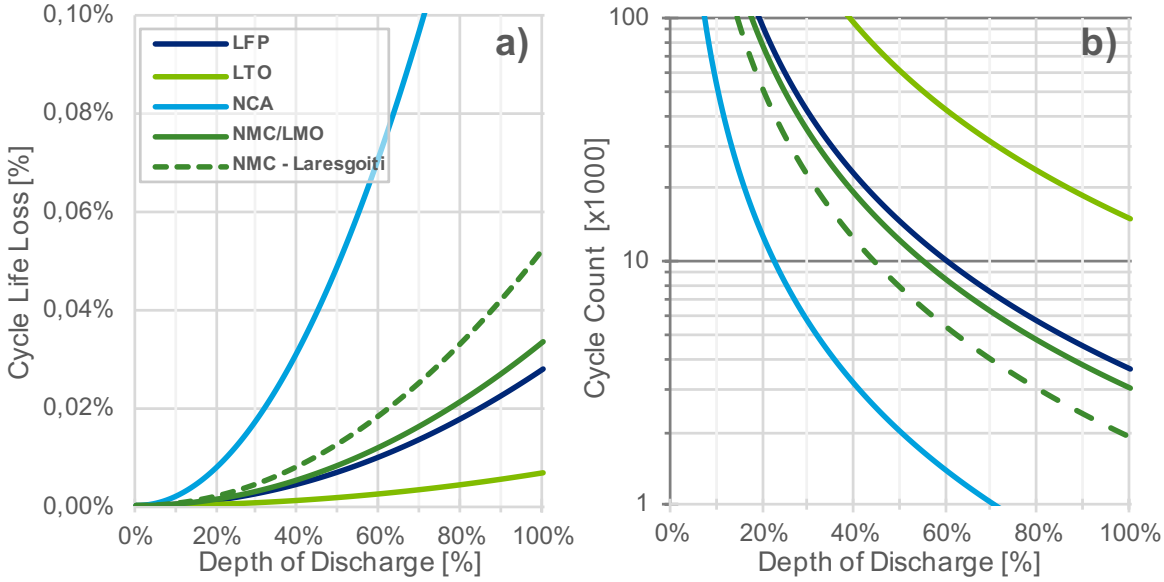

FIGURE 4.5: Calculated cycle life loss (a) and expected total cycle count (b) as a function of the depth of discharge. Source: Own representation.

It can be seen in Figure 16, that NCA as the cheapest of all chemistries with only 352 €/kWh has the weakest cycle performance, while LTO outperforms all other chemistries. This comes with the price of 1050 €/kWh, which is comparably cheap considering its performance is 24 times better, while only being three times more expensive (refer to Table 4.1). Moreover, a significant difference between the experimentally validated value for NMC by Laresgoiti et al. [47] and the proposed calculation method can be obtained. The resulting accuracy, though deviating from experimental data, is considered sufficient for this thesis, but should be addressed in future research within the INVADE project.

4.3.2 C-Rate

The C-rate is considered an important degradation stress factor. With higher C-rates the stress on the battery increases exponentially, moreover the total amount of energy which can be withdrawn from the battery decreases [34]. Mosely et al. [59] quantified the capacity loss of an NMC cell at around 5 % when increasing the C-rate from C/2 to 2C.

As a consequence, the C-rate in this project are kept constant between C/2 and 1 C, this way the losses and the degradation are considered negligible.

4.3.3 Over Charge and Discharge

Aside from the C-rate, the SoC-range, in which the charging takes place, plays an important role. As aforementioned in the introduction, Birkl et al. [44] and Vetter et al. [45] discuss damages to the electrolyte when batteries are over discharged and decomposition processes take place at the cathode and the electrolyte, when the battery is over charged. These physical constraints have been taken into consideration within the INVADE projects and respective charging and discharging power constraints are implemented. This is achieved by limiting the charging to the designated limitations:

$$\sigma^{ch} \leq Q^{ch} \tag{4.5}$$

$$\sigma^{dis} \leq Q^{dis} \tag{4.6}$$

With σ^{ch},σ^{dis} as the variable value and Q^{ch},Q^{dis} the physical constraints for charging and discharging in kW imposed by the battery design respectively.

To avoid overworking conditions in high and low SoC conditions, a limitation of the SoC region is proposed:

$$O^{min} \leq \sigma^{SoC} \leq O^{max} \tag{4.7}$$

With O^{min} the minimum and O^{max} the maximum value of σ^{SoC}. Within this work 15 % and 95 % of the total installed capacity $E_{installed}$ for O^{min} and O^{max} have been assumed respectively.

The SoC limitation comes with the advantage, that neglected discharge efficiency losses which deviate in high and low SoC areas, are described more accurately [34].

Furthermore, a tapering method to ensure that the energy charged σ^{ch} and discharged σ^{dis} are linearly decreased, when approaching high and low SoC areas, is assumed:

$$\sigma^{ch} \leq \frac{-Q^{ch}}{1-S^{ch}} \cdot \left(\frac{\sigma^{SoC}}{O^{max}} - 1 \right) \tag{4.8}$$

$$\sigma^{dis} \leq \frac{-Q^{dis}}{S^{dis}} \cdot \left(\frac{\sigma^{SoC}}{O^{max}} \right) \tag{4.9}$$

S^{ch} and S^{dis} are the upper and lower power limitations thresholds. The values are typically 0.8 (80 % SoC) and 0.1 (10 % SoC) [38], [60]. The emerging constraints during charging and discharging are illustrated in Figure 4.6.

Table 4.2 presents the previously mentioned parameters introduced in this section, which will be used over the course of this work.

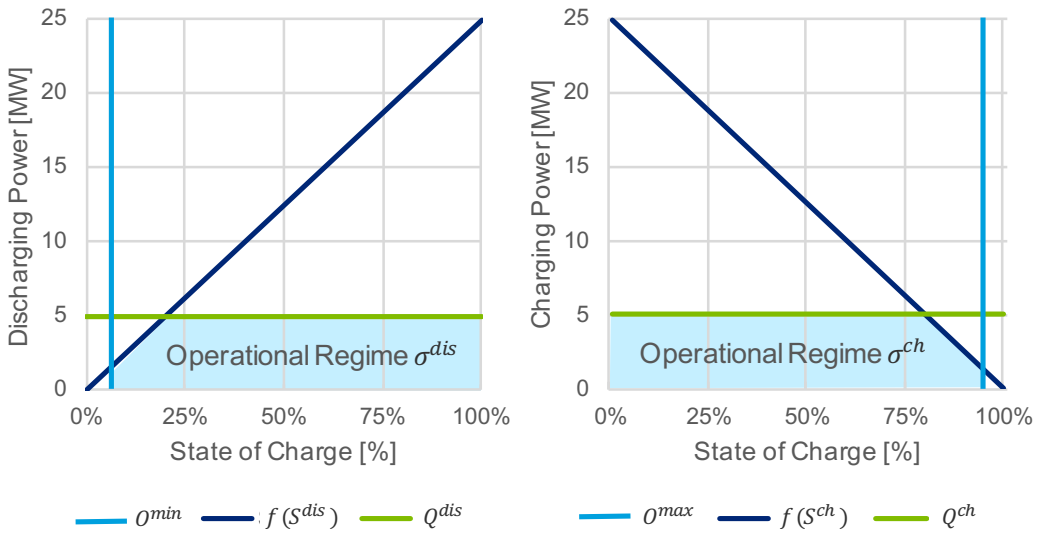

FIGURE 4.6: Discharging (left) and charging (right) power constraints [34].

TABLE 4.2: Charge and discharge control parameters.

Variable	O^{min}	O^{max}	S^{dis}	S^{ch}
Value	$15\,\% \cdot E_{installed}$	$95\,\% \cdot E_{installed}$	0.1	0.8

4.4 State of Health

The cycle and calendar aging factors give indication of the State of Health (SoH) of the battery. SoH is used to describe the condition of a battery, with which the current capacity can be calculated. The SoH ranges from 0 to 100 % and directly correlates with the expected remaining capacity. Contrary to the expectance, the end of life (EoL) of a battery is reached when the SoH has a remaining capacity of around 80 %. The battery is considered as unusable due to tremendous performance fluctuations, in which the output voltage cannot be maintained [52].

The SoH is calculated as follows:

$$L_{cyc}[\%] = \sum_{t} \Phi(\delta_t) \tag{4.10}$$

With L_{cyc} representing the total annual cycle stress caused by depth of discharges δ_t within one year.

$$L_{cal}[\%] = \frac{1}{T_{Bat}} \tag{4.11}$$

With L_{cal} being the total annual calendar degradation, based on the expected battery lifetime, guaranteed by the manufacturer. The total annual proceeded degradation L_{total}, given in percentage of the total life

of the battery can be calculated as the sum of both:

$$L_{tot}[\%] = L_{cal} + L_{cyc} \tag{4.12}$$

The resulting life expectancy of the battery T_{exp} in years, based on the annual degradation can be simply calculated as follows:

$$T_{exp} = \frac{100\,\%}{L_{tot}} \tag{4.13}$$

With D_{EoL} representing the guaranteed remaining capacity after reaching the end of life, the SoH is derived as follows:

$$SoH[\%] = 100\,\% - (1 - D_{EoL}) \cdot L_{tot} \tag{4.14}$$

The remaining capacity can be expressed as function of the SoH:

$$E_{remaining} = SoH \cdot E_{installed} \tag{4.15}$$

4.5 Rainflow Cycle Counting Mechanism

While calendar aging relies on linear, constant parameters, such as the elapsed time, cycle aging is tremendously complicated by the process of cycle counting. This is the result of the batteries agility to charge and discharge freely along a prescribed SoC range. Again, this problem is already known in material fatigue studies, in which the sample undergoes non-symmetrical and undefined stress pattern.

A battery cycle, in this sense, can be described as a physical fatigue event, in which injected and extracted power represent the stress imposed to the battery [61]. As described in Section 4.3.1, the depth of discharge causing higher stress to the battery while shallow processes, won't affect the battery that much. This complies with understandings in fatigue, which allows the usage of the Rainflow cycle method. This is used extensively in materials fatigue stress analysis to count cycles and quantify their depth [62], [63], and has also been broadly applied to battery life assessment [61], [64]–[66].

As an input for the Rainflow algorithm, the SoC profile with a series of local extrema of the examined time period is required. An example is provided to illustrate the procedure (refer to Figure 4.7). This example utilises the Rainflow MATLAB toolbox, developed by Adam Niesłony [62] based on the standards of ASTM International [63]. The algorithm identifies, 1) the relative DoD δ, 2) its type δ_{type}, whether it is a half or a full cycle, and 3) the actual cycle count δ_{count}. The Rainflow logic is shown in the Appendix C in detail.

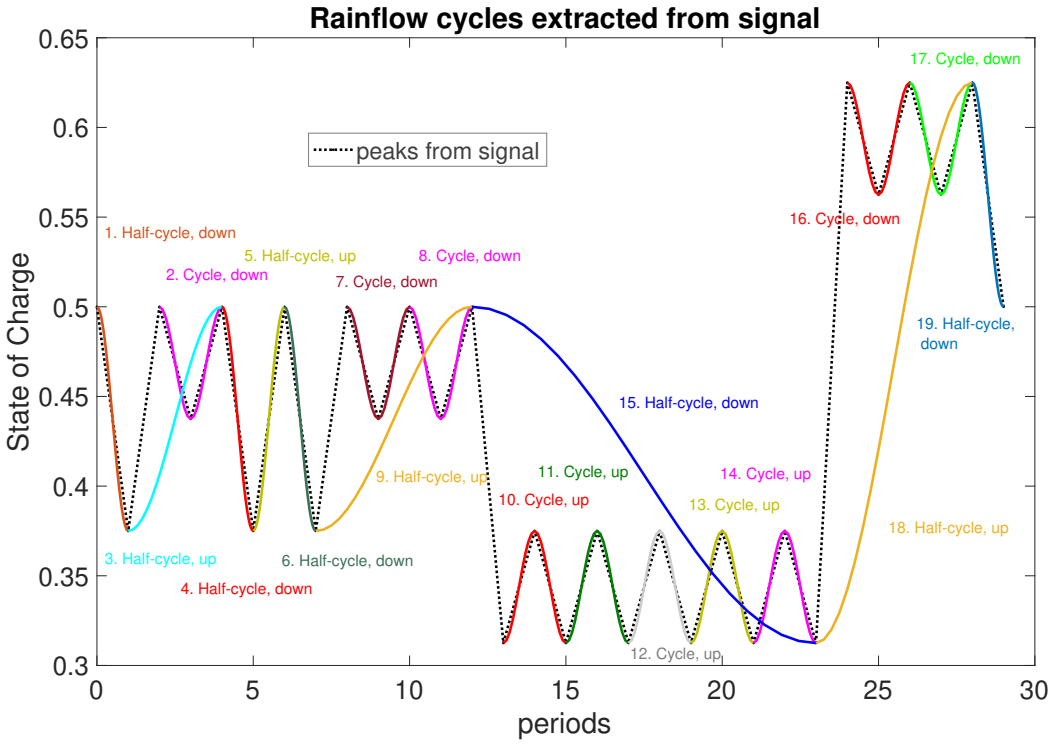

FIGURE 4.7: Half and full cycles in a SoC profile identified by the Rainflow algorithm using the Rainflow MATLAB toolbox by [62].

As can be seen in Figure 4.7, the algorithm successfully distinguishes between half and full cycles. The total life loss L_{cyc} caused by this SoC profile can be calculated accordingly:

$$L_{cyc}[\%] = \sum_{t} \delta_{count} \cdot \delta_{type} \cdot K_1 \cdot (\delta_t)^{k_2} \tag{4.16}$$

Assuming, that the battery in this example is of type NMC and the coefficients are as previously introduced, $k_1 = 5.24 \times 10^{-4}$ and $k_2 = 2.03$, it can be derived, that the onehalf cycle of 31 % causes approximately as much degradation as the seven cycles of a depth of discharge of 13 %, although only 34 % of the energy has been provided compared to the seven cycles (refer Table 4.3). This discrepancy between energy provided and degradation caused, and the resulting non-linearity is one of the main challenges faced in degradation modelling Additionally, the Rainflow algorithm, which enables the proper identification of the equivalent cycles in a battery, does not have a mathematical description and is therefore unsuitable for the integration in optimisation problems [43]. The decision variables would affect the local extreme points on the energy curve and then the identification of the half cycle should be conducted for each feasible bidding strategy to calculate the battery cycle life. He et al. [65] states, that "[t]he relation between the decision variables and the local extreme points can be only analytically expressed in a very complicated form, so it is difficult to embed the identification of the half cycle into a model that can be

TABLE 4.3: Quantified output of the Rainflow algorithm, DoD, cycle type, total cycle number and the calculated cycle depth stress.

DoD δ	**Cycle type** , δ_{type}	**Total number** δ_{count}	**Cycle depth stress** $\Phi(\delta)$
6 %	1	10	0.0019 %
13 %	0.5	7	0.0027 %
19 %	0.5	1	0.0009 %
31 %	0.5	1	0.0025 %

solved by a commercial optimisation solver."

4.6 Linearised Degradation Model

With the increase of implementation of batteries in the energy sector, a need of accurate models is building up. Thus, researchers are constantly improving the precision of theoretical and empirical models. While a high precision model seems to be a reasonable goal to achieve, the operation of batteries in the electric grid involves market interaction, which demands fast algorithm solving for the economic and physical feasibility. These time windows are inherently very small and comprise between 2 hours to 15 minutes. Thus, algorithms commonly used for market dispatch demand linear problems.

On the other hand, degradation mechanisms, such as the cycle aging (refer to Figure 4.5) are highly non-linear and cannot be implemented without certain degree of simplification, e.g. linearisation. Additionally, the aforementioned issue of an accurate cycle counting method implementation presents researcher with a challenge.

In the following a literature review on current linearised degradation models is conducted, and thereafter a substantiated solution is provided.

4.6.1 Literature Review on Degradation Models

In the following, literature research with the focus on cycle counting and cycle-based degradation has been conducted:

- Pelletier et al. [67] compares empirical degradation methods and applies and focuses on the energy throughput and the C-rate as the main cause. This way no advanced cycle counting methods is

needed. Moreover, they propose an electrical equivalent circuit to determine the capacity fade in battery for their application in EVs.

- Similarly, Millner et al. [49] uses an equivalent circuit model of the battery cell as well, to provide terminal characteristics as a function of time, age, state of charge, and charge or discharge rate. The problem of cycle counting is tackled by introducing the average state of charge over the time interval of cycling which is put in relation to the actual depth of discharge. The resulting model, though providing reasonable values, is non-linear.
- Wang et al. [68] expresses the degree of degradation imposed to the battery based on the prevailing SoC and relates it to the cycle life loss curve, which eventually is linearised and implemented in a model.
- Koller et al. [48] defines a cycle as the period between battery charging and discharging transitions. The resulting DoD cycles are put into an exponential cost function which represents the stress function. Eventually, the piece-wise problem is used for a market dispatch algorithm integrating Model Predictive Control (MPC).
- He et al. [65] proposes an algorithm using the decomposition method which separates decision variables from cycle identification method. This causes small inaccuracies compared to the Rainflow algorithm. According to Xu et al. [47], this method yields more accurate dispatch results, but is too complicated to be incorporated in an economic dispatch calculation.
- You et al. [66] proposes an economic dispatch algorithm, but does not fix the problem of solving for degradation as part of the optimisation, rather considers the degradation as an ex-post analysis using the Rainflow algorithm.
- Abdulla et al. [69] introduce an optimisation, which uses a fixed per kWh and static multi-factor degradation model. According to the authors the fixed per kWh damage model should be accurate when all charge-discharge cycles occur at very restricted domains, while the multi-factor degradation, using the current output and input in combination with the SoC and DoD, works better in wider ranges.
- Quite related, Tran et al. [70] relates the cycle depth and the resulting life loss with the energy output within each control time interval.
- Xu et al. [43] presents an integrated solution for the cycle identification and the linearisation of the stress function by splitting the battery into segments and allocating the degradation cost accordingly on-the-go. The error between the proposed method and the ex-post analysis using the Rainflow algorithm is low for a number of segments higher than 10. This approach allocates degradation cost as part of the discharging, arguing that a battery is usually operated with symmetrical charging and discharging [71]. Moreover, Shi et al. [54] proves the convexity of the algorithm, which allows it to be used in a mixed integer linear problem (MILP) problem.

The method proposed by Xu et al. [43] was decided to be used within this work. The fact, that it provides a good accuracy and can be solved by linear solvers also makes it an attractive candidate for the INVADE project.

4.6.2 Marginal Cost of Cycle Aging

One challenge described by Xu et al. is the piece-wise segmentation of the degradation stress function (refer to Figure 4.5) and implementation of the same in a cost function. This is done by taking into consideration the total number of segments J, that evenly divide the cycle depth range (from 0 to 100 %), the known stress function $\Phi(\delta)$ and the total replacement cost of the BESS c_r.

$$c(\delta_t) = \begin{cases} c_1 & \text{if} \quad \delta_t \in [0, \frac{1}{J}] \\ \vdots & \\ c_j & \text{if} \quad \delta_t \in [\frac{j-1}{J}, \frac{j}{J}] \\ \vdots & \\ c_J & \text{if} \quad \delta_t \in [\frac{J-1}{J}, 1] \end{cases} \tag{4.17}$$

Where c_j is calculated based on the DoD of the current operation:

$$c_j = \frac{c_r}{\eta^{dis} \cdot E_{installed}} \cdot J \cdot \left[\Phi\left(\frac{j}{J}\right) - \Phi\left(\frac{j-1}{J}\right) \right] \tag{4.18}$$

Figure 4.8 shows how the increase of segments approximates the plotted cycle life loss curve. Thus, the precision of the cost function increases with the number of segments. Keeping in mind, that the computational effort increases at the same time [43]. Within this work the number of segments throughout all analysis is chosen to be 32.

A small example will demonstrate the plausibility of the marginal cost function, considering the following values (refer to Table 4.4).

TABLE 4.4: Parameters for marginal cycle depth cost function example.

Replacement Cost c_r	**Fitting parameter** k_1	**Fitting parameter** k_2	**Discharge efficiency** η^{dis}	**Installed Capacity** $E_{installed}$	**Number of Segments** J
420000 €	5.24×10^{-4}	2.03	95 %	1 MWh	10

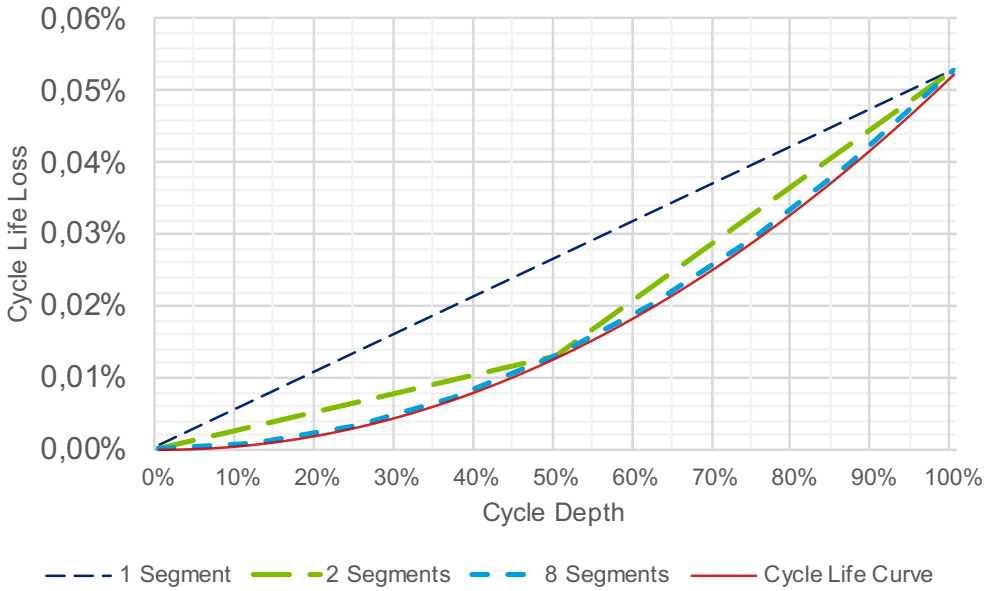

FIGURE 4.8: Segmentation of the cycle depth aging stress function.

The resulting values for c_j are independent of the actual installed capacity $E_{installed}$, therefore these values do not properly represent the actual cost per segment. The actual average cost per MWh c_y^{real} in case the battery is discharged from a shallow $j = 1$ to a deep $j = y$ segment is calculated as follows (refer to Table 4.5).

$$c_y^{real} = \sum_{y=1}^{y} \frac{c_j \cdot E_{installed}}{J} \tag{4.19}$$

This calculation is only a support to visualise the actual cost. This step will be accordingly integrated in the objective function. In this example, the cost to discharge the battery in a full cycle would be 232 €/MWh. The cost for two half cycles, which discharge the same amount of energy, would be 114 €/MWh (refer to Table 4.5) only. This way the cost function is drastically penalising the usage of deep cycles. Since the battery is only operating in shallower cycles, the cost of discharging is normally tremendously lower.

The average of the actual cost c_y^{real} is around 88 €/MWh for NMC/LMO-blend, 11 €/MWh for LTO, 47 €/MWh for LFP and 340 €/MWh for NCA.

TABLE 4.5: Marginal cost function example. Comparison between calculated and corrected, actual cost.

Segment j	c_j [€/MWh]	c_y^{real} [€/MWh]
1	21.62	2
2	66.68	9
3	112.8	20
4	159.51	36
5	206.63	57
6	254.07	82
7	301.76	112
8	349.68	147
9	397.8	187
10	446.08	232

Chapter 5

Spanish Imbalance Settlement

This chapter provides a quick overview of the relevant market mechanism of the Iberian Electricity Market (Mercado Ibérico de la Electricidad, MIBEL), focusing on the Spanish wholesale market including the day-ahead (DA) market and intraday (ID) markets, as well as the adjustment services. A closer description of the balancing markets is provided in Appendix D.

5.1 Short-Term Electricity Market

Short-term procurement of electricity in Spain is done through a spot market organised as a sequence of markets, which are described in the following (refer to Figure 5.1). demand

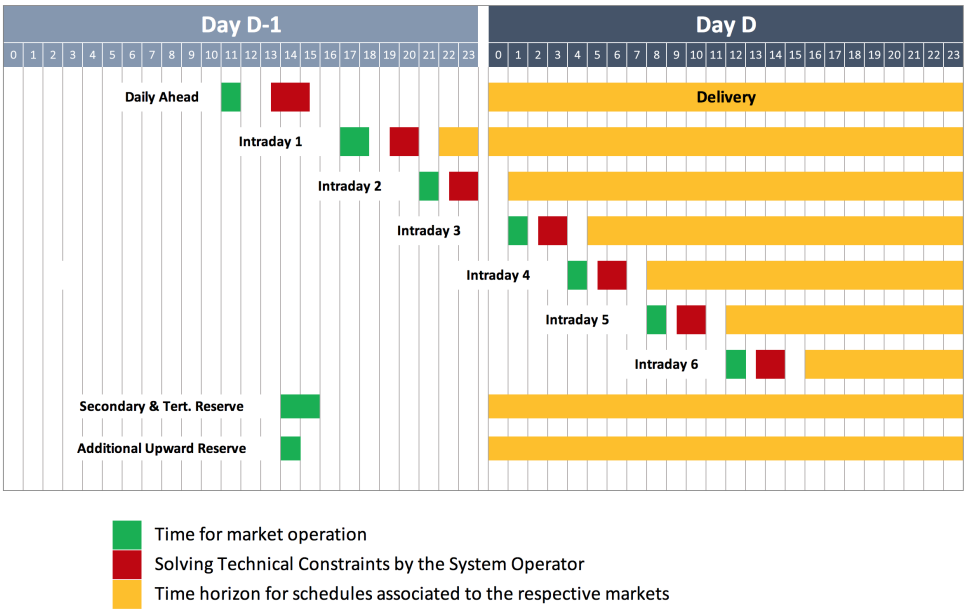

FIGURE 5.1: Timing of the Spanish short-term electricity markets [26].

5.1.1 Day-Ahead Market

The markets of Spain and Portugal are integrated and managed by the Iberian Electricity Market (MIBEL), which is operated by OMI-Polo Español S.A. (OMIE). The market's volume allocates to more than 76 % of the total electricity demanded. The trading is single-price auction, in which hourly bids and offers for each delivery period are submitted by a specified deadline. The auction takes place once a day and at 12 p.m. the auction is conducted for the 24 hours of the next day. The market outcome is defined by the equilibrium market price (EP), which is obtained through merit order by compiling bids and offers in descending and ascending price order respectively. Consequently, the EP is the price at which the cumulative quantity of bids is equal to the cumulative quantity of offers. A producer can place up to 25 different bids per production unit and hour within the price range from 0 to 180 €/MWh, a price cap established by the government.

The average price of electricity in the day-ahead market OMIE in Spain in 2017 has been 52.24 €/MWh. During this first half of the year the lowest hourly price of 2.30 €/MWh year took place. The most expensive hourly price this year occurred, 102.00 €/MWh, which was recorded on day 25 between 20:00 and 21:00. In Figure 5.2 the daily arithmetic average of the day ahead market clearing prices of the MIBEL are shown. In case the transmission between Portugal and Spain is not sufficient, the market is split and results in two different prices for each region.

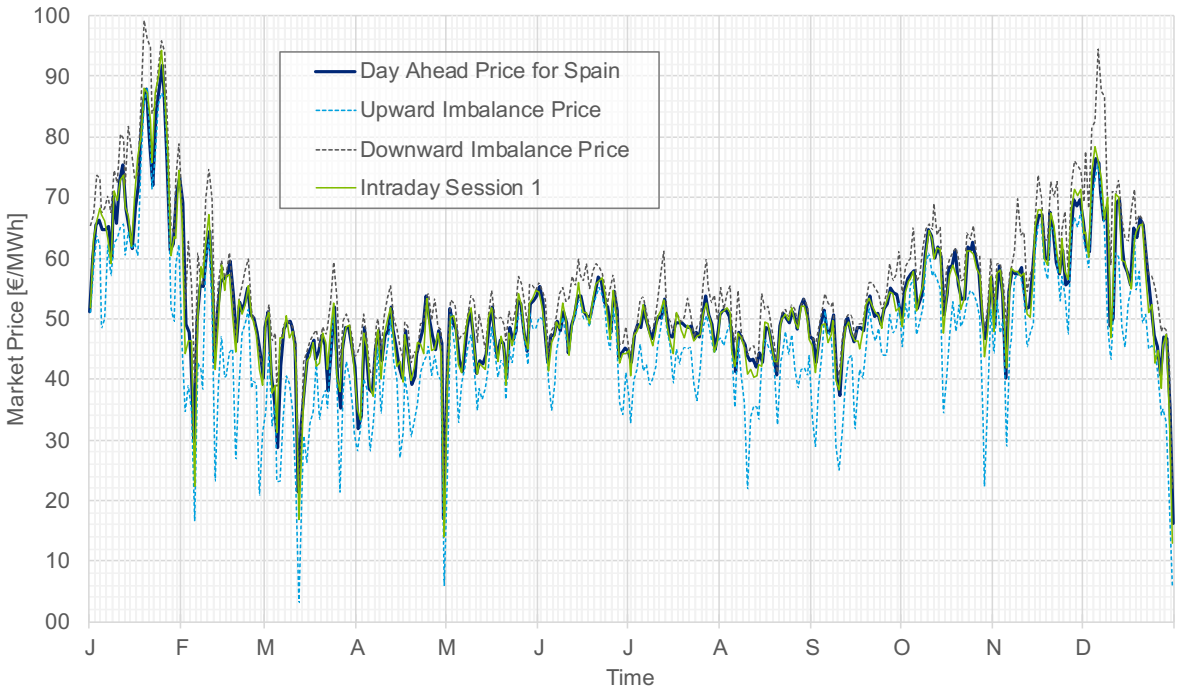

FIGURE 5.2: Day-ahead market MIBEL clearing, upward and downward imbalance and intraday session 1 prices for 2017.

5.1.2 Intraday Market

The intraday markets allow traders to adapt their bids and enables the consideration of time-sensitive information, such as weather and consumption forecasts in order to have their production and consumption covered. The trade on these markets is, just as the day-ahead market, checked for transmission overloads by the transmission system operator, Red Eléctrica de España (REE). The price influence and volumes traded on the different intraday markets are substantially lower than the trade on the day ahead market [72].

The intraday market is divided into six sessions, and the intersection between supply and demand is calculated in each one. The first session covers 28 hours (the last four in D-1 and 24 on day D); the sixth covers the last nine hours of day D (refer to Figure 5.1) [73].

5.1.3 Balancing Market

The third market, chronologically following after the day-ahead and the intraday market, is the balancing market, which comprises the Secondary Reserves, the Tertiary Reserve and the Deviation Management market. Each of these are of importance for the stabilisation of the frequency and are therefore used by the TSO. The precise market mechanism of each of the markets are only of secondary importance for this project, thus can be found in Appendix D.

5.2 Payment of Technical Services

The TSO determines the imbalance price for each imbalance settlement period, imbalance price area and imbalance direction. A penalty to a balance responsible is applied if its scheduled deviations are opposite or against the system´s needs.

In Spain, a dual pricing mechanism is applied for settling energy imbalances. Therefore, the imbalance price depends on the direction of the market party deviation in relation to the system imbalance [26].

The cost of procuring balancing services is allocated to the imbalanced market parties through the imbalance settlement. The balance responsible defines the obligation of market participants, such as generators, consumers and traders to send schedules to the system operator and the financial responsibility for deviating from those schedules. In this regard, market participants are Balance Responsible Parties (BRPs).

The following four scenarios can occur according to different balances with regards to whole control area and individual BRP's portfolios (refer to Figure 5.3).

1. A unit in the BRP's portfolio produces less than what it is scheduled for and the deviation supports the system. As a result, it pays the Day-Ahead-Market-Price (DMP) for balancing generation.

2. A unit in the BRP's portfolio produces less than what it is scheduled for and the deviation is opposing the system's needs. Thus, it pays a penalty based on the amount of energy used to meet system needs, which is the maximum of either the DMP or the Imbalance Price.
3. A unit in the BRP's portfolio produces more than what it is scheduled for and the deviation supports the system's needs. It receives the DMP for the excess energy produced.
4. A unit in the BRP's portfolio produces more than what it is scheduled for and the deviation is opposing the system's needs. It receives the average of the "penalty" for the excess energy produced, which is the minimum of either the DMP or the Imbalance Price

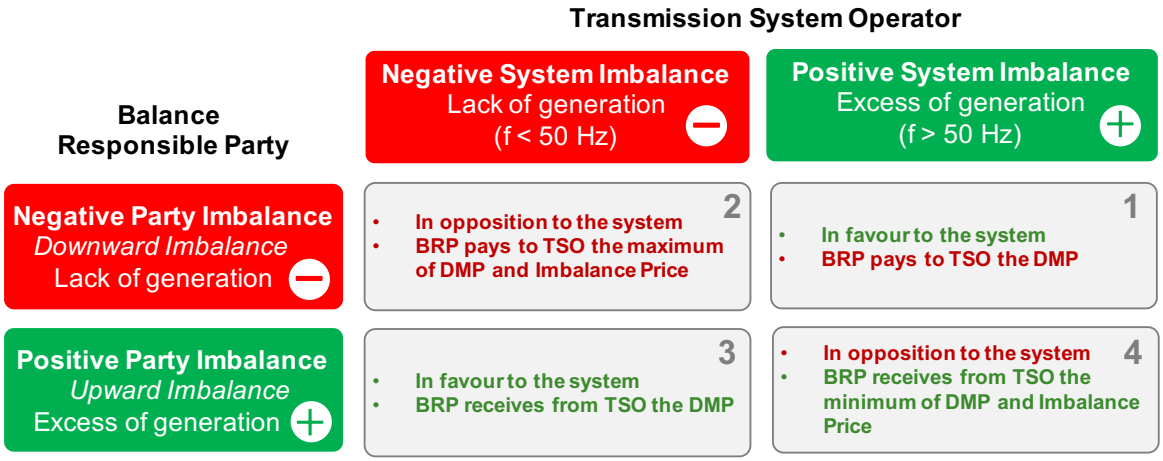

FIGURE 5.3: Calculation of Spanish imbalance prices according to different system and BRP circumstances.

In Figure 5.3 the sign convention used in the data published by REE is shown. A positive system imbalance means that the system suffered an energy deficit and negative signifies an excess of energy produced. Upwards unit imbalance means the generator produced more than its schedule, and vice versa, downwards unit imbalance means it produced less than its schedule.

Figure 5.4 shows the calculation of the penalty as an example for deviations opposing the system needs for each BRP. In case of a deviation in a control area, the TSO activates the timely respective balancing services with regards to the settled prices on the various markets. The Weighted Average of Cost (WAC) will be compared to the DMP. The WAC is calculated according to Equations 5.1, 5.2, 5.3 and 5.4 for the Secondary Reserve, Tertiary Reserve and Deviation Management Market respectively. The maximum of both will be considered for the penalty and together with the deviation of each individual BRP to calculate the penalty.

$$\text{Cost}_{SR} = P_{SR}[€/\text{MWh}] \cdot E_{SR}[\text{MWh}] \tag{5.1}$$

$$\text{Cost}_{TR} = P_{TR}[€/\text{MWh}] \cdot E_{TR}[\text{MWh}] \tag{5.2}$$

$$\text{Cost}_{DM} = P_{DM}[€/\text{MWh}] \cdot E_{DM}[\text{MWh}] \tag{5.3}$$

$$\text{WAC} = \frac{(\text{Cost}_{SR} + \text{Cost}_{TR} + \text{Cost}_{DM})}{(E_{SR} + E_{TR} + E_{DM})} \tag{5.4}$$

$$P_{\text{IMBALANCE}} = \max(\text{WAC}, P_{DMP}) \tag{5.5}$$

$$\text{Penalty for BRP}_j \text{ to pay} = (P_{\text{IMBALANCE}}\ [€/\text{MWh}] \cdot \text{Imbalance}_{\text{BRP}_j}\ [\text{MWh}] \tag{5.6}$$

Chaves-Ávila et al. points out that "since imbalance prices in Spain are only related to the DA market prices, there is no direct relationship between [intraday] prices and imbalance prices. Therefore, [intraday] prices give an arbitrage opportunity for BRPs between [day-ahead] and imbalance prices" [26].

This arbitrage possibility will be in the focus of the case study, which is further explained in the following.

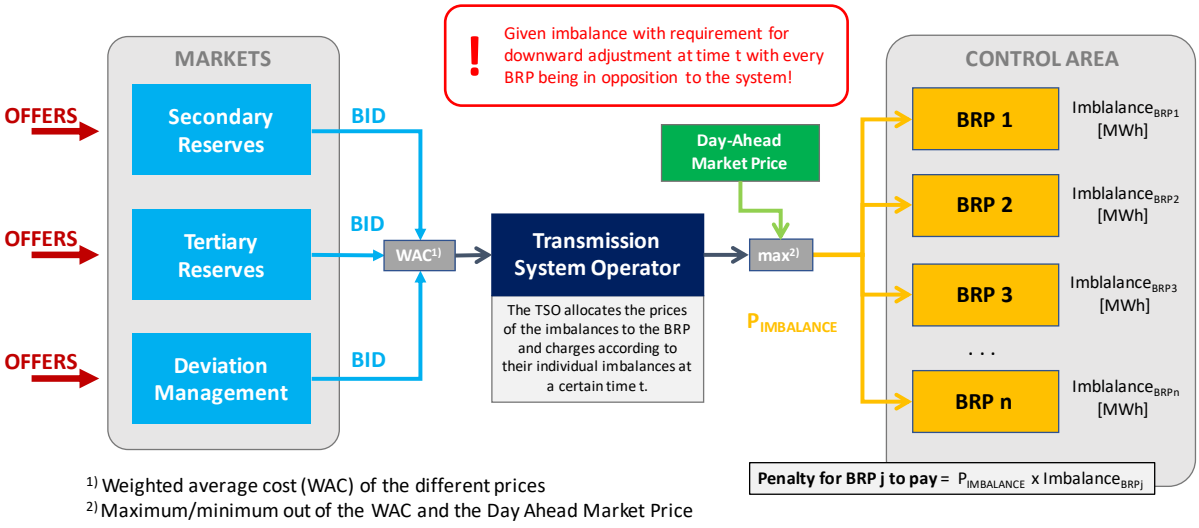

FIGURE 5.4: Calculation of the penalty of Scenario 2; The BRP's portfolio is producing less than scheduled and it is opposing the grid state.

5.3 Imbalance Prices and Arbitrage Potential

The business opportunity of imbalance management is based on the dual pricing mechanism applied in Spain. As described in Section 5.2, the imbalance price depends on the direction of the market party deviation in relation to the system imbalance. If the market party helps the system (i.e. the deviation is in the opposite direction to the system), this market party usually receives or pays the DA market price. However, if the BRP deviates from its schedule in the same direction as the system imbalance, it pays an imbalance price based on the balancing costs (i.e. energy costs of activated reserves) [26], [74].

Figure 5.5 shows the monthly average imbalance prices as a percentage of the daily average day-ahead market prices from January 2017 until December 2017. During this period, on average, imbalance prices for negative (downward) imbalances were 7.7 % higher than DMP. On the other hand, the imbalance prices for positive (upward) imbalances were 13.1 % lower than the DMP.

The arbitrage time window for a battery is 24 to 48 hours, depending on the optimisation horizon and the imbalance forecasting. Based on the data from 2017, the arbitrage potential has been calculated as the maximum upward imbalance price minus the minimum downward imbalance price within 24 hours. The results are shown in Figure 5.5.

FIGURE 5.5: Arbitrage possibility in the Spanish Balancing market. At the top daily averages of the up- and downward imbalance prices for the year 2017. At the bottom the calculated arbitrage possibilities within 24 hours.

It can be seen that especially in the winter months, in which the electricity consumption is higher, the arbitrage possibility peaks at 111 €/MWh and 90 €/MWh. The average is calculated at 38.47 €/MWh. The frequency of days with a specific arbitrage possibility is shown in Figure 5.6. This scenario assumes, that the BRP always has an imbalance position which favours the maximum trading potential. Moreover,

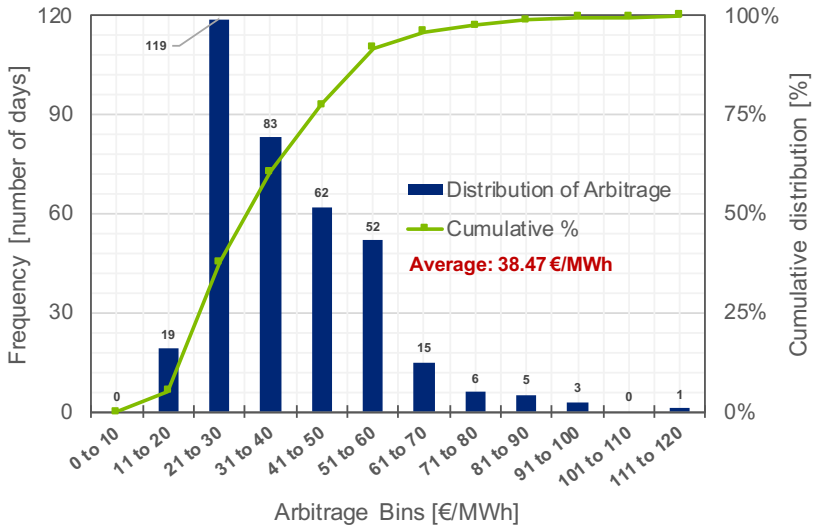

FIGURE 5.6: Distribution of number of days sorted by arbitrage possibility.

a perfect prediction of the imbalances is considered. Extreme values above 90 €/MWh due to their low probability in occurrence, are hardly to be forecasted and used efficiently.

5.4 Imbalance Data

As part of the engagement in the INVADE project, Estabanell Energia provided hourly negative imbalance data for the year 2017, in order to validate the use case of the battery for the usage of deviation management. To assess the whole potential of imbalances, the positive imbalances are needed as well and therefore have been assumed to follow the same pattern as the system imbalance. The hourly data for the year 2017 is shown in Figure 5.7.

In the context of imbalances, the negative imbalances are the only cause of cost, while positive bring revenue. Still, in order to use the arbitrage window of imbalance prices, information about the size of positive imbalance are essential. For this purpose, the known system imbalances have been analysed and used to interpolate the missing positive imbalances, considering the same statistical distribution and a slight excess of negative imbalances (refer to Figure 5.8).

Figure 5.9 provides a first analysis. It shows that the BRP, Estabanell Energia, had a total negative Imbalance of 2.05 GWh in the year 2017, which allocates to 0.73 % of the total energy traded or a total cost of 109,618 € with an average negative imbalance of 0.412 MWh and an average cost of 57.13 €/MWh. An hourly peak has been recorded on the 26. December 2017 at 8 a.m., as the BRP's portfolio was short 8.93 MWh, causing a penalty of 516 €.

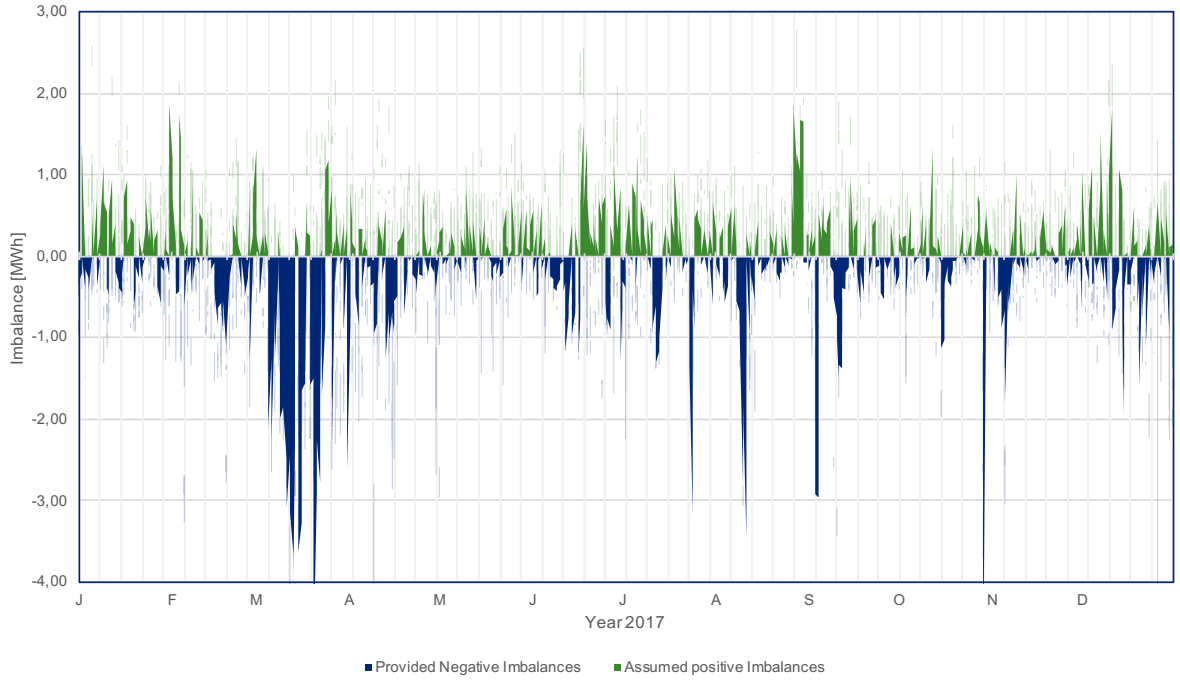

FIGURE 5.7: Imbalance data; provided (blue) and assumed (green).

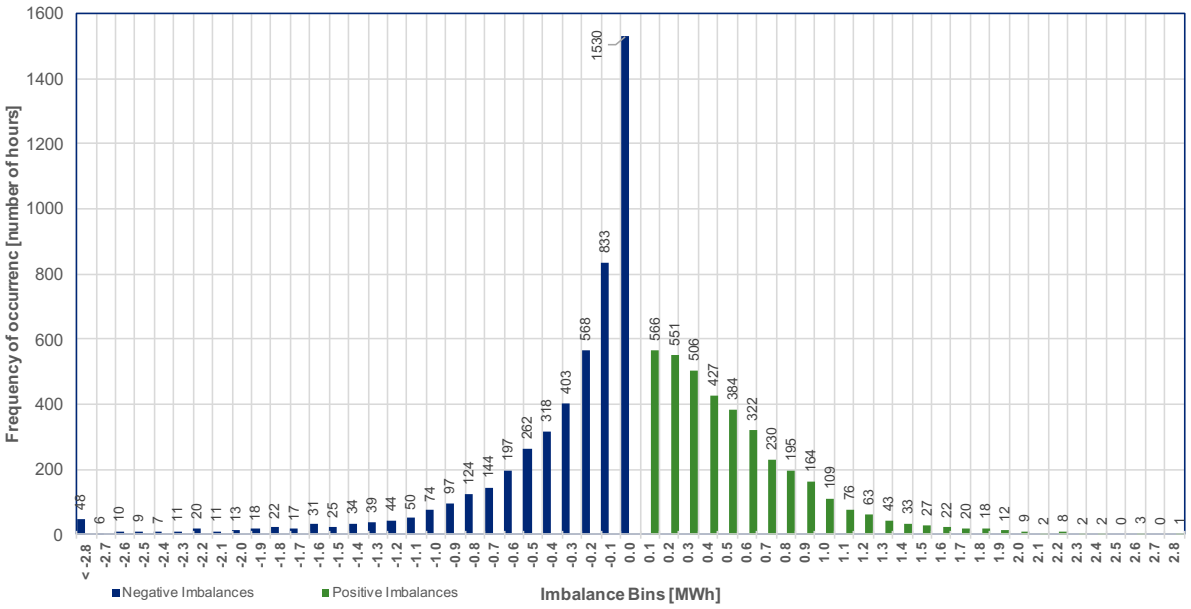

FIGURE 5.8: Statistical distribution of the BRP imbalances over the year 2017.

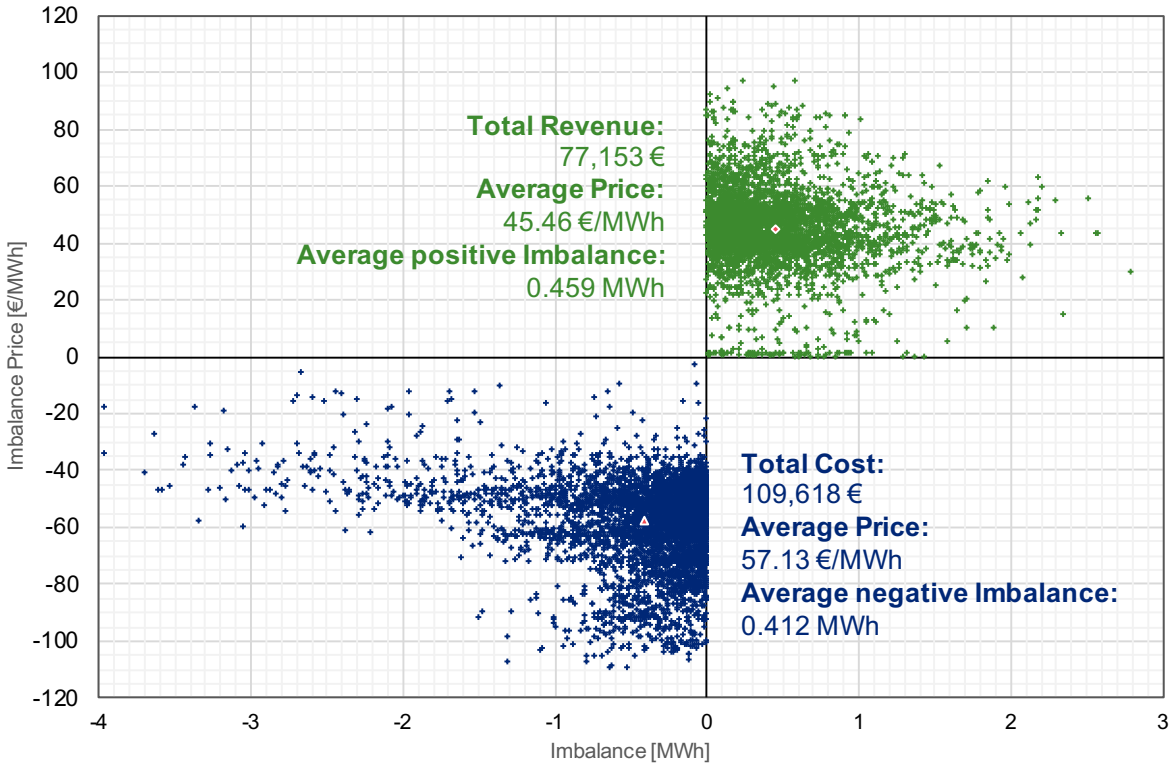

FIGURE 5.9: Data correlation between imbalance prices and energy. Prices for negative Imbalances have been converted into negative values for visual reasons.

A surplus in the BRP's portfolio causes a transaction from the TSO to the BRP, therefore the resulting penalty, caused by positive imbalances is accounted as revenue. In total, only 44 % of the time Estabanell had a surplus, which caused a total revenue of 77,153 € with an average price of 45.46 €/MWh and an average positive position of 0.459 MWh. As can be seen in Figure 5.9, the imbalances do not necessarily correlate with the prices, which means that Estabanell's imbalances are not during times in which the balancing market is highly demanded, and thus the imbalance prices are not that high.

Together with the imbalance data, the arbitrage window and thus the business opportunity for the BESS can be quantified.

Chapter 6

Model Description

This work aims to quantify, whether BESS are eligible for imbalance management in order to avoid deviation penalties imposed to BRPs. All cases presented in the following are considering the full information case, in which the BRP knows the upcoming imbalances. The imbalance forecasting is a research topic on its own and therefore will be not touched in this work. In this context, the work will solely give indication about what accuracy of forecasting is needed to obtain a financially feasible deviation management utilising a battery and the intraday trading.

6.1 Problem Formulation

The formulated problem aims to walk the thin line of mitigating the deviation penalties, complying with the Iberian market regulations and technical battery constraints while considering state-of-the art battery degradation mechanism, up-to-date battery economics and real imbalance data provided by Estabanell Energia.

Moreover, the problem is dominated by the opposing goals of a high accuracy while maintaining a low computational effort. The chosen method is based on linearisation and results in a Mixed-Integer-Linear-Problem (MILP), which allows it to be solved by non-commercial solvers in less than 15 minutes.

The sets, parameters and variables used in the following are defined in the preface of this work.

6.1.1 Model Overview

The aforementioned parameters introduced in the respective chapters are considered in different steps of the algorithm. Figure 6.1 gives a better understanding about the necessary input and the calculated output. The imbalance data and the battery information are the only parametrised input from Excel-spreadsheets. The data is read into the Python-based imbalance optimisation algorithm using the Panda library. For repetitive analysis, e.g. for one year, the battery status is created and readout in each iteration. The corresponding Excel-file contains the state of health and degradation specific parameters.

Eventually, the output file consists of the final results of the objective functions, which helps to analyse the overall finances of the battery use case. This again is done in a separate spreadsheet. While the optimisation results are a snapshot of the optimisation period analysed, the financial calculation sets out to put them in a project context with a planning horizon of 10 years. This two-fold analysis has been chosen to understand whether savings within the optimisation horizon are sufficient to pay back a purposely installed BESS.

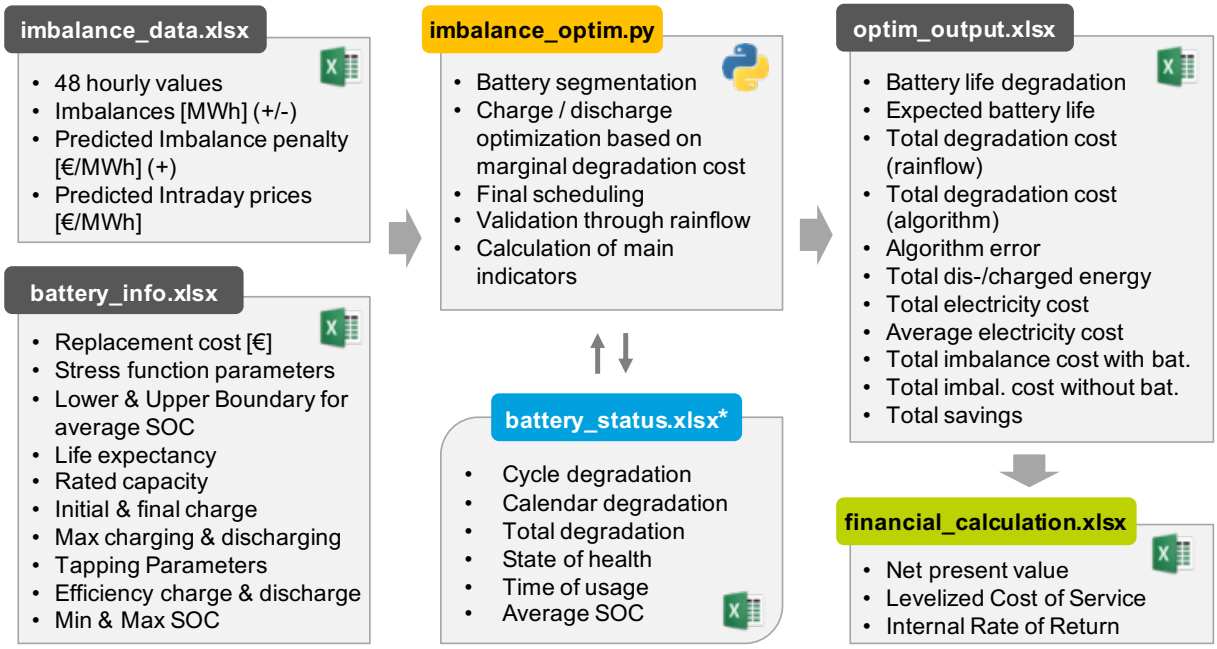

FIGURE 6.1: Model overview.

6.1.2 Time Horizon

The advantage of the full information scenario is that the algorithm can optimise the battery schedule for the whole day. The optimisation horizon is to 24 to 48 hours. A more realistic model would comprise a multi-stage model, which deals with forecasted and updated market information within the optimisation horizon and updates the model on the fly.

Further time constraints need to be considered, such as the intraday bidding window, which closes for each session minimum three hours before delivery. Consequently, current forecasting techniques have to provide accurate information at least three hours before delivery in order to supply sufficient data for market bidding. The closer the state of time to the point of delivery is, the easier it is to predict the exact

amount of supply and demand. Trading flexibility can provide a cost-competitive solution together with short-term forecasting[1], which might be less complex to implement.

6.1.3 Battery Segmentation

The segment parameters are derived from the input parameters of the battery, to keep the program modular and flexible with regards to the number of batteries and number of segments needed. The segment energy maximum $o_{b,j}^{max}$ is defined as follows:

$$o_{b,j}^{max} = \frac{O_b^{max}}{J} \qquad \forall\, b \in B,\ \ j \in J \tag{6.1}$$

The initial segments are filled based on the initial charge of the battery unit b. The segments are filled from the shallowest to the deepest. The sum of all the segments at $t = 0$ has to equal the initial state of charge of the battery.

$$\sum_{j=0}^{J} o_{b,j}^{initial} = O_b^{initial} \qquad \forall\, b \in B \tag{6.2}$$

6.1.4 Marginal Cost of Cycle Aging

As described in Section 4.6.2, the marginal cost of cycle aging is calculated based on the stress function $\Phi(\delta)$, the number of segments J, the battery cell replacement cost $c_{f,b}$, the installed capacity $E_b^{installed}$ and the discharge efficiency η_b^{dis}. Since the cycle depth aging stress function is non-linear, the marginal cost is linearised with different numbers of segments j with $j \in J$.

$$c_j = \frac{c_{r,b}}{\eta_b^{dis} \cdot E_b^{installed}} \cdot J \cdot \left[\Phi\left(\frac{j}{J}\right) - \Phi\left(\frac{j-1}{J}\right) \right] \qquad \forall\, j \in J \tag{6.3}$$

6.1.5 Objective Function

The aim of the objective function is to minimise cost. In the context of this optimisation algorithm the cost is expressed with a positive sign, while revenue is negative. Thus, the optimisation direction is to minimise the overall expenses caused by imbalances by means of charging and discharging batteries and trading on the intraday market. As can be seen in Figure 6.2, the objective function can be split in six parts.

- **Imbalance cost** refers to the deviation forecasted by the BRP. Positive imbalances are cost, negative imbalances are revenues. If no measure is taken, the BRP is subjected to this cost.

[1] Short-term forecasting in this context refers to upcoming information up to 5 min before the delivery.

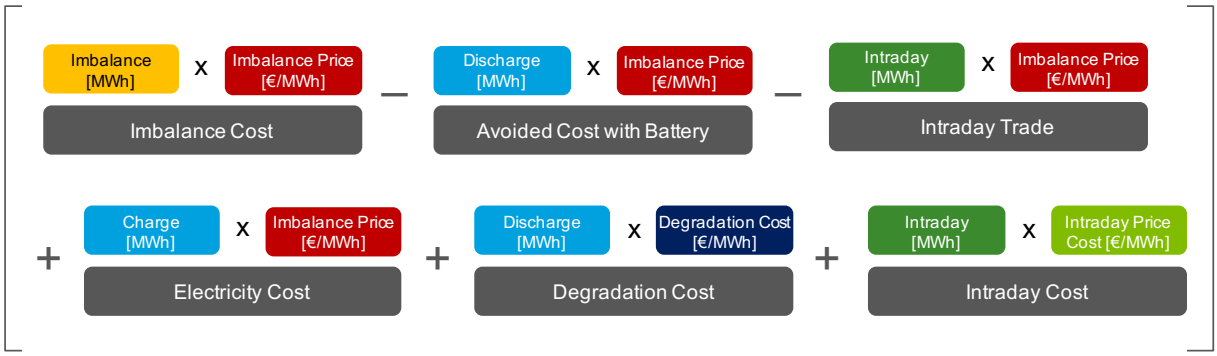

FIGURE 6.2: Objective minimisation function and its six cost segments.

- **Avoided cost with battery** is the opportunity cost the battery causes by discharging and mitigating the imbalance cost. The higher the avoided imbalance price, the larger the savings.
- The same can be achieved by **trading on the intraday**. The energy bought on the intraday for a certain hour causes a decrease of the imbalance cost. If energy is bought on the intraday market, the downward imbalance costs are reduced, thus the sign is positive.
- **Electricity cost** refers to the energy the battery is charging. The act of charging, if no energy is bilaterally bought, causes an imbalance and needs to be considered. The battery is aiming to charge during upward imbalance, when the imbalance price is lower than the Day-Ahead-Market Price.
- **Degradation cost** is the cost of usage, which penalises an extensive use of the battery which might lead to a quick degradation.
- **Intraday cost** accounts to the price of the bought energy. If energy is sold, the sign is negative, and it becomes revenue.

The mathematical formulation is less neatly arranged but contains the exact same cost segments. The imbalance price p_t^{IB} can be identified as a common factor of the first four constituents. More than one battery can be applied, thus the summation of the total charge $C_{t,b}$ and discharge $D_{t,b}$ needs to be considered. The cycle aging cost is the sum of the cycle aging costs associated with each segment over the horizon. The cost function as a whole is summed over the total optimisation period T.

The first part calculates the imbalance cost, while the second part calculates the cost of discharge. The objective is to minimise the cost imposed to the BRP while keeping the cost of the battery as small as

possible.

$$\begin{aligned} \text{min cost} \quad C := \sum_{t=0}^{T} \Bigg[\left(d_t^{BRP} - \sigma_t^{ID} - M \cdot \sum_{b=0}^{B} (D_{t,b} - C_{t,b}) \right) \cdot p_t^{IB} \\ + \sigma_t^{ID} \cdot p_t^{ID} + \sum_{b=0}^{B} \sum_{j=1}^{J} (M \cdot \sigma_{t,b,j}^{dis} \cdot c_{b,j}) \Bigg] \end{aligned} \tag{6.4}$$

6.1.6 Imbalance Constraints

If the forecasted imbalance is negative, the optimised imbalance is not allowed to be positive and vice versa. A change of sign would cause a different imbalance price to be allocated (refer to Figure 5.3), which would increase the complexity of the algorithm due to an additional decision variable added.

The imbalance should not be amplified by any activities. Even though the algorithm would find an economic reasoning in increasing positive and negative imbalances, which results in higher revenues, it is quite controversial and won't be used in this optimisation.

$$0 \leq \left[d_t^{BRP} - \sigma_t^{ID} - M \cdot \sum_{b=0}^{B} (D_{t,b} - C_{t,b}) \right] \leq d_t^{BRP} \qquad \forall\, d_t^{BRP} \geq 0, \quad \forall\, t \in T \tag{6.5}$$

$$d_t^{BRP} \leq \left[d_t^{BRP} - \sigma_t^{ID} - M \cdot \sum_{b=0}^{B} (D_{t,b} - C_{t,b}) \right] \leq 0 \qquad \forall\, d_t^{BRP} \leq 0, \quad \forall\, t \in T \tag{6.6}$$

6.1.7 Intraday Constraints

The intraday market provides a tool to trade energy on the day of delivery in order to react to new information about demand and supply, such as unplanned events or updated weather forecast. Ergo, the intraday market is the BESS's competitor in the context of deviation management. Therefore, the intraday bidding under full information was added to see the remaining potential for the BESS to alleviate imbalances. For simplicity, only the intraday session 1 (refer to Section 5.1.2) will be added into the decision process (refer to Figure 5.2). The analysis comprising the intraday market is not conducted in all scenarios, due to the fact that the focus of this work is on the economic feasibility of BESS systems as an alternative to Intraday trading.

In the following the battery constraints are presented, which are based on the INVADE publication 5.3 [38] and Xu et al. [43]. As for the intraday market activity, only one activity constraint has been defined, which refers to the manual input, whether intraday trading should be performed or not.

$$\sigma_t^{ID} \cdot (1 - v^{ID}) = 0 \qquad \forall\, t \in T \tag{6.7}$$

6.1.8 Battery Constraints

At any time, the sum of charging power $\sigma^{ch}_{b,t,j}$ and the sum of discharging power $\sigma^{dis}_{b,t,j}$ over all the segments j need to be equal the power taken from and fed into battery, $D_{t,b}$ and $C_{t,b}$ respectively.

$$C_{t,b} = \sum_{j=1}^{J} \sigma^{ch}_{b,t,j} \qquad \forall\, t \in T,\ b \in B \tag{6.8}$$

$$D_{t,b} = \sum_{j=1}^{J} \sigma^{dis}_{b,t,j} \qquad \forall\, t \in T,\ b \in B \tag{6.9}$$

To avoid any spontaneous charging and discharging at the same time within the same battery, an activity constraint is introduced. The necessity of this binary variable has been studied in detail, concluding that constraints 6.10 and 6.11 can be written without $v_{t,b,j}$ as long the charging and discharging processes are allocated to a cost. The results of the analysis can be found in Appendix E.1: Solver Comparison.

$$C_{t,b} \leq Q^{in}_{b} \cdot v_{t,b,j} \qquad \forall\, t \in T,\ b \in B,\ j \in J \tag{6.10}$$

$$D_{t,b} \leq Q^{out}_{b} \cdot (1 - v_{t,b,j}) \qquad \forall\, t \in T,\ b \in B,\ j \in J \tag{6.11}$$

Each battery b has efficiency factors for charging η^{ch}_{b} and discharging η^{dis}_{b}, respectively. The battery state of charge, i.e. the storage content $\sigma^{SOC}_{b,t,j}$ for segment unit j in period t depends on the state of charge in the previous period and charging $\sigma^{ch}_{b,t,j}$ or discharging $\sigma^{dis}_{b,t,j}$ in current period.

$$\sigma^{SOC}_{b,t,j} - \sigma^{SOC}_{b,t-1,j} = M \cdot \sigma^{ch}_{b,t,j} \eta^{ch}_{b} - \frac{\sigma^{dis}_{b,t,j}}{M \cdot \eta^{dis}_{b}} \qquad \forall\, t > 0,\ b \in B,\ j \in J \tag{6.12}$$

The maximal segment capacity is constrained:

$$\sigma^{SOC}_{b,t,j} \leq o^{max}_{b,j} \qquad \forall\, t \in T,\ b \in B,\ j \in J \tag{6.13}$$

In order to decrease extreme operational regimes, the minimum and maximum SoC of the battery is constrained:

$$\sum_{j=1}^{J} \sigma^{SOC}_{b,t,j} \leq (S^{max}_{b} \cdot E^{installed}_{b}) \qquad \forall\, t \in T,\ b \in B \tag{6.14}$$

$$\sum_{j=1}^{J} \sigma^{SOC}_{b,t,j} \geq (S^{min}_{b} \cdot E^{installed}_{b}) \qquad \forall\, t \in T,\ b \in B \tag{6.15}$$

The initial and the final state of charge at $t = 0$ and T is provided respectively:

$$\sigma_{b,0,j}^{SOC} = o_{b,j}^{initial} \qquad \forall\, b \in B,\ \ j \in J \tag{6.16}$$

$$O_b^{final} = \sum_{j=1}^{J} \sigma_{b,T,j}^{SOC} \qquad \forall\, b \in B \tag{6.17}$$

To avoid spontaneous charging and discharging in $t = 0$, the variables are disabled in this period:

$$\sigma_{b,0,j}^{dis} = \sigma_{b,0,j}^{ch} = 0 \qquad \forall\, b \in B,\ \ j \in J \tag{6.18}$$

Previous constraints assume that the batteries are completely adjustable in terms of power input and output. However, the following constraint ensures that the energy charged $\sigma_{b,t,j}^{ch}$ and discharged $\sigma_{b,t,j}^{dis}$ to the battery b is linearly decreased from S_b^{ch} and S_b^{dis} state of charge. This constraint is described in Section 4.3.3.

$$\sigma_{b,t,j}^{ch} \leq \frac{-Q_b^{ch}}{1 - S_b^{ch}} \cdot \left(\frac{\sigma_{b,t,j}^{SOC}}{O_b^{max}} - 1 \right) \qquad \forall\, t \in T,\ \ b \in B,\ \ j \in J \tag{6.19}$$

$$\sigma_{b,t,j}^{dis} \leq \frac{-Q_b^{dis}}{S_b^{ch}} \cdot \left(\frac{\sigma_{b,t,j}^{SOC}}{O_b^{max}} \right) \qquad \forall\, t \in T,\ \ b \in B,\ \ j \in J \tag{6.20}$$

Eventually, the average SoC is introduced in order to increase the cell life of the battery.

This constraint origins from Section 4.2.2, in which one concludes, that the battery's lifetime can be increased when operated at favourable SoC conditions. Based on studies by M. Ecker et al. [53], the electrochemistry benefits when kept around 50 %. However, a strict constraint of the upper and lower boundary would result in too little operational regime. Therefore, the concept of average state of charge is introduced, which supports the operation in between $A_b^{low} = 40\,\%$ and $A_b^{high} = 60\,\%$.

The complexity of Equation 6.21 derives from the fact, that the average SoC is updated after every optimisation period and readout again. The significance of every new optimisation period is put in relation with the elapsed time. This way a new optimisation horizon affects the average SoC less.

$$A_b^{low} \leq \frac{(A_b^{status} \cdot T_b^{status}) + \left[\sum_{t=0}^{T} \left(\frac{\sum_{j=1}^{J} \sigma_{b,t,j}^{dis}}{E_b^{installed}} \right) \cdot \frac{1}{T_{optim}} \right] \cdot M \cdot T_{optim}}{M \cdot T_{optim} + T_b^{status}} \leq A_b^{high} \qquad \forall\, b \in B \tag{6.21}$$

6.1.9 Calculation of Evaluation Indicators

The individual components of the objective functions provide good insight about the optimisation. In order to validate the plausibility and accuracy of the cycle counting and degradation algorithm, the error between the algorithm and Rainflow method is calculated. Therefore, the obtained SoC evolution is fed

into the Rainflow method as described in Section 4.5, and the cycle life loss L_{cyc} is calculated with the cycle stress function $\Phi(\delta_t)$. The relative error ε on the cycle aging cost is calculated as:

$$\varepsilon = \frac{|C - c_r \cdot L|}{c_r \cdot L} \tag{6.22}$$

C is the cycle aging cost as part of the objective function:

$$C = \sum_{b=0}^{B} \sum_{j=0}^{J} (M \cdot \sigma_{b,t,j}^{dis} \cdot c_{b,j}) \tag{6.23}$$

The obtained error is assessed by means of a sensitivity analysis in the following Section 6.2. Based on the obtained cycle degradation, the expected battery life can be calculated. The life expectancy is assuming the BESS repeats the same operating pattern in future years. It extrapolates the cycles calculated for the optimisation horizon T_{opt} to a whole year. The life estimation $T_b^{expected}$ includes calendar aging L_b^{cal} as well as cycle aging L_b^{cyc} and is calculated as follwos:

$$T_b^{expected} = 100\,\% \left(\frac{8760\,\text{hr/yr}}{m \cdot T_{opt}} \cdot L_b^{cyc} + L_b^{cal} \right) \qquad \forall\, b \in B \tag{6.24}$$

The accuracy of the calculated expected lifetime increases with longer optimisation periods.

6.2 Model Error Sensitivity

To validate the accuracy of the proposed cycle counting and degradation cost calculation method a sensitivity analysis has been conducted by implementing the problem in a simple market arbitrage problem. The market prices used in this analysis, are presented in Figure 6.3. The aforementioned error between the Rainflow algorithm and the linearised marginal cost function (see Equation 6.22), together with the overall runtime of the solver is the focus of this assessment.

In total, 8 different battery specification have been tested to assure the accuracy of the code. The base case was represented by a 1 MW/1 MWh NMC/LTO battery with the replacement cost of 420 €/kWh. Thereafter, seven other variations have been tested, including different size, price, E/P-ratio, and initial and final charge (refer to Table 6.1).

As can be seen in Table 6.2, the runtime of the solver is very short for all number of segments. The problem with 72 time-steps was executed in Gurobi through Pyomo using a MacBookPro10,1 with Intel Core i7 (8 threads) and 8GB of RAM. In this context it needs to be mentioned, that all batteries have been simulated simultaneously per number of segments, which underlines the low computational effort the algorithm. The total runtime of all 20 iterations including 8 batteries was 10:38 minutes. From the results the following conclusions can be drawn:

TABLE 6.1: Different battery specification for the sensitivity analysis.

Battery	Description	Power capacity [MW]	Energy capacity [MWh]	Replacem. cost [€/kWh]	E/P Ratio	Initial charge	Final charge
Bat.1	*Basecase (BC)*	1	1	420 €	1	50 %	50 %
Bat.2	*Bigger battery*	10	10	as BC	as BC	as BC	as BC
Bat.3	*Cheaper battery*	as BC	as BC	42 €	as BC	as BC	as BC
Bat.4	*More expensive bat.*	as BC	as BC	4200 €	as BC	as BC	as BC
Bat.5	*Low E/P*	2	as BC	as BC	as BC	as BC	as BC
Bat.6	*High E/P*	0.5	as BC	as BC	as BC	as BC	as BC
Bat.7	*Low initial charge*	as BC	as BC	as BC	as BC	15 %	50 %
Bat.8	*Low final charge*	as BC	as BC	as BC	as BC	50 %	15 %

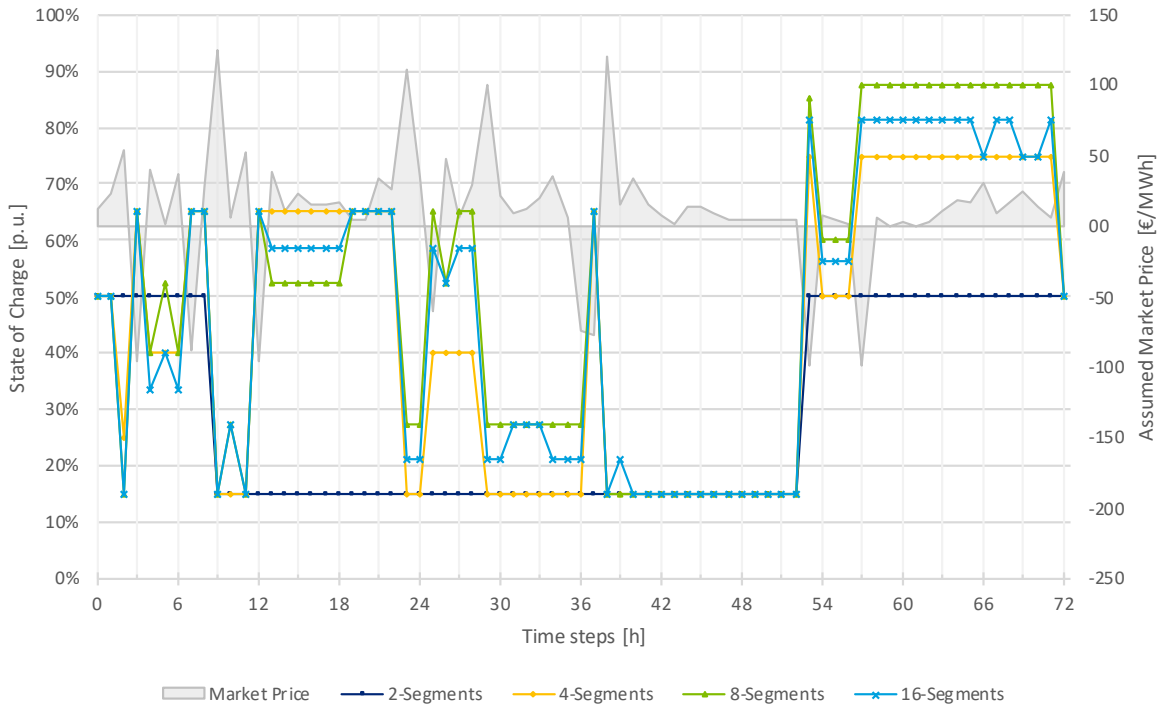

FIGURE 6.3: Assumed market prices for the sensitivity analysis and the SoC evolution for the base case for 2, 4, 8 and 16 segments.

TABLE 6.2: Obtained errors for different battery specifications and number of segments.

Number of segments	Bat. 1	Bat. 2	Bat. 3	Bat. 4	Bat. 5	Bat. 6	Bat. 7	Bat. 8	Runtime [s]
1	inf	inf	44.5 %	nan	inf	inf	nan	inf	3
2	7.9 %	7.9 %	8 %	nan	5.7 %	15.2 %	5.2 %	18.5 %	4
3	0.4 %	0.4 %	3.8 %	nan	0.4 %	8.9 %	9.7 %	16.9 %	7
4	1.2 %	1.2 %	3.8 %	nan	1.2 %	3.2 %	0.5 %	15 %	10
5	0.2 %	0.2 %	1.6 %	nan	0.2 %	5.9 %	4.7 %	18 %	12
6	0.6 %	0.6 %	1.9 %	nan	0.6 %	3 %	0.1 %	15 %	15
7	0.6 %	0.6 %	0.9 %	nan	0.6 %	2.3 %	3.5 %	13.9 %	16
8	0.2 %	0.2 %	1.4 %	nan	0.2 %	3.2 %	9.6 %	18.8 %	20
9	0.5 %	0.5 %	1.6 %	nan	0.5 %	2.4 %	9.4 %	16.2 %	24
10	0 %	0 %	0.6 %	100 %	0 %	1.9 %	9.4 %	15.3 %	28
11	0.3 %	0.3 %	1.2 %	50 %	0.3 %	3.3 %	9.5 %	17.1 %	30
12	0.6 %	0.6 %	1.5 %	50 %	0.6 %	2.7 %	10 %	16.6 %	37
13	0.2 %	0.2 %	0.9 %	33.3 %	0.2 %	2.1 %	9.6 %	15.5 %	44
14	0.4 %	0.4 %	1.1 %	25 %	0.4 %	3.1 %	9.9 %	17.3 %	54
15	0.6 %	0.6 %	1.3 %	0.7 %	0.6 %	2.7 %	10 %	16.6 %	56
16	0.2 %	0.2 %	0.9 %	0.6 %	0.2 %	2.1 %	9.8 %	15.8 %	56
17	0.4 %	0.4 %	1.1 %	0.6 %	0.4 %	3.1 %	10.1 %	17.5 %	58
18	0.6 %	0.6 %	0.8 %	0.6 %	0.6 %	2.4 %	9.7 %	15.8 %	60
19	0.3 %	0.3 %	1 %	0.5 %	0.3 %	2.1 %	9.9 %	15.9 %	71
20	0.2 %	0.2 %	1 %	0.5 %	0.2 %	1.8 %	9.9 %	15.5 %	77

- The algorithm should only be used above 10 segments. At low number of segments, the marginal cost is either too high, and the battery does not trigger at all. Thus, the error is “nan” (not-a-number). On the other hand, the error suddenly jumps to infinity ("inf"). The battery cost is still high, but some activities of the battery are recognised, resulting in a small fluctuation in the SoC, which are too small for the Rainflow algorithm to recognise resulting in 0. Consequently, the error becomes infinity.
- The size of the battery, as long the E/P-ration stays constant does not play a role. It can be seen that the error for the 10 MW and 1 MW are identical.
- The replacement cost, which determines the marginal cost functions, directly affects the activity of the algorithm. Ten times lower prices even lead to an activity with only one segment, while a ten times more expensive battery won’t respond to any arbitrage. Only when reaching higher segments, starting from 10 segments, an activity is noted, resulting in relatively high errors, which normalise when the granularity of segmentation exceeds 14 segments.
- The increase of the power capacity does not lead to a different error, compared to the base case. Whereas the reduction of the same leads to a small increase of the overall error.
- Eventually, the initial and final state have been modified, causing the highest notated error. One key assumption in the implemented algorithm is that the SoC evolution is symmetrical, which allows to confine the allocation of the degradation cost to the discharging process. Changing the initial or the final state the charging discharging symmetry is not given. The system has either a surplus energy, the final state is higher than the initial state, or a lack of energy, the final state is lower than the initial state. In either case the Algorithm cost differs from the Rainflow, hence producing an error. The initial and final state should always be tied together in a static analysis to avoid any discrepancy between the Algorithm and she Rainflow. Conclusively, it needs to be said, that the discharging and charging processes statistically equalises over the lifetime of the battery. Thus, the errorless usage of the linearised Algorithm in optimisations which implement a rolling horizon is justified.

As can be seen in Figure 6.3, the number of segments determine the activity of the battery. This behaviour is in alignment with the results by Xu et al. [43].

Chapter 7

Operational Analysis

This chapter aims to validate the operation of the algorithm considering the cycle-based degradation cost. Energy and cost balances for two consecutive sample days are generated and hereafter discussed.

7.1 Assumptions

- The battery type in this analysis is a 1 MWh / 1 MW Li-Ion BESS of type NMC/LMO. For this analysis the type of battery is only of secondary relevance, as the focus rests mainly on the qualitative integrity.
- Intraday trading was considered, and the respective prices have been assumed to be known.
- The sample days are the 11th and 12th of December 2017, which have a calculated arbitrage potential of 86.24 €/MW and 47.92 €/MWh respectively (refer Figure 5.6).
- For the marginal cost function, 32 segments ($J = 32$) was assumed. In the following, different scenarios with less segments, and one scenario with no cost is presented.

7.2 Hourly Results: 32-Segments

To understand fully the algorithm's logic, two representations of the optimisation are provided: 1) in the energy and 2) in the cost domain.

Figure 7.1 presents the energy domain as function of time. The values above zero refer to negative imbalances and vice versa (as defined in Figure 5.3):

- The dotted bars [▦] symbolise the given imbalance, before any optimisation. Thus, if neither intraday nor the battery is scheduled, the resulting imbalance [▬] is congruent with the one before.

- The turquoise bars [▬] are assigned to intraday trading. E.g. if the intraday energy is identical with the initial imbalance, the full imbalance was traded on the intraday market.
- A different way to optimise negative and positive imbalances is the charging [▨] and discharging [▨] of the battery, resulting in a modification of the SoC [—].
- Two important constraints are present: 1) the optimised imbalance [▬] at any time t is never amplified and 2) the sign of the imbalance at any given time t does not change through the optimisation.

On the other hand, Figure 7.2 presents the cost domain as function of time of the same optimisation. Keeping in mind the objective function with its six cost blocks (refer to Figure 6.2):

- Important to notice in Figure 7.2, the values below the x-axis refer to revenue and the positive values to cost.
- By trading energy on the intraday market [▬], revenues and cost savings can be achieved. By selling excess energy (positive imbalance), a small increase in revenue is noticed. Contrarily, when buying energy on the intraday market, cost savings are observed. This results in difference between the imbalance cost before [▬] and the lower intraday cost [▬]. This is likely the case when the intraday prices [·····] are lower than the imbalance penalties [- - -].
- The battery activity allocates in three different cost and savings. Charging [▨] is constrained and can only take place during positive imbalances. It results in an avoided revenue, since the excess energy won't get remunerated through the imbalance settlement. On the other hand, discharging the battery [▨] results in savings. By definition of the degradation algorithm, the discharging triggers the degradation cost [▨] and consequently lowers the savings induced by the battery.

As can be seen in Figure 7.1 and Figure 7.2, the battery takes advantages of the low imbalance prices in point ❶ and charges from 0.50 MWh to 0.71 MWh [—]. Once the imbalance prices peak at around 81 €/MWh [- - -] in point ❷, the battery discharges from 0.71 MWh to 0.62 MWh [—]. In the cost perspective (refer to Figure 7.2), it can be seen that even though the amount of charged energy is significantly higher, the avoided revenue is smaller than the savings obtained. The calculated degradation cost [▨] is in all cases lower than the savings earned. Keeping in mind that the degradation cost is only an optimisation penalty and not a real cost in the strict sense that the BRP has to pay it. The charging and discharging pattern repeat itself throughout the optimisation, as can be seen in point ❸ and point ❹, in which the battery is charging and discharging respectively.

In point ❺ and ❻, it can be seen that the ID trading triggers, every time during positive imbalances when the ID prices [·····] are higher than the IB prices [- - -]. Thus, the forecasted excess energy is sold to achieve a higher income. On the other hand, during negative imbalances, when the imbalance price is lower, the algorithm disregards intraday trading and uses the cheaper imbalance prices. The differences between the two prices are rarely very big, which is appreciated from a system point of view, since it favours a low-risk trading on the intraday market.

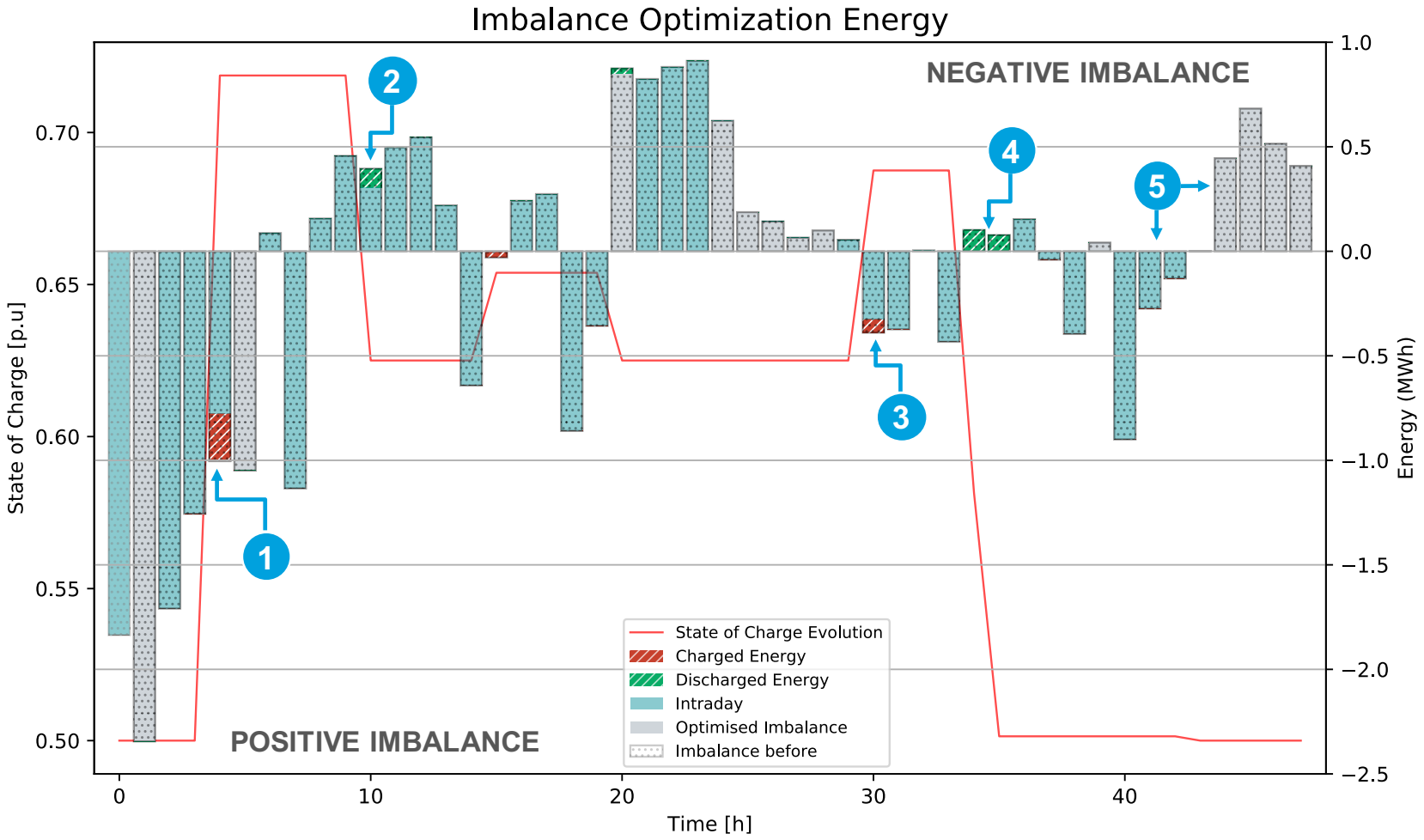

FIGURE 7.1: Hourly analysis of imbalance energy before and after the optimisation for 32-Segments.

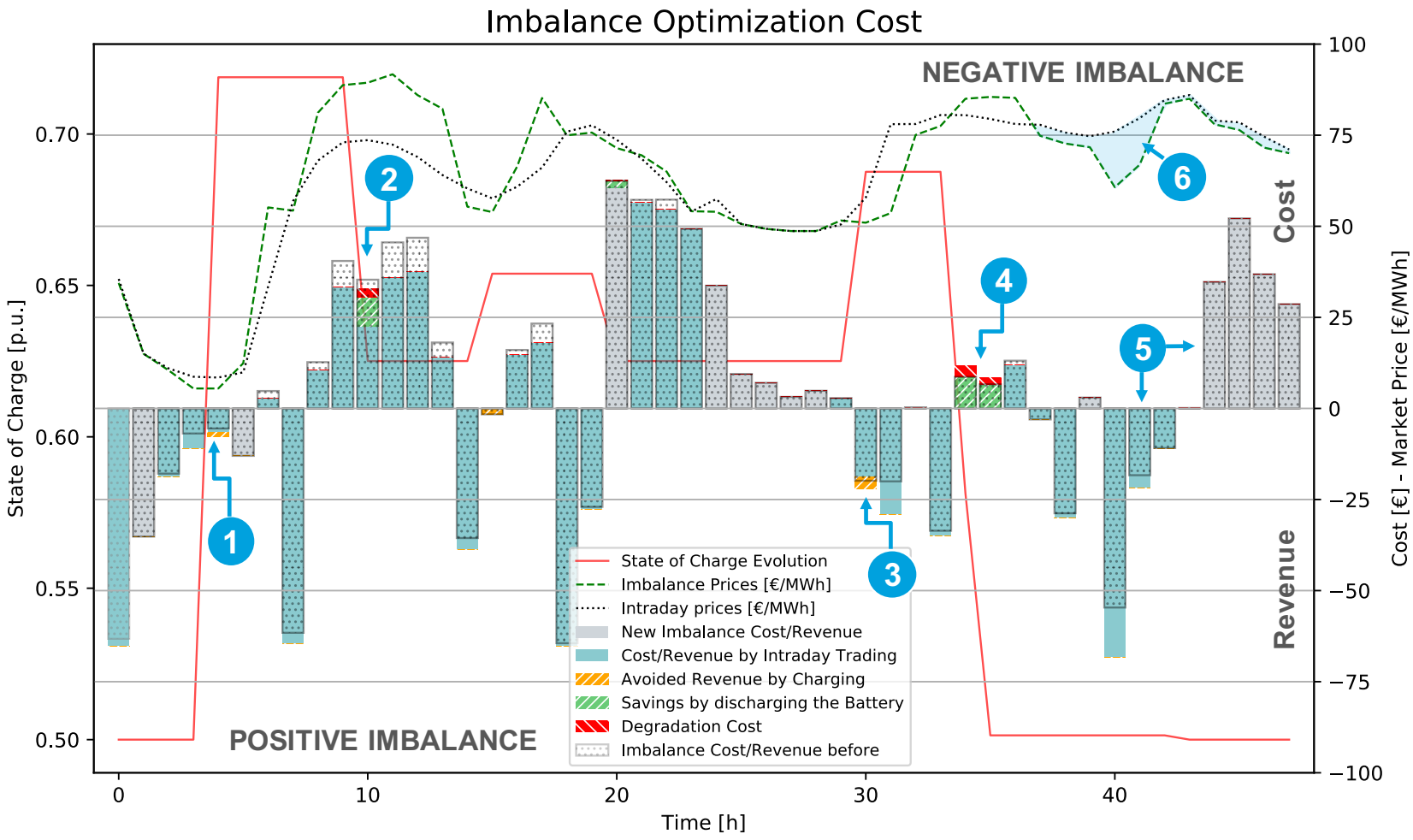

FIGURE 7.2: Hourly analysis of imbalance cost before and after the optimisation for 32-Segments.

7.3 Profitability Analysis

When decreasing the number of segments up to the point where no degradation cost is allocated, the integrity and way of operation of the algorithm maintains the same. However, the calculated results vary. Table 7.1 summaries the economics for the four cases: 32-segments; 16-segments; 1-segment and no degradation cost. To understand, how the results emerge, it is advisable to have a look at the SoC evolution for each case, which is shown in Figure 7.3.

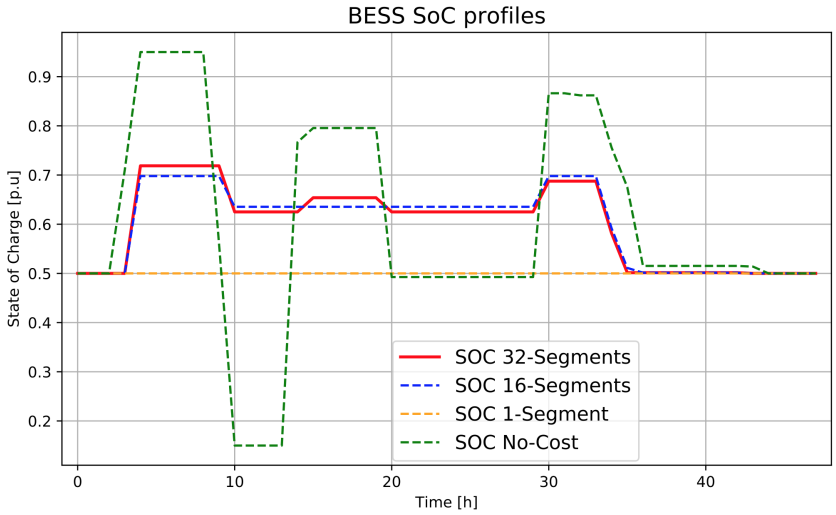

FIGURE 7.3: SoC evolution for different cost functions.

In the 32-segments use case, the savings are maximised throughout the optimisation horizon, while it gauges the cost of degradation, resulting in a low total cost. When lowering the number of segments, the battery activity decreases, while the intraday trading becomes more attractive up to the point where the battery activity freezes, because the arbitrage window is too small, and the battery cannot participate.

Compared to the 32-segment model, the no cost model results in a more aggressive operation of the BESS, while the 1-segment model is more conservative. Because the no-cost model encourages arbitrage in response to all price differences, it results in a very large negative profit and a very short battery life expectancy in all market scenarios.

Even though in the last case, no cost for the usage of the battery is allocated, the hypothetical degradation cost was calculated using the Rainflow algorithm. The high activity of the battery results in the largest savings of 139.69 € but produce the biggest degradation cost of 93.46 € and the shortest expected lifetime 8.06 years. Taking this into account, the 32-segments case is the most profitable with savings of 110.08 €.

TABLE 7.1: Results for hourly optimisation considering intraday trading and a 1 MWh NMC/LMO battery for no operating cost, single segment cycle aging cost, 16 and 32-segment cycle aging cost.

	Value	32-Segments	16-Segments	1-Segment	No-Cost
Battery	Charge [MWh]	0.323	0.27	0	1.53
	Discharge [MWh]	0.297	0.25	0	1.41
	Degradation Cost*	7.36 €	6.10 €	0 €	93.46 €
	Electricity Cost	6.18 €	4.45 €	0 €	59.60 €
	Opportunity Cost	-25.36 €	-21.55 €	0 €	-71.76 €
	Savings (without Degradation)	-19.18 €	-17.10 €	0 €	-12.16 €
	Total degradation	0.0017536 %	0.0014523 %	0	0.02225 %
	Expected Lifetime	11.55 y	11.63 y	12 y	8.06 y
Intraday	Bought Energy [MWh]	5.61	5.62	5.88	4.77
	Sold Energy [MWh]	11.44	11.49	11.76	10.23
	Cost	365.05 €	366.48 €	385.98 €	303.30 €
	Revenue	- 514.97 €	-516.89 €	-522.41 €	-455.34 €
	Opportunity Cost	51.66 €	51.56 €	34.57 €	71.76 €
	Savings	-98.26 €	-98.85 €	-101.86 €	-80.28 €
Total	Imbalance Cost (before optimisation)	193.69 €			
	Total Cost (after optimisation)	76.25 €	77.74 €	91.84 €	54 €
	Savings without Degradation	117.44 €	115.95 €	101.85 €	139.69 €
	Savings with Degradation	110.08 €	109.85 €	101.85 €	46.23 €

7.4 Full Year vs. Day-to-Day Optimisation

The algorithm optimisation is usually 24 to 48 hours with possibility to adapt the time step to quarterly, half-hourly or hourly PTUs (programme time units). In order to examine the performance of the algorithm for every hour in year 2017, two approaches were identified:

- **One Full Year Optimisation:** This way, the input data was extended to the whole year, which comprises 8760 PTUs and the battery will be scheduled for the whole year in one single optimisation considering full information. The downsides are, that the computational time is significantly longer and the battery SoH, which is updated after the optimisation is ignored for the daily optimisation.
- **Day-to-Day Optimisation:** This method keeps the optimisation window of 24 hourly PTUs and accordingly creates 365 outputs, which will be then aggregated to one yearly result. This requires some modification in the code, to execute all 365-consecutive optimisation in single run. The advantage over the other method is that after every optimisation, the battery status file is updated and read out for the next optimisation period. The computational time is considerably shorter. Furthermore, the ongoing battery degradation, which reduces the available overall capacity, is considered as well.

Generally, it can be concluded that in the full year analysis, the savings and the battery activity in comparison to the day to day analysis are slightly lower. On the other hand, the battery does not have to be at 50 % state of charge at the end of each day, thus, it can take advantage of very low or high imbalance prices and create more value per MWh discharged. The missing state of charge constraint leads to larger cycles, which cause an increase in degradation cost and hence a non-linear increase of degradation cost.

The main take-away of this analysis is that both approaches produce very similar results, moreover, the day-to-day optimisation, which will be eventually play a bigger role in the final application within the INVADE project, does not perform significantly worse. This means that even with a perfect forecast for the whole year, the value of withdrawn from a perfect battery schedule is not outperforming a day-to-day optimisation in which the forecasted data does not exceed one day. Thus, the results presented in the following refer to the Day-to-Day Optimisation.

Chapter 8

Case Studies

The focus of this chapter is on the project-based assessment of BESS flexibility for deviation management. While Section 7 mainly focused on the hourly analysis of the optimisation, this chapter forges a bridge to the yearly analysis. It aims to assess the financial feasibility of a BESS system utilising imbalance management as the main value stream. Thus, two case studies have been identified.

- **Case study I: INVADE Spanish Pilot** (see Chapter 8.1) comprises the assessment of the existing centralised BESS by Estabanell for the imbalance deviation management. It aims to be as close as possible to a real implementation. The results will reveal, whether the current battery design is financially and technologically suitable for Estabanell's imbalance management. This study splits into two scenarios, one with and another without Intraday trading.
- **Case study II: Li-Ion Performance Comparison** (see Chapter 8.2) encompasses the application of different chemistries, their distinctive performance in a techno-economic context. The evaluation is divided in four scenarios corresponding to the four commercially available LiB chemistries, which have been introduced in Section 3.2.

In total, six different scenarios with different specifications for the centralised BESS within the imbalance market are evaluated. All scenarios assume perfect forecasting and full information. Thus, results should be handled with precaution, since they represent an ideal case.

8.1 Case Study I: INVADE Spanish Pilot

According to the proposal within the INVADE project, the Spanish pilot consists of a centralised battery with a capacity of 200 kWh and a limited charge and discharge power of 60 kW. The battery is owned and operated by Estabanell Energia. 50 % of the battery capacity has to be reserved to provide supply to the controlled islanding in case of electricity cuts. The rest of the capacity can then be used for BRP imbalance management. The utilised Lithium-chemistry is an NMC/LMO blend with the aforementioned assumed characteristics. The required lifetime of the battery is 10 years, 2 years less than the expected calendar lifetime of NMC/LMO. The emerging conflict between the two value streams show the necessity

of an integrated degradation model. One half of the battery has remained as constant backup and is paid to stand by for emergency. The contractual time horizon is assumed to be 10 years. The other half of the battery can be used to maximise the profit of the project owner. Without considering the degradation cost, an extensive usage could result in a tremendously short lifetime due to cycle aging and jeopardise the first value stream. The data for the different simulation is summarised in Table F.2 of Appendix F. The case study focuses on the following research questions:

- Can imbalance management contribute positively to the finances of the BESS project?
- How does the second value stream (the backup power) affect the financial performance?
- How does perfect Intraday trading affect the battery imbalance management?
- What is the value of having degradation cost integrated in the decision making?

8.1.1 Results Case Study Ia

The scope of Scenario Ia is to demonstrate the financial feasibility for an NMC-based BESS for deviation management. As assessed previously in Section 7, the battery does create savings, but these alone do not make a project profitable. As can be seen in Table 8.1, the BESS of 200 kWh would create real savings of around 226.2 € per year. This value excludes the degradation cost, which is only used for optimisation reasons. The total charged, and discharged energy allocates to 8.1 and 7.5 MWh respectively. The calculated cost results in approximately 0.13 % with an expected lifetime of 11.86 years. The calculated LCoS for this battery corresponds to 0.41 €/kWh. The value created by deviation management is only 0.0469 €/kWh. Using this use case as the only value stream, the calculated NPV and IRR would be -148,216 € and -17.4 % respectively.

As the battery's service comprises the provision of Uninterruptible Power Supply (UPS) of 60 kW and 100 kWh, the necessary income from this additional value stream to make the battery profitable was calculated at 21,997.89 € per year. This value is more than twice as much as the single investment in a conventional backup Diesel generator with a similarly rated power [75].

Apparently, using the battery for imbalance management does not use the BESS capacity to its full extent and the investment into the BESS cannot be recovered. Additional value streams are recommended to be integrated to reach the break-even for the investment.

8.1.2 Result Case Study Ib

Scenario Ib focusses more on the value of ideal imbalance forecasting and whether the battery system can compete with intraday trading under perfect information. The emerging imbalance cost allocate to more than 32,465 €. Perfect imbalance trading together with the battery of Scenario Ia, could reduce the cost by 21,942.2 €/year. Whereas the battery only contributes with 0.3 % to these savings. Furthermore,

TABLE 8.1: Results for Scenario Ia and Ib.

Value	Ia	Ib	Value	Ia	Ib
IRR	-17 %	-18 %	Total Charge [MWh]	8.1	2.1
LCOS [€/MWh]	414.62	414.62	Total Discharge [MWh]	7.5	2.0
LCOS [€/kWh]	0.41	0.41	Imbalance Cost [€]	32465.5	32465.5
NPV [€]	-148,216	-149,623	Opportunity Cost [€]	-479.9	-131.7
Value Stream [€/MWh]	46.9	41.3	Electricity Cost [€]	253.6	74.4
Value Stream [€/kWh]	0.047	0.041	Intraday Savings [€]	0.0	-34569.0
Total possible energy [MWh/yr]	48	48	Intraday Cost [€]	0.0	12664.0
Used Energy by Value Stream [MWh]	7	2	Degradation Cost [€]	111.6	20.2
Percentage of Capable Energy	16 %	4 %	Optimised Savings [€]	114.6	21942.2
Percentage of LCOE	10 %	9 %	Real Savings [€]	226.2	21962.4

the battery activity is being reduced by 74 %, which means that in many cases the battery cannot compete with the imbalance prices, resulting in an even worse business case for the BESS of an NPV and IRR of -149,623 € and -18 % respectively (Table 8.1). The value of perfect imbalance forecasting with the goal to trade all the excess and needed energy on the ID is not more than 21,942.2 €/year.

8.2 Case Study II: Li-Ion Performance Comparison

One of the main outcomes of this work is the detailed battery model, which enables the allocation of cycle-based degradation mechanism. As previously explained, this effect is highly dependent on the battery electrochemistry used. Therefore, four scenarios compare different commercially available Lithium chemistries with regards to their cyclability and investment cost. A relatively big installed capacity of 1 MWh has been assumed, keeping in mind that the operational pattern and economics are assumed constant above 100 kW[1]. The data for the different simulation is summarised in Table F.2 of Appendix F. The case study focuses on the following research questions:

- Which Lithium chemistry provides the best cost-benefit?
- How much does the degradation cost affect the optimisation?

8.2.1 Results Case Study II

As can be seen in Table 8.2, the different chemistries, even though having the same rated power and energy capacities, perform quite differently, due to the distinctive structure of the marginal cost function derived from the replacement cost and cyclability of the chemistry. The calculated LCoS for LFP, LTO, NCA and NMC/LMO-blend are 0.56, 0.20, 1.53 and 0.54 €/kWh respectively (refer Figure 8.1a). In this context, LTO outperforms the other chemistries, though being the most expensive chemistry. It has the highest number of expected cycles and therefore it has the lowest average degradation cost (refer Figure 8.1d)

The imbalance management use case reaches a plateau for all chemistries around 0.46 €/kWh (refer Figure 8.1b), which is slightly more but still consistent with the Scenario Ia and Ib.

Taking both into account, the investment cost and the generated savings, LTO provides the best cost-benefit, followed by NMC/LMO, LFP and NCA (refer Figure 8.1c).

The charged and discharged energy correlate with the total degradation accounted for each battery. The marginal degradation cost for NCA is the highest, followed by NMC, LFP and eventually LTO. The total cost, due to the correlation with the discharged energy is the other way around.

[1] This assumption neglects economies of scale, which are undoubtedly important when installing large-scale BESS.

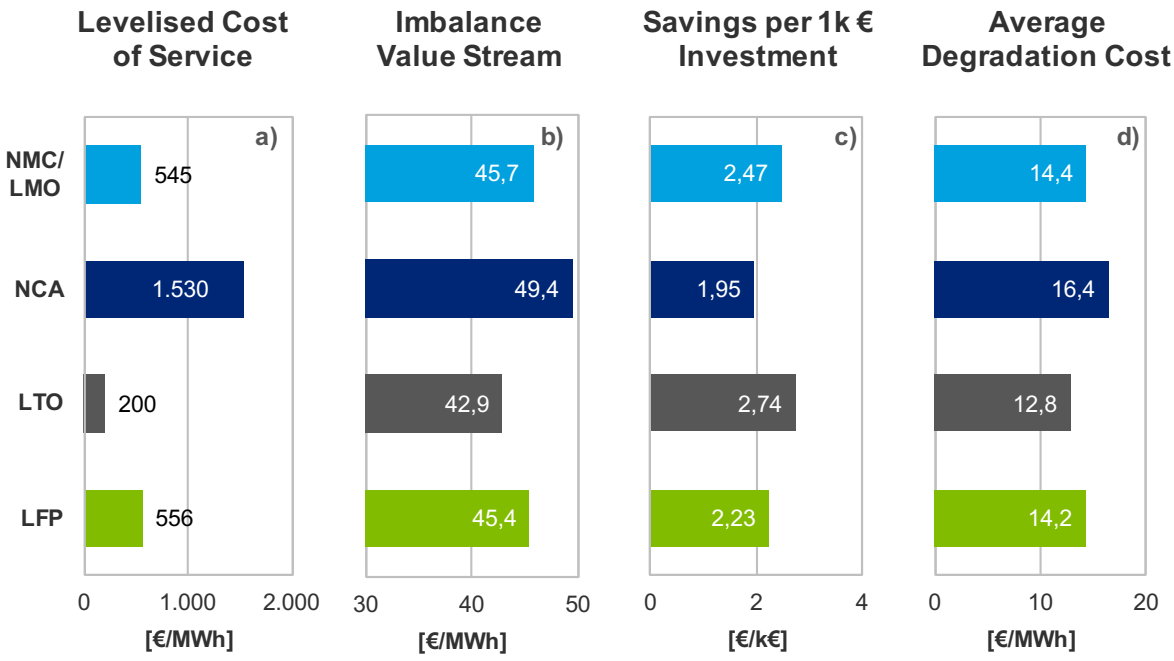

FIGURE 8.1: a) LCoS, b) imbalance value stream, c) savings per investment and d) average degradation cost for Case Study IIa (LFP), IIb (LTO), IIc (NCA) and IId (NMC/ LMO).

From a project point of view, again considering the imbalance management as the only income, the NPVs and IRRs are negative for all chemistries, which make this project unprofitable (refer to Table 8.2).

8.3 Importance of Degradation Cost

For both case studies it can be concluded, that the degradation cost positively contributed to real savings. Reminding, that the Degradation Cost, as part of the objective function negatively, but in actual fact needs to be added.

The results are in compliances with research by Xu et al. [11] and Correa-Florez et al. [76]. Both conclude that if cycling cost is ignored in the optimisation model, batteries can cycle without any constraint of frequency or depth, which results in suboptimal operating costs for the BESS operator.

In the case of Spanish imbalance prices, the market prices are quite stable, the expected arbitrage revenue is small and the BESS owner may therefore opt to pass on cycling to prolong the battery lifetime and reduce its cycle aging cost. However, without considering the degradation cost, certain periods of arbitrage are not profitable because the price fluctuations are small, and the aging cost from cycling is likely to be higher than the revenue from arbitrage.

In other cases in which the market is exposed to large price fluctuations, such as the Tesla BESS in Australia (see Appendix F.1), the BESS owner could cycle the BESS multiple times a day to maximise its profits. This case, again, proves the necessity of degradation as an integrated cost-block in the decision making.

8.4 Profitability Analysis

Independent of the degradation cost, the economic results for the BESS imbalance use case can be described as rather disillusioning, since its project KPI are significantly negative, resulting in a poor payback of the initial investment. Putting this in context with the triumphal march and the corresponding positive attention Lithium based BESS have, one might assume this is contradictory. However, battery use cases nowadays, aside from some exceptional projects such as the Tesla powerpack in Australia, only work by stacking several value streams (VS) together in order to break-even. As can be seen Figure 8.2, in many cases one value stream is not sufficient to cover the system cost, otherwise the NPV of the BESS is negative and losses are accumulated.

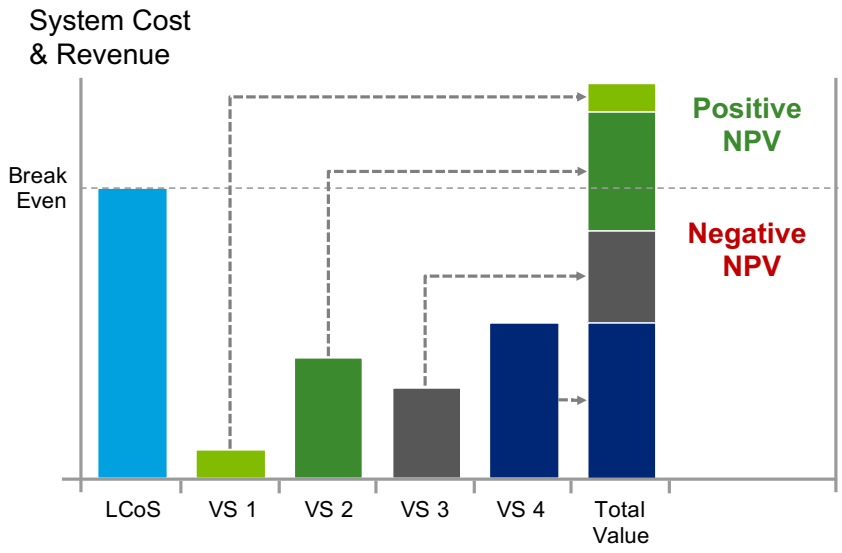

FIGURE 8.2: Battery system cost and revenue structure [42].

The stacking of the different services is not as straight forward as suggested in the figure. The needed activity in form of discharged energy for each VS needs to be calculated and weighted together with the income stream. For every battery, the maximal discharged energy is based on the warranted cycles, DoD and discharge efficiency.

Simple example: The maximal discharged energy for the battery in Scenario IIa is 288 MWh per year. The imbalance optimisation only uses 44 MWh of the discharged energy per year, which results in 15 %.

However, the value stream creates 0.045 €/kWh, which is only 8 % of the battery's LCoS. Consequently, it would be not advisable to integrate this use case in the battery operation, because the value stream uses disproportionately much energy compared to the revenue it brings.

This being said, only the Scenario Ib and IIb (LTO) are eligible for integration in a BESS project with several use cases, assuming that the activities of the other value stream would not influence the profitability of the calculated use case too much.

TABLE 8.2: Results for Case Study IIa, b, c and d.

Case Study	**IIa - LFP**	**IIb - LTO**	**IIc - NCA**	**IId - NMC/LMO**
Total Charge [MWh]	47.379	105.193	21.932	37.841
Total Discharge [MWh]	43.664	101.027	21.932	34.874
Imbalance Cost [€]	32,465	32,465	32,465	32,465
Opportunity Cost [€]	-2796.814	-6452.130	-1412.472	-2236.297
Electricity Cost [€]	1505.667	3579.872	725.313	1200.665
Degradation Cost [€]	620.60	1,292.68	359.93	500.4
Average Degr. Cost [€MWh]	14.21	12.80	16.41	14.35
Optimised Savings [€]	670.55	1,579.58	327.23	535.23
Real Savings [€]	1,291.15	2,872.26	687.16	1,035.63
IRR	-16.28 %	-10.16 %	-16.43 %	- 16 %
LCOS [€/MWh]	555.87	200.29	1,529.94	544.79
LCOS [€/kWh]	0.56	0.20	1.53	0.54
NPV [€]	-1,088,321	-1,308,146	-900,138	-955,370
Value Stream [€/MWh]	45.44	42.86	49.43	45.70
Value Stream [€/kWh]	0.045	0.043	0.049	0.046
Total possible Energy [MWh/yr]	288	980	81	240
Used Energy by Value Stream [MWh/year]	44	101	22	35
Percentage of Capable Energy	15 %	10 %	27 %	15 %
Percentage of LCOE	8 %	21 %	3 %	8 %

Chapter 9

Project Summary

The objective of this chapter is to give an overview of the activities conducted within this project and estimate the research and development cost as well as the environmental impact caused.

9.1 Project Planning

TABLE 9.1: Gantt diagramm.

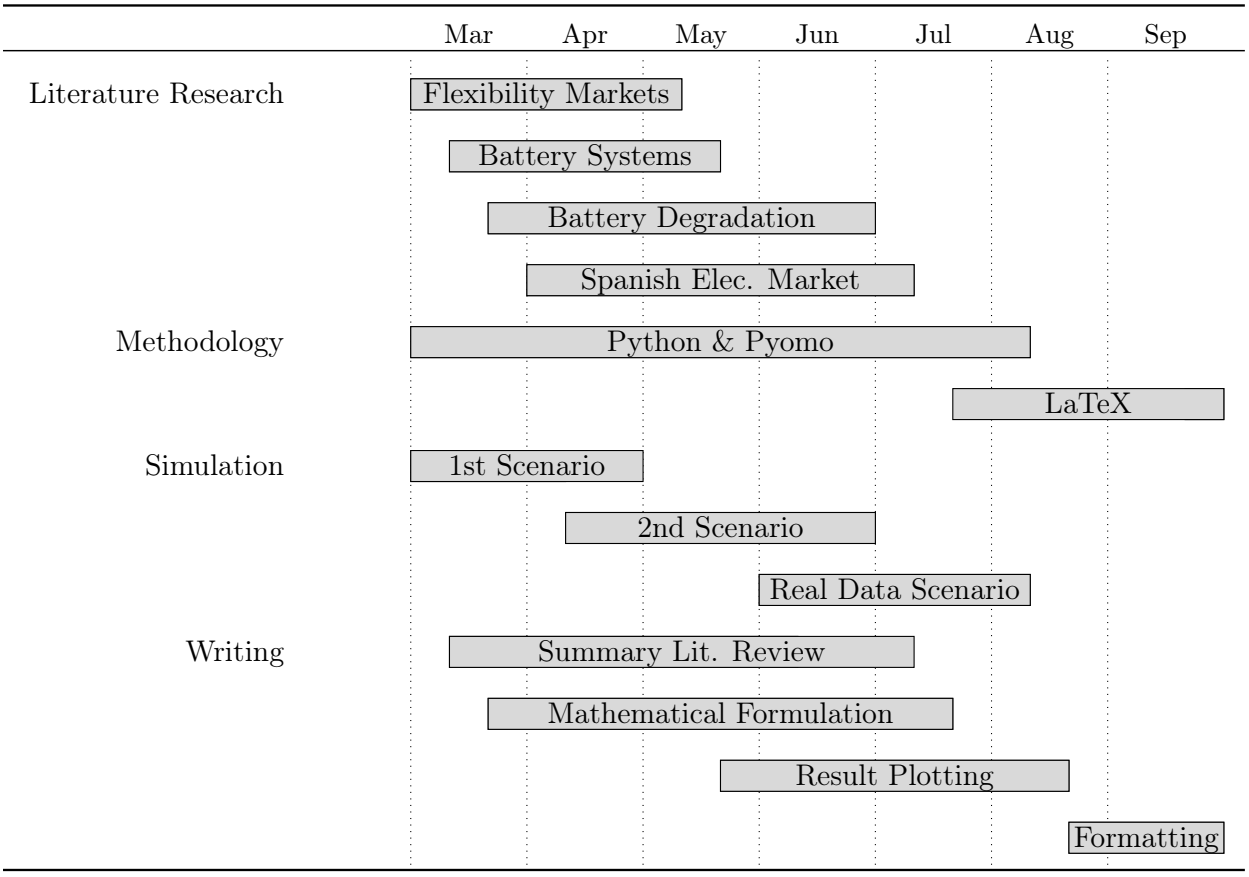

The thesis can be structured in four main work packages. The allocation of work can be found in Table 9.1. The project was carried out in seven months, starting from March and finishing in September. A weekly average of 30-week hours was dedicated. It may seem that the process is consecutive, but it rather followed a synchronous approach, due to constant feedback loops. E.g. new insights in battery modelling mirrored in updated simulations and mathematical formulation.

9.2 Budget Estimation

The budget of this project takes into consideration the research and development of this present thesis, as well as the required material to carry out this work. Personal labor costs are calculated in Table 9.2. The cost for software was neglected due to the fact, that mainly open source libraries were used. The total cost, considering that the labor cost is subjected to 21 % VAT, accounts for around 23595 €.

TABLE 9.2: Project labor costs

Concept	**Hourly Wage (€/h)**	**Hours (h)**	**Total (€)**
Literature Research	30	150	4500
Methodology	30	60	1800
Simulation	30	240	7200
Writing	30	200	6000
Subtotal	-	**650**	**19500**
VAT 21 %	-	-	4095
TOTAL	-	-	**23595**

9.3 Environmental Impact

The present chapter studies the environmental impact produced by the realisation of this project, not by its supposed execution.

Two emission sources were identified: Electricity usage and the indirect pollution caused by thermal units and the usage of public transportation in Barcelona.

The calculation carried out in Table 9.3 are separated in the calculation of the electrical consumption of the laptop used. Almost whole of the time an external monitor used. Moreover, when working in

the office of CITCEA-UPC during the winter and summer months, a air conditioning (AC) unit was used. The energy consumption of this AC-unit has been divided by the number of people working in the office (10). By considering the average environmental footprint of the Spanish grid in 2017 of 392 g·CO_{2eq}/kWh [77], the amount of greenhouse gases caused is around 57 kg.

The subway was used to get to the office in Barcelona. According to public transportation company TMB [78], the Barcelona subway emits around 15 g/CO_{2eq} per passenger per kilometre. Considering around 96 work days and a roundtrip of 13 km, the total emissions are 18.72 kg of greenhouse gases.

The amount of CO_{2eq} produced for by this project is estimated to be 75.71 kg.

TABLE 9.3: Environmental impact.

Electrical Consumption	**Power [kW/person]**	**Operating hours [h]**	**Energy [kWh]**	**CO_{2eq} produced [kg]**
Laptop	0.085	650	55.25	-
External screen	0.055	650	35.75	-
Heating/Cooling unit	0.125	435	54.375	
Subtotal	-	-	**145.375**	**56.99**
Transport	**Distance [km]**	**Days [d]**	**Total distance [km]**	-
Subway	13	96	1248	**18.72**
TOTAL	-	-	-	**75.71**

Conclusion

This work proposes a method for accurately modelling the battery degradation when dispatching in Spanish imbalance markets. Having battery degradation implemented in the decision making reveals a more considerate operation of the battery, which prolongs the battery's lifetime and improves the project economics. Moreover, the analysis revealed that the LTO chemistry performs the best from a operational and project-based perspective when applied to imbalance management. Eventually, the business case of using centralised battery flexibility for deviation management using the example of Spain was assessed and concluded to be insufficient to reach break-even for the investment.

From this work, the following conclusions can be drawn:

- Based on simulations performed, using a full year of actual market price data, the effectiveness and accuracy of the proposed model was demonstrated. These simulation results show that modelling battery degradation using the proposed model significantly improves the actual BESS profitability and life expectancy regardless of the arbitrage potential.
- The cycle aging model closely approximates the actual electrochemical battery cycle aging mechanism, while being simple enough to be incorporated into market models such as economic dispatch. The code developed is convincing by having small computational needs and a reasonably high accuracy compared to the Rainflow algorithm.
- Spanish imbalance prices in the year 2017 are quite stable and do not offer high arbitrage potential when combined with the real portfolio data provided by Estabanell Energia.
- The arbitrage possibility emerging from imbalance management in Spain, even considering perfect forecasting and full information, is not sufficient for a battery use case.
- To successfully implement BESS in the Spanish electricity market, the stacking of several use cases needs to be considered.
- Intraday trading for deviation management can perform significantly better than current batteries. The battery often cannot compete on a financial level with intraday prices. This needs to be considered when aiming to implement the use case. In case, intraday trading is performed, it weakens the revenue generated by the battery.

For future work, the following proposals are suggested:

- A possible increase of fluctuations in the imbalance market combined with a decrease of battery economics in the next years may change the business case to the point in which it becomes lucrative.

- Intraday trading with non-anticipativity constraint can show what accuracy for forecasting will be needed. It is expected that the intraday market provides a quite simple cost competitive tool for deviation management.
- In this context, a more sophisticated control of battery scheduling for deviation management can consider the dual price optimisation. This includes an extra decision variable, which will apply a different price, in case the battery operation leads to a change of imbalance's sign.
- Other important degradation mechanism should be considered as well. Especially, the battery cell temperature and the C-Rate are strongly affect the expected lifetime.
- Future research should look into the holistic battery dispatch optimisation, not only considering cycle-based degradation mechanism, but also the expected lifetime based on calendar and cycle life. This might maximise the operational life while maintaining the operational profits on a high level.
- The performance of the algorithm in more remunerative markets can be subject of future studies. As can be seen in Appendix F.1, the algorithm can be easily adapted and used in different environments and prevent burning of capital by avoiding deep cycling.
- The algorithm was designed to implement more than one battery. This function was not closer researched in this work. However, it might be of interest to analyse the algorithm performance when using a number of decentralised batteries as a virtual battery network.

Acknowledgements

A Master's Thesis

Written & Directed by *Leon Haupt*

Examined by *Francisco Diaz*
Pol Olivella-Rosell

Supported by *Justin Scholz*
Sigurd Bjarghov
Pau Lloret Gallego
Sara Barja Martínez

The Cast

Thomas Kreuzer & *Tanja Mollenhauer*
Natalia Escobosa Pineda *Martin Udo Hillenbrand*
David Hirt *Konrad Erker*
Konrad & *Susanne Auenhammer (+1)*
Tara Maya Trafton *Srilakshmi Gopalakrishnan*
Luigi Ghiani *Krzysztof Działo*
Jalomi Maayan Tardif *Riccardo Toffanin*
Łukasz Chmielnicki *Natasha Pillai*
Jose Miguel Hernandez *Kiran Raj Rajan*
Carlo Favero Falconi *Benedek Pasztor*

The SELECT Family *and all I forgot...*

The Family *Angelika &*
Carlo Haupt

The Flat *Alba Monclus &*
Ricard Gili Menéndez
Gissel Moya Choque &
Albert Gili Menéndez

The CommUnity *by InnoEnergy*

Bibliography

[1] PWC, *Spain Corporate - Taxes on corporate income*, 2018. [Online]. Available: http://taxsummaries.pwc.com/ID/Spain-Corporate-Taxes-on-corporate-income.

[2] Trading Economics, *Spain Consumer Price Index (CPI) (1954-2018)*, 2018. [Online]. Available: https://tradingeconomics.com/spain/consumer-price-index-cpi.

[3] N. Hatziargyriou, *Microgrids: architectures and control*. John Wiley & Sons, 2014.

[4] R. A. van der Veen and R. A. Hakvoort, "The electricity balancing market: Exploring the design challenge", *Utilities Policy*, vol. 43, pp. 186–194, 2016, ISSN: 09571787. DOI: 10.1016/j.jup.2016.10.008. [Online]. Available: http://dx.doi.org/10.1016/j.jup.2016.10.008.

[5] L. Einhellig, "Die Einbettung der Komponenten des Smart Markets", in *Smart Market*, Springer, 2014, pp. 345–382.

[6] L. Haupt and L. Einhellig, "Smart Grid 2016 Die Digitalisierung der Energiewende", Munich, Tech. Rep., 2016.

[7] P. Lloret, P. Olivella, G. T. Berger, J. Timbergen, and P. Rademakers, "INVADE Deliverable 4.1: Overall INVADE architecture", Smart system of renewable energy storage based on INtegrated EVs, bAtteries to empower mobile, Distributed, and centralised Energy storage in the distribution grid, Tech. Rep., 2017.

[8] USEF Foundation and Universal Smart Energy Framework, *USEF: The Framework explained*. 2015, pp. 1–55, ISBN: 9789082462517.

[9] Smart Grid Task Force, "2015 Regulatory Recommendations for the Deployment of Flexibility - EG3 REPORT", no. January, pp. 1–94, 2015.

[10] M. Jaradat, M. Jarrah, A. Bousselham, Y. Jararweh, and M. Al-Ayyoub, "The internet of energy: Smart sensor networks and big data management for smart grid", *Procedia Computer Science*, vol. 56, pp. 592–597, 2015.

[11] B. Xu, "Batteries in Electricity Markets: Economic Planning and Operations", PhD thesis, 2018.

[12] European Union's Horizon 2020 Research, *Horizon 2020 INVADE - Partners*, 2018. [Online]. Available: http://h2020invade.eu/ (visited on 03/27/2018).

[13] Directorate-General for Communication and The European Commission, "Sustainable, secure and affordable energy for Europeans", Brussels, Tech. Rep., 2014. DOI: 10.2775/60236.

[14] A. K. Dash, *From Darkness to Light: The Five 'Ds' can Lead the Way*, 2016. [Online]. Available: https://www.infosys.com/insights/business-responsibility/Pages/darkness-to-light.aspx (visited on 03/19/2018).

[15] European Commission, *Paris Agreement*, 2016. [Online]. Available: https://ec.europa.eu/clima/policies/international/negotiations/paris_en (visited on 03/19/2018).

[16] ——, "Delivering the internal electricity market and making the most of public intervention", Brussels, Tech. Rep., 2013.

[17] P. Olivella-Rosell, P. Lloret-Gallego, Í. Munne-Collado, R. Villafafila-Robles, A. Sumper, J. Rajasekharan, S. Ottessen, and B. Bremdal, "Local Flexibility Market Design for Aggregators Providing Multiple Flexibility Services at Distribution Network Level", *Energies*, vol. 11, no. 4, p. 822, 2018, ISSN: 1996-1073. DOI: 10.3390/en11040822. [Online]. Available: http://www.mdpi.com/1996-1073/11/4/822.

[18] P. Olivella-Rosell, E. Bullich-Massagué, M. Aragüés-Peñalba, A. Sumper, S. Ø. Ottesen, J.-A. A. Vidal-Clos, and R. Villafáfila-Robles, "Optimization problem for meeting distribution system operator requests in local flexibility markets with distributed energy resources", *Applied Energy*, vol. 210, no. August, pp. 881–895, 2018, ISSN: 03062619. DOI: 10.1016/j.apenergy.2017.08.136.

[19] EU, "Proposal directive", vol. 0359, 2016.

[20] S. Ø. Ottesen, A. Tomasgard, and S.-E. Fleten, "Multi market bidding strategies for demand side flexibility aggregators in electricity markets", *European Journal of Operational Research*, vol. 149, pp. 120–134, 2017, ISSN: 03605442. DOI: 10.1016/j.energy.2018.01.187. [Online]. Available: https://doi.org/10.1016/j.energy.2018.01.187.

[21] T. Van Der Schoor and B. Scholtens, "Power to the people: Local community initiatives and the transition to sustainable energy", *Renewable and Sustainable Energy Reviews*, vol. 43, pp. 666–675, 2015, ISSN: 13640321. DOI: 10.1016/j.rser.2014.10.089. [Online]. Available: http://dx.doi.org/10.1016/j.rser.2014.10.089.

[22] N. Sajn, "Electricity Prosumers", *European Parliamentary Research Service*, no. Briefing Novemeber 2016, 2016. [Online]. Available: http://www.europarl.europa.eu/RegData/etudes/BRIE/2016/593518/EPRS_BRI(2016)593518_EN.pdf.

[23] Brooklyn Microgrid, *Brooklyn Microgrid*, 2018. [Online]. Available: http://brooklynmicrogrid.com/.

[24] G. Fitzgerald, J. Mandel, J. Morris, and H. Touati, "The Economics of Battery Energy Storage: how multi-use, customer-sted batteries deliver the most services and value to customers and the grid", *Rocky Mountain Institute*, no. October, p. 41, 2015.

[25] A. Malhotra, B. Battke, M. Beuse, A. Stephan, and T. Schmidt, "Use cases for stationary battery technologies: A review of the literature and existing projects", *Renewable and Sustainable Energy Reviews*, vol. 56, pp. 705–721, 2016.

[26] B. Battke and T. Schmidt, "Cost-efficient demand-pull policies for multi-purpose technologies-The case of stationary electricity storage", *Applied Energy*, vol. 155, pp. 334–348, 2015.

[27] E. F. Bødal, P. C. del Granado, H. Farahmand, M. Korpa s, P. Olivella, I. Munné, and P. Lloret, "INVADE Deliverable 5.1: Challenges in distribution grid with high penetration of renewables",

Smart system of renewable energy storage based on INtegrated EVs, bAtteries to empower mobile, Distributed, and centralised Energy storage in the distribution grid, Tech. Rep., 2017.

[28] Popular Science Monthly, "A Ten-Mile Storage Battery", *Popular Science Monthly*, 1930.

[29] Office of Electricity Delivery & Energy Storage, *DOE Global Energy Storage Database*, 2018. [Online]. Available: https://www.energystorageexchange.org/.

[30] C. Kost, J. N. Mayer, J. Thomsen, N. Hartmann, C. Senkpiel, S. Philipps, S. Nold, S. Lude, N. Saad, and T. Schlegl, "Levelized cost of electricity renewable energy technologies", *Fraunhofer Institute for Solar Energy Systems ISE*, 2013.

[31] A. Sumper, F Diaz-Gonzalez, O. Gomis-Bellmunt, F. Díaz-González, A. Sumper, and O. Gomis-Bellmunt, *Energy Storage in Power Systems*. Wiley, 2016, pp. 25–59, ISBN: 9781118971321. DOI: 10.1002/9781118971291. [Online]. Available: https://books.google.es/books?id=wfpcCgAAQBAJ.

[32] International Renewable Energy Agency IRENA, "Costs and Markets to 2030", International Renewable Energy Agency, Tech. Rep. October, 2017.

[33] G. Huff, A. B. Currier, B. C. Kaun, D. M. Rastler, S. B. Chen, D. T. Bradshaw, and W. D. Gauntlett, "DOE/EPRI 2013 electricity storage handbook in collaboration with NRECA", *Report SAND2013- ...*, no. July, p. 340, 2013. DOI: SAND2013-5131. [Online]. Available: http://www.emnrd.state.nm.us/ECMD/RenewableEnergy/documents/SNL-ElectricityStorageHandbook2013.pdf.

[34] J. Hentunen, Ari and Forsström, S. Jenu, S. Tuurala, A. Manninen, S. Bjarghov, T. Glen, J. Timbergen, and P. R. Elaadnl, "INVADE Deliverable 6.2: Battery Techno-Economics Tool", Smart system of renewable energy storage based on INtegrated EVs, bAtteries to empower mobile, Distributed, and centralised Energy storage in the distribution grid, Tech. Rep. 731148, 2018.

[35] Battery University, *Types of Lithium-ion*. [Online]. Available: http://batteryuniversity.com/learn/article/types{_}of{_}lithium{_}ion.

[36] "The handbook of lithium-ion battery pack design: Chemistry, components, types and terminology", in *The Handbook of Lithium-Ion Battery Pack Design*, J. Warner, Ed., Amsterdam: Elsevier, 2015, p. xv, ISBN: 978-0-12-801456-1. DOI: https://doi.org/10.1016/B978-0-12-801456-1.04001-X. [Online]. Available: http://www.sciencedirect.com/science/article/pii/B978012801456104001X.

[37] F. D. González, "Energy storage systems for power networks Module 2. Overview of energy storage technologies", 2017.

[38] S. Ø. Ottesen, P. Olivella-Rosell, P. Lloret, A. Hentunen, P. C. del Granado, S. Bjarghov, V. Lakshmanan, J. Aghaei, M. Korpås, and H. Farahmand, "INVADE Deliverable 5.3: Simplified Battery Operation and Control Algorithm", INVADE; Tech. Rep., 2017.

[39] B. Nykvist and M. Nilsson, "Rapidly falling costs of battery packs for electric vehicles", *Nature Climate Change*, vol. 5, no. 4, pp. 329–332, 2015, ISSN: 17586798. DOI: 10.1038/nclimate2564.

[40] A. S. Sidhu, M. G. Pollitt, and K. L. Anaya, "A social cost benefit analysis of grid-scale electrical energy storage projects: A case study", *Applied Energy*, vol. 212, no. October 2017, pp. 881–

894, 2017, ISSN: 0306-2619. DOI: 10.1016/J.APENERGY.2017.12.085. [Online]. Available: https://www.sciencedirect.com/science/article/pii/S0306261917318068.

[41] N. Di Orio, A. Dobos, and S. Janzou, "Economic Analysis Case Studies of Battery Energy Storage with SAM", *National Renewable Energy Laboratory: Denver, CO, USA*, no. November, 2015.

[42] Lazard, "Lazard's levelised cost of storage v2.0", *Climate Policy*, vol. 6, no. 6, pp. 600–606, 2016, ISSN: 1469-3062. DOI: 10.1080/14693062.2006.9685626. arXiv: arXiv:1011.1669v3.

[43] B. Xu, J. Zhao, T. Zheng, E. Litvinov, and D. S. Kirschen, "Factoring the Cycle Aging Cost of Batteries Participating in Electricity Markets", *IEEE Transactions on Power Systems*, vol. 8950, no. c, pp. 1–12, 2017, ISSN: 08858950. DOI: 10.1109/TPWRS.2017.2733339. arXiv: 1707.04567.

[44] C. R. Birkl, M. R. Roberts, E. McTurk, P. G. Bruce, and D. A. Howey, "Degradation diagnostics for lithium ion cells", *Journal of Power Sources*, vol. 341, pp. 373–386, 2017, ISSN: 03787753. DOI: 10.1016/j.jpowsour.2016.12.011. [Online]. Available: http://dx.doi.org/10.1016/j.jpowsour.2016.12.011.

[45] J. Vetter, P. Novák, M. R. Wagner, C. Veit, K. C. Möller, J. O. Besenhard, M. Winter, M. Wohlfahrt-Mehrens, C. Vogler, and A. Hammouche, "Ageing mechanisms in lithium-ion batteries", *Journal of Power Sources*, vol. 147, no. 1-2, pp. 269–281, 2005, ISSN: 03787753. DOI: 10.1016/j.jpowsour.2005.01.006.

[46] G. Ning and B. N. Popov, "Cycle Life Modeling of Lithium-Ion Batteries", *Journal of The Electrochemical Society*, vol. 151, no. 10, A1584, 2004, ISSN: 00134651. DOI: 10.1149/1.1787631. [Online]. Available: http://jes.ecsdl.org/cgi/doi/10.1149/1.1787631.

[47] I. Laresgoiti, S. Käbitz, M. Ecker, and D. U. Sauer, "Modeling mechanical degradation in lithium ion batteries during cycling: Solid electrolyte interphase fracture", *Journal of Power Sources*, vol. 300, pp. 112–122, 2015.

[48] M. Koller, T. Borsche, A. Ulbig, and G. Andersson, "Defining a degradation cost function for optimal control of a battery energy storage system BT - 2013 IEEE Grenoble Conference PowerTech, POWERTECH 2013, June 16, 2013 - June 20, 2013", 2013. DOI: 10.1109/PTC.2013.6652329. [Online]. Available: http://dx.doi.org/10.1109/PTC.2013.6652329.

[49] A. Millner, "Modeling lithium ion battery degradation in electric vehicles", *2010 IEEE Conference on Innovative Technologies for an Efficient and Reliable Electricity Supply, CITRES 2010*, no. August, pp. 349–356, 2010. DOI: 10.1109/CITRES.2010.5619782.

[50] B. Xu, A. Oudalov, A. Ulbig, G. Andersson, and D. S. Kirschen, "Modeling of lithium-ion battery degradation for cell life assessment", *IEEE Transactions on Smart Grid*, vol. 9, no. 2, pp. 1131–1140, 2018, ISSN: 19493053. DOI: 10.1109/TSG.2016.2578950. arXiv: ‘‘‘‘.

[51] S. Grolleau, A. Delaille, H. Gualous, P. Gyan, R. Revel, J. Bernard, E. Redondo-Iglesias, and J. Peter, "Calendar aging of commercial graphite/LiFePO4cell - Predicting capacity fade under time dependent storage conditions", *Journal of Power Sources*, vol. 255, pp. 450–458, 2014, ISSN: 03787753. DOI: 10.1016/j.jpowsour.2013.11.098. [Online]. Available: http://dx.doi.org/10.1016/j.jpowsour.2013.11.098.

[52] B. Xu, "Degradation-limiting Optimization of Battery Energy Storage Systems Operation", *Power Systems Laboratory, ETH Zurich*, no. September 2013, 2013.

[53] M. Ecker, N. Nieto, S. Käbitz, J. Schmalstieg, H. Blanke, A. Warnecke, and D. U. Sauer, "Calendar and cycle life study of Li(NiMnCo)O2-based 18650 lithium-ion batteries", *Journal of Power Sources*, vol. 248, pp. 839–851, 2014, ISSN: 03787753. DOI: 10.1016/j.jpowsour.2013.09.143. [Online]. Available: http://dx.doi.org/10.1016/j.jpowsour.2013.09.143.

[54] Y. Shi, B. Xu, Y. Tan, and B. Zhang, "A Convex Cycle-based Degradation Model for Battery Energy Storage Planning and Operation", no. March, 2017. arXiv: 1703.07968. [Online]. Available: http://arxiv.org/abs/1703.07968.

[55] K. Uddin, S. Perera, W. Widanage, L. Somerville, and J. Marco, "Characterising Lithium-Ion Battery Degradation through the Identification and Tracking of Electrochemical Battery Model Parameters", *Batteries*, vol. 2, no. 2, p. 13, 2016, ISSN: 2313-0105. DOI: 10.3390/batteries2020013. [Online]. Available: http://www.mdpi.com/2313-0105/2/2/13.

[56] R. Frank and A. Poblocka, "Integration of electricity from renewables to the electricity grid and to the electricity market – RES-", *RES-INTEGRATION - Country report Denmark*, no. December, p. 48, 2011.

[57] V. Ramadesigan, P. W. C. Northrop, S. De, S. Santhanagopalan, R. D. Braatz, and V. R. Subramanian, "Modeling and Simulation of Lithium-Ion Batteries from a Systems Engineering Perspective", *Journal of the Electrochemical Society*, vol. 159, no. 3, R31–R45, 2012, ISSN: 0013-4651. DOI: 10.1149/2.018203jes. arXiv: 1602.06747. [Online]. Available: http://jes.ecsdl.org/cgi/doi/10.1149/2.018203jes.

[58] Victron Energy, "Victron Energy24V 180Ah / 100Ah Lithium-Ion Battery and Lynx Ion + Shunt",

[59] P. T. Moseley, *Electrochemical Energy Storage for Renewable Sources and Grid Balancing - Google Livres*. 2015, p. 197, ISBN: 9780444626165.

[60] G. Chandra Mouli, "Charging electric vehicles from solar energy: Power converter, charging algorithm and system design", PhD thesis, Delft University of Technology, 2018.

[61] B. Xu, Y. Shi, D. S. Kirschen, and B. Zhang, "Optimal Regulation Response of Batteries Under Cycle Aging Mechanisms", no. December, 2017. DOI: 10.1109/CDC.2017.8263750. arXiv: 1703.07824. [Online]. Available: http://arxiv.org/abs/1703.07824.

[62] A. Niesłony, "Determination of fragments of multiaxial service loading strongly influencing the fatigue of machine components", *Mechanical Systems and Signal Processing*, vol. 23, no. 8, pp. 2712–2721, 2009, ISSN: 08883270. DOI: 10.1016/j.ymssp.2009.05.010.

[63] ASTM E 1049-85, *Standard Practices for Cycle Counting in Fatigue Analysis*, 2011.

[64] V. Muenzel, J. de Hoog, M. Brazil, A. Vishwanath, and S. Kalyanaraman, "A Multi-Factor Battery Cycle Life Prediction Methodology for Optimal Battery Management", *Proceedings of the 2015 ACM Sixth International Conference on Future Energy Systems - e-Energy '15*, pp. 57–66, 2015, ISSN: 9781450336093. DOI: 10.1145/2768510.2768532. [Online]. Available: http://dl.acm.org/citation.cfm?doid=2768510.2768532.

[65] G. He, Q. Chen, C. Kang, P. Pinson, and Q. Xia, "Optimal bidding strategy of battery storage in power markets considering performance-based regulation and battery cycle life", *IEEE Transactions on Smart Grid*, vol. 7, no. 5, pp. 2359–2367, 2016, ISSN: 19493053. DOI: 10.1109/TSG.2015.2424314.

[66] S You and C. Rasmussen, "Generic modelling framework for economic analysis of battery systems", in *IET Conference Proceedings*, Stevenage: The Institution of Engineering & Technology, 2011, ISBN: 978-1-84919-536-2. [Online]. Available: http://search.proquest.com/docview/1775431305/.

[67] S. Pelletier, O. Jabali, G. Laporte, and M. Veneroni, "Goods Distribution with Electric Vehicles: Battery Degradation and Behaviour Modeling", no. September, 2015.

[68] Y. Wang, Z. Zhou, A. Botterud, K. Zhang, and Q. Ding, "Stochastic coordinated operation of wind and battery energy storage system considering battery degradation", *Journal of Modern Power Systems and Clean Energy*, vol. 4, no. 4, pp. 581–592, 2016, ISSN: 21965420. DOI: 10.1007/s40565-016-0238-z.

[69] K. Abdulla, J. de Hoog, V. Muenzel, F. Suits, K. Steer, A. Wirth, and S. Halgamuge, "Optimal Operation of Energy Storage Systems Considering Forecasts and Battery Degradation", *IEEE Transactions on Smart Grid*, vol. 9, no. 3, pp. 1–1, 2016, ISSN: 1949-3053. DOI: 10.1109/TSG.2016.2606490. [Online]. Available: http://ieeexplore.ieee.org/document/7562406/.

[70] D. Tran and A. M. Khambadkone, "Energy management for lifetime extension of energy storage system in micro-grid applications", *IEEE Transactions on Smart Grid*, vol. 4, no. 3, pp. 1289–1296, 2013, ISSN: 19493053. DOI: 10.1109/TSG.2013.2272835.

[71] S. S. Choi and H. S. Lim, "Factors that affect cycle-life and possible degradation mechanisms of a Li-ion cell based on LiCoO2", *Journal of Power Sources*, vol. 111, no. 1, pp. 130–136, 2002, ISSN: 03787753. DOI: 10.1016/S0378-7753(02)00305-1.

[72] P. Bennerstedt and J. Grelsson, "Spain's electricity market design - A case study", 2012. [Online]. Available: http://urn.kb.se/resolve?urn=urn:nbn:se:kth:diva-98488.

[73] MIBEL Regulatory Council, "Description of the operation of the mibel", no. November, p. 246, 2009.

[74] J. P. Chaves-Ávila, *European Short-term Electricity Market Designs under High Penetration of Wind Power*. 2014, p. 260, ISBN: 9789079787630.

[75] Hampshire Generators, *CPS Perkins AP60S 60kVA / 66kVA Diesel Generator*, 2018. [Online]. Available: https://www.hampshiregenerators.co.uk/product/cps-perkins-ap60s-60kva-66kva-diesel-generator/ (visited on 07/30/2018).

[76] C. A. Correa-Florez, A. Gerossier, A. Michiorri, and G. Kariniotakis, "Stochastic operation of home energy management systems including battery cycling", *Applied Energy*, vol. 225, no. June, pp. 1205–1218, 2018, ISSN: 03062619. DOI: 10.1016/j.apenergy.2018.04.130. [Online]. Available: https://doi.org/10.1016/j.apenergy.2018.04.130.

[77] Oficina Catalana del Canvi Climàtic, "Nota informativa sobre la metodología de estimación del mix eléctrico por parte de la oficina catalana del cambio climático", Tech. Rep., 2014, pp. 0–1.

[78] TMB, *TMB Public Transport Barcelona*.

[79] Universal Smart Energy Framework, *USEF: The Framwork Specifications 2015*. 2015, ISBN: 9789082462517.

[80] CENELEC, CEN-CENELEC-ETSI Smart Grid Coordination Group, and CENELEC, "SG-CG / M490 / L Flexibility Management Overview of the main concepts of flexibility management", *Overview of the main concepts of flexibility management Version 3.0*, pp. 1–36, 2014.

[81] M. Van Den Berge, M. Broekmans, B. Derksen, A. Papanikolaou, and C. Malavazos, "Flexibility provision in the Smart Grid era using USEF and OS4ES", *2016 IEEE International Energy Conference, ENERGYCON 2016*, 2016. DOI: 10.1109/ENERGYCON.2016.7514067.

[82] D. B. Nguyen, J. M. A. Scherpen, B Haar, B ter Haar, and F. Bliek, "Modeling and optimization in USEF-compliant hierarchical energy markets", in *PES Innovative Smart Grid Technologies Conference Europe (ISGT-Europe), 2016 IEEE*, IEEE, 2016, pp. 1–6, ISBN: 9781509033584.

[83] BDEW German Association of Energy and Water Industries, "Smart Grid Traffic Light Concept - Design of the amber phase", BDEW German Association of Energy and Water Industries, Berlin, Tech. Rep. March, 2015.

[84] H. Zoeller, S. A. G. Germany, S. A. G. Germany, and S. A. G. Germany, "Managing volatility in distribution networks with active network management", no. 0078, pp. 1–4, 2016.

[85] The European Commission, "METIS Technical Note T4: Overview of European Electricity Markets", no. February, 2016.

[86] C. Contreras, "System imbalance forecasting and shortterm bidding strategy to minimze imbalance costs of transacting in the spanish electricity market", PhD thesis, 2015.

[87] ENTSO-E, "ENTSO-E Operation Handbook", Tech. Rep., pp. 2–5.

[88] REE (Red Eléctrica de España), "Ancillary Services in Spain : dealing with High Penetration of RES", Tech. Rep., 2010, p. 42. [Online]. Available: http://www.reshaping-res-policy.eu/downloads/topicalevents/de-la-Fuente_Ancillary-Services-in-Spain1.pdf.

[89] KUL Energy Institute, "The current electricity market design in Europe", *KUL Energy Institute*, p. 4, 2015.

[90] NEOEN, *Hornsdale Power ReserveDemand*, 2018. [Online]. Available: https://hornsdalepowerreserve.com.au/.

[91] Australian Energy Markets Operator AEMO, *Data Dashboard - Electricity Price and Demand*, 2018. [Online]. Available: https://www.aemo.com.au/Electricity/National-Electricity-Market-NEM/Data-dashboard#price-demand.